Exploration of the active site of β4GalT7

Synthesis of substrates and inhibitors

CENTER FOR ANALYSIS AND SYNTHESIS | LUND UNIVERSITY
KARIN THORSHEIM

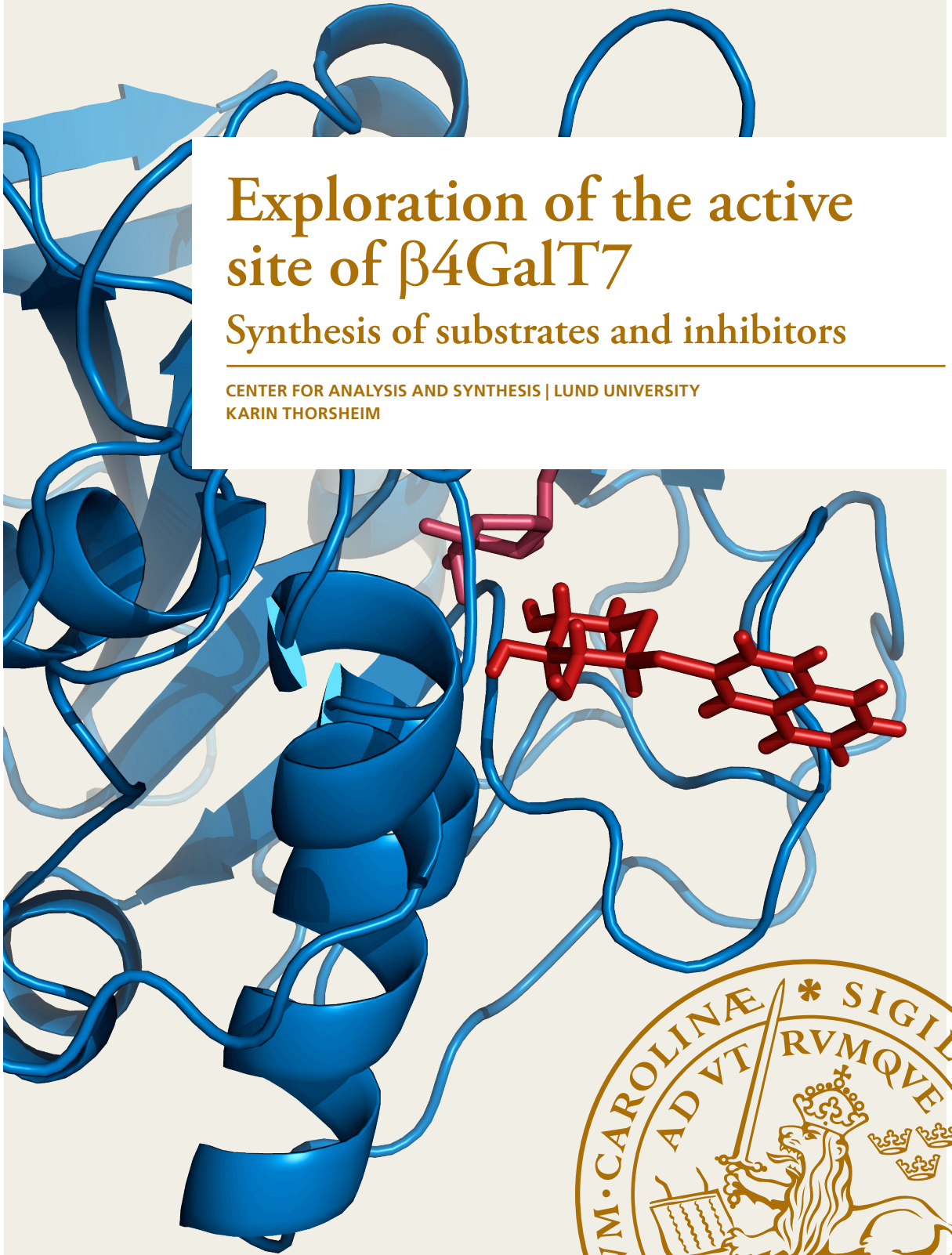

Exploration of the active site of β4GalT7

Synthesis of substrates and inhibitors

Karin Thorsheim

LUND
UNIVERSITY

DOCTORAL DISSERTATION

by due permission of the Faculty of Science, Lund University, Sweden.
To be defended in lecture hall K:A, Kemicentrum,
on Friday 15th of September 2017 at 9.00 a.m.

Faculty opponent

Associate Professor Anja Sandström
Department of Medicinal Chemistry, Uppsala University, Sweden

Organization LUND UNIVERSITY	Document name DOCTORAL DISSERTATION
	Date of issue 2017-08-22
Author(s) Karin Thorsheim	Sponsoring organization

Title and subtitle

Exploration of the active site of β4GalT7 – Synthesis of substrates and inhibitors

Abstract

β-1,4-Galactosyltransferase 7 (β4GalT7) is a key enzyme in the biosynthesis of proteoglycans (PGs) and glycosaminoglycan (GAG) chains, which are important macromolecules involved in many biological processes such as cell growth and cell signaling as well as in cancer pathobiology and viral and bacterial infections. Despite its pivotal role, much is still unknown regarding the specific structure of GAGs and how the structure affects its functions. GAG synthesis can be regulated by xylosides acting on β4GalT7 as either substrates or inhibitors. In an effort to find efficient substrates and inhibitors of β4GalT7, which would be valuable tools applicable in GAG research, we set out to investigate the active site of β4GalT7 by synthesizing and examining xylosides and xyloside analogs with modifications in the xylose moiety, the endocyclic and exocyclic positions, as well as the aglycon. The overarching aim with these investigations was to pinpoint the requirements of efficient substrates and efficient inhibitors. The synthesized compounds were evaluated in a β4GalT7 assay in combination with molecular docking simulations and conformational analysis by NMR spectroscopy. We found that efficient substrates are formed when keeping the xylose moiety unmodified, but exchanging the endocyclic and/or exocyclic oxygen atoms for sulfur, as well as connecting the xyloside to an aglycon consisting of a fused aromatic system, preferably separated from the xylose part by a short oligoethylene glycol spacer. These structural features can not directly be transferred to a xyloside analog possessing inhibitory activity to gain efficient inhibitors of β4GalT7.

Key words

Xylosides, β4GalT7, β-1,4-galactosyltransferase 7, glycosaminoglycan, synthesis

Classification system and/or index terms (if any)

Supplementary bibliographical information		Language English
ISSN and key title		ISBN 978-91-7422-535-8
Recipient's notes	Number of pages 226	Price
	Security classification	

Exploration of the active site of β4GalT7

Synthesis of substrates and inhibitors

Karin Thorsheim

LUND
UNIVERSITY

Cover by Karin Thorsheim and Emil Tykesson

Faculty of Science
Department of Chemistry

ISBN 978-91-7422-535-8

Printed in Sweden by Media-Tryck, Lund University
Lund 2017

Populärvetenskaplig sammanfattning

Ytan av alla celler är dekorerad med kolhydrater som står för mycket av den information en cell överför till omgivande celler. Många av kolhydraterna tillhör en föreningsklass som kallas proteoglykaner som består av ett protein sammanbundet med en eller flera långa kolhydratkedjor. Dessa kolhydratkedjor kallas glykosaminoglykaner och är bundna till proteinet via kolhydraten xylos. Än så länge har vi bara en vag aning om sambanden mellan strukturen hos glykosaminoglykanerna och den information de överför. Denna avhandling handlar om att skapa verktyg som kan ge oss insikter i hur glykosaminoglykanerna bildas.

Xylosider, det vill säga molekyler baserade på xylos kopplat till en annan molekyl – en aglykon, kan gå in i celler och starta eller blockera bildandet av glykosaminoglykaner genom att efterlikna det naturliga substratet för ett visst enzym – β4GalT7. För att öka förståelsen för hur en xylosid ska se ut för att vara ett bra substrat eller en bra hämmare för β4GalT7 har vi syntetiserat och testat aktiviteten av olika xylosider.

Vi har valt att systematiskt undersöka tre olika delar av xylosidmolekylerna - själva kolhydraten, kopplingen och aglykonen. Vi har hittat ett antal nya molekyler som fungerar som bra substrat för β4GalT7 och vi har också hittat substanser som fungerar som hämmare.

Resultaten i den här avhandlingen lägger en grund för vilka strukturelement som kan inkorporeras i xylosider för att ge effektiva substrat samt grundläggande krav för en hämmare.

List of papers

This thesis summarizes and supplements the following papers, referred to by Roman numerals I-XI. Paper I, IV, and VI are reprinted with kind permission of Elsevier. Paper II and III are reprinted with kind permission of The Royal Society of Chemistry. Paper V is reprinted with kind permission of Springer.

I **K. Holmqvist**, A. Persson, R. Johnsson, J. Löfgren, K. Mani, U. Ellervik. "*Synthesis and biology of oligoethylene glycol linked naphthoxylosides*", Bioorg. Med. Chem., **2013**, *21*, 3310-3317.

Contribution: Performed the majority of the synthetic work, contributed to the interpretation of data, and to writing the manuscript.

II A. Siegbahn, S. Manner, A. Persson, E. Tykesson, **K. Holmqvist**, A. Ochocinska, J. Rönnols, A. Sundin, K. Mani, G. Westergren-Thorsson, G. Widmalm, U. Ellervik. "*Rules for priming and inhibition of glycosaminoglycan biosynthesis: Probing the β4GalT7 active site*", Chem. Sci., **2014**, *5*, 3501-3508.

Contribution: Performed synthetic work, contributed to the interpretation of data, and to writing the manuscript

III A. Siegbahn, **K. Thorsheim**, J. Ståhle, S. Manner, C. Hamark, A. Persson, E. Tykesson, K. Mani, G. Westergren-Thorsson, G. Widmalm, U. Ellervik. "*Exploration of the active site of β4GalT7: Modifications of the aglycon of aromatic xylosides*", Org. Biomol. Chem., **2015**, *13*, 3351-3362.

Contribution: Performed the majority of the synthetic work, contributed to the formulation of the research problem, the interpretation of data, and to writing the manuscript.

IV **K. Thorsheim**, A Siegbahn, R. E. Johnsson, H. Stålbrand, S. Manner, G. Widmalm, U. Ellervik. "*Chemistry of xylopyranosides*", Carbohydr. Res., **2015**, *418*, 65-88.

Contribution: Performed the majority of the writing work.

V **K. Thorsheim**, A. Persson, A. Siegbahn, E. Tykesson, G. Westergren-Thorsson, K. Mani, U. Ellervik. "*Disubstituted naphthyl β-D-xylopyranosides: Synthesis, GAG priming, and histone acetyltransferase (HAT) inhibition*", Glycoconj. J., **2016**, *33*, 245-257.

Contribution: Performed all the synthetic work, contributed to the formulation of the research problem, the interpretation of data, and to writing the manuscript.

VI **K. Thorsheim**, S. Clementson, E. Tykesson, D. Bengtsson, D. Strand, U. Ellervik. "*Hydroxylated oxanes as xyloside analogs for determination of the minimal binding requirements of β4GalT7*", Tetrahedron Lett., **2017**, *58*, 3466-3469.

Contribution: Performed all the synthetic work on the chiral pool approach, contributed to the formulation of the research problem, the interpretation of data, and to writing the manuscript.

VII **K. Thorsheim**, S. Manner, U. Ellervik. "*Expanding the scope of methyl xanthate esters - from Barton McCombie reaction auxiliary to versatile protective group*", Submitted.

Contribution: Performed all the synthetic work, contributed to the formulation of the research problem, the interpretation of data, and to writing the manuscript.

VIII **K. Thorsheim**, D. Willén, E. Tykesson, J. Ståhle, J-P. Praly, S. Vidal, M. T. Johnson, G. Widmalm, S. Manner, U. Ellervik. "*Naphthyl thio- and carba-xylopyranosides for exploration of the active site of β4GalT7 – The role of the endocyclic oxygen atom*", Manuscript.

Contribution: Performed synthetic work, contributed to the formulation of the research problem, the interpretation of data, and to writing the manuscript.

IX P. Blasco Morales, J. Ståhle, **K. Thorsheim**, A. Siegbahn, U. Ellervik, G. Widmalm. "*Synthesis, conformational analysis and biological activity of xylopyranosyl sulfur-containing glycosides: Dependence of sulfur atom configuration*", Manuscript.

Contribution: Performed all the synthetic work, performed the enzymatic assay, contributed to the formulation of the research problem, the interpretation of data, and to writing the manuscript.

Abbreviations

AIBN	Azobisisobutyronitrile
β4GalT7	β-1,4-Galactosyltransferase 7
CS	Chondroitin sulfate
DBN	1,5-Diazabicyclo[4.3.0]non-5-ene
DBU	1,8-Diazabicyclo[5.4.0]undec-7-ene
DMG	Directed metalation group
DMP	Dess–Martin periodinane
D*o*M	Directed *ortho* metalation
DS	Dermatan sulfate
GAG	Glycosaminoglycan
HAT	Histone acetyltransferase
HDAC	Histone deacetylase
HS	Heparan sulfate
IC_{50}	The concentration at which 50% of maximal inhibition is reached
*m*CPBA	*meta*-Chloroperoxybenzoic acid
OEG	Oligoethylene glycol
PG	Proteoglycan
PrtG	Protective group
TBAHS	Tetrabutylammonium hydrogen sulfate
TBAI	Tetrabutylammonium iodide

Abbreviations found in the ACS Style Guide are not included.

Content

1 Introduction

1.1 Xylosides

1.1.1 Classification and nomenclature

Xylose is a monosaccharide, which means that it does not decompose to smaller subunits when treated with aqueous acid. Xylose is also an aldose, indicating that the carbonyl functionality is an aldehyde, in contrast to a ketose wherein the carbonyl functionality is a ketone. In addition, xylose is a pentose meaning that it contains five carbon atoms. Carbohydrates consisting of six carbon atoms, such as glucose and galactose, are subsequently referred to as hexoses.

All carbohydrates are chiral and have stereocenters. Generally, the Fischer projection shows the carbohydrate in an open, two-dimensional form with the carbonyl at the top and the vertical line representing the carbon backbone (Figure 1). Atoms and groups on the right side are on the bottom face in a cyclic structure and atoms and groups on the left side are on the top face. Carbohydrates with the hydroxyl group pointing to the right at the stereocenter with highest location (center of reference) are referred to as D sugars, whereas carbohydrates with this hydroxyl group pointing to the left are referred to as L sugars. Hence, D/L gives the absolute configuration of the stereocenter with highest location while the trivial names, such as xylose and arabinose, gives the relative stereochemistry of the remaining stereocenters. (+) And (-) may be added, indicating how plane-polarized light is rotated.[1]

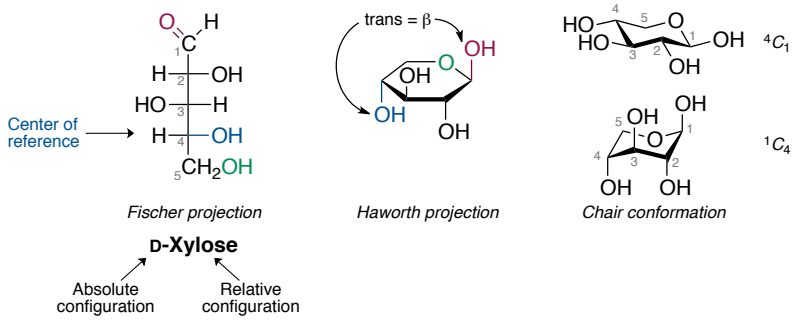

Figure 1. Different representations of D-xylose.

Carbohydrates exist to a large extent in cyclic forms where a hydroxyl group has reacted with the carbonyl group to yield either a five membered ring, i.e. a furanose, or a six membered ring, i.e. a pyranose. Other ring sizes are possible, but unusual. The cyclization generates a new stereogenic center at the former carbonyl carbon, referred to as the anomeric carbon, and the diastereomers formed are called anomers. When the newly formed hydroxyl group at the anomeric carbon is situated cis to the hydroxyl group at the stereocenter with highest location, this configuration is called α, whereas a trans relation between these hydroxyl groups is referred to as β (Figure 1). In an aqueous solution, xylose exists as 36.5% α-pyranose, 63.0% β-pyranose, less than 1% as furanoses, and in a negligible extent in the acyclic form.

The cyclic form can be represented as a Haworth projection where the ring is almost perpendicular to the plane of the paper, but viewed slightly from above (Figure 1). The hydrogen atoms are often excluded from this representation and hydroxyl groups are positioned vertically pointing either up or down in relation to the plane. However, this is not a good representation of the conformation of carbohydrates. Xylose, as well as other pyranoses, usually resides in a chair conformation (*C*). The chair can exist in two different forms where O-C2-C3-C5 define the reference plane of the ring. To define the chair, carbon atoms positioned above this plane are given as a superscript and atoms below the plane are given as a subscript, i.e. ${}^{4}C_{1}$ and ${}^{1}C_{4}$.

Several factors affect which chair conformation (or other forms) that is adopted. Taking sterics into account, equatorial positions of the substituents are favored. However, the anomeric effect, i.e. a stereoelectronic effect, may influence the conformation to a large extent. In short, electronegative substituents at the anomeric carbon is favorably positioned axially since a lone pair of electrons of the endocyclic oxygen atom can interact with the unoccupied, anti-bonding orbital σ* of the axial glycosidic bond. This is a stabilizing interaction, and indeed a slight shortening of the bond between the endocyclic oxygen atom and C1 is observed as well as a lengthening of the bond between C1 and the anomeric substituent, compared to the anomer.

1.1.2 Reactivity of xylosides

Xylose connected to another molecule at C1 is referred to as a xyloside and the group that is bound to xylose is referred to as an aglycon. The chemistry of xylopyranosides has recently been reviewed by us (Paper IV), including formation of xylosyl donors, protective group chemistry, modifications of the xylose moiety, and conformational analysis. Thus, this will not be discussed here, and only a few comments will be given.

Generally, xylosides can be formed through glycosylation under either basic conditions, usually with xylosyl halides through an S_N2 type mechanism, or under acidic conditions, via an S_N1 type mechanism (Scheme 1). The stereochemical

outcome of a Lewis acid promoted xylosylation is usually directed by the anomeric effect. However, participating groups at C2, e.g. esters, may interact with the intermediate oxocarbenium ion forming a cyclic acyloxonium ion (Figure 2). The acyloxonium ion is subsequently opened by the aglycon, also called acceptor, in an S_N2 manner resulting in an equatorial glycosidic bond, hence β-D-xylosides are fairly easy to synthesize by standard methods, whereas α-D-xylosides can be formed by anomerization of the kinetic β-products.

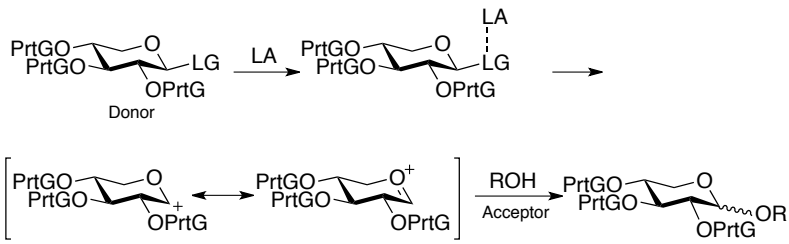

Scheme 1. General mechanism for acid-promoted glycosylation reaction. PrtG = Protective group, LG = Leaving group, LA = Lewis acid.

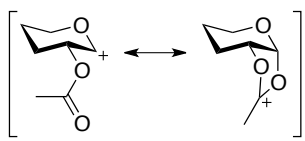

Figure 2. A participating group, such as acetate, at C2 directs the nucleophile, promoting β-attack.

Peracetylated xylose is a common donor since it is easily available and generally forms β-xylosides in good yields. However, if an α-xyloside is to be synthesized, xylosyl halides are generally the donor of choice, performing the glycosylation reaction using tetraalkylammonium bromide as catalyst (Lemieux protocol). Trichloroacetimidate donors may be preferred if the donor and/or acceptor is sensitive towards harsh conditions. On the other hand, if a robust donor is wanted, thioxylosides are the donor of choice.[2]

When β-D-xylosides reside in a $^4C_1$ chair conformation, all hydroxyl groups are equatorial, and since they are all secondary, they show similar reactivity. This must be taken into account when protective group strategies and modifications are planned. However, a general trend in reactivity has been observed, and for β-xylosides this is O4 > O3 > O2, whereas the trend for α-xylosides is O2 > O4 > O3.[2]

1.2 Proteoglycans and glycosaminoglycans

Proteoglycans (PGs) are located in the extracellular matrix, on cell surfaces, or inside mammalian cells and consist of a core protein with one or several, covalently attached glycosaminoglycan (GAG) chains, i.e. long, linear, anionic polysaccharides. PGs and GAGs appear to be synthesized by virtually all cell types and their function is highly diversified, including involvement in cellular processes such as differentiation, migration, adhesion, and cell growth, as well as functioning as mechanical support. The biological activities exerted by PGs are largely due to the interactions of the GAG chains with growth factors, cytokines, enzymes, and other signaling molecules.[3] PGs and GAGs are also involved in cancer pathobiology as well as bacterial and viral infections.[4-7]

GAG chains are composed of disaccharide units consisting of one hexosamine [*N*-acetyl-D-glucosamine (D-GlcNAc) or *N*-acetyl-D-galactosamine (D-GalNAc)] and one hexuronic acid or hexose [D-glucuronic acid (D-GlcA), L-iduronic acid (L-IdoA), or galactose (Gal)]. Based on this disaccharide structure, GAGs are classified into four families, i.e. heparin/heparan sulfate (HS), chondroitin sulfate/dermatan sulfate (CS/DS), keratan sulfate (KS), and hyaluronan (HA). CS/DS and HS GAG chains are connected to a core protein forming PGs via a tetrasaccharide linker: GlcAβ1–3Galβ1–3Galβ1–4Xylβ1–*O*-(Ser) (Figure 3).[3]

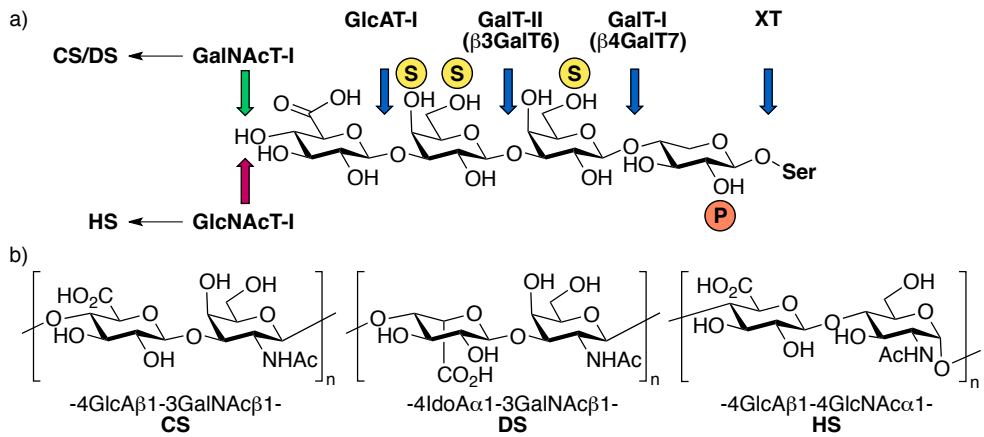

Figure 3. a) Schematic figure over linker tetrasaccharide synthesis with involved enzymes. Modifications, i.e. phosphorylation and sulfation, are indicated at the possibly affected positions by "P" or "S", respectively, enclosed by a cirle. b) Disaccharide composition of CS/DS and HS GAG chains.

The biosynthesis of CS/DS and HS PGs takes place in the endoplasmic reticulum (ER) and Golgi compartments and is initiated by xylosylation of a specific serine residue in the core protein, mediated by a xylosyltransferase[8-9] (XT). Galactosyltransferase I[10-11] (GalT-I also known as β4GalT7) and galactosyltransferase II[12] (GalT-II also known as β3GalT6) subsequently add two galactose residues and then a glucuronic acid is added by the aid of glucuronyltransferase I[13] (GlcAT-I). The subsequent addition of β-GalNAc by β-*N*-acetylgalactosaminyltransferase I (GalNAcT-I) triggers CS/DS synthesis, whereas the addition of α-GlcNAc by α-*N*-acetylglucosaminyltransferase I (GlcNAcT-I) initiates HS synthesis (Figure 3). During GAG chain polymerization, site-specific deacetylation, sulfation, and epimerization occurs, which leads to their structural and biological diversification. In addition, the linker tetrasaccharide is also modified where the xylose residue can be phosphorylated as well as dephosphorylated at O2. This modification can be found in both CS/DS and HS chains, and the phosphorylated trisaccharide seems to be a good substrate for GlcAT-I. Sulfation of C6 of the first galactose unit and of C4 and/or C6 of the second galactose unit in the linker is only found in CS/DS. These modifications may therefore have a regulatory function.[3, 14-15]

Defects in the biosynthesis of GAGs and PGs, caused by mutations in the genes encoding the enzymes involved, causes a number of rare genetic disorders.[16] One of these, Ehlers-Danlos syndrome (EDS), is a heterogeneous group of inherited connective tissue disorders, comprising deficiency in collagen and connective tissue structure and synthesis. Several different mutations of β4GalT7 have been found in patients suffering from progeroid variant of EDS.[11, 17-20] These mutations affect the putative catalytic domain and the folding of the enzyme, and results in reduction or loss of β4GalT7 activity.

1.3 β4GalT7

1.3.1 Structure and function

In 1999, Almeida et al. cloned, expressed, and characterized the seventh member of the human β-1,4-galactosyltrasferase family,[11] which also almost simultaneously was reported by Okajima et al.[10] The six already known members catalyze the biosynthesis of Galβ1-4GlcNAc and/or Galβ1-4Glc and possess highly conserved sequence motifs in the putative catalytic domain that includes four conserved cysteine residues. However, β4GalT7 does not contain any of the conserved cysteine residues, and the

enzyme was found to catalyze the Galβ1-4Xylβ1-R linkage, in the presence of Mn^{2+}. Thus, β4GalT7 show galactosyltransferase I activity (EC 2.4.1.133)*.

ITC measurements of β4GalT7 have shown that binding of UDP-Gal strongly promotes the binding of the acceptor substrate (xyloside), where the binding of the β-phosphate of UDP-Gal largely contributed to the binding energy and the uridine moiety contributed to the positioning of the donor. The contribution of the galactose moiety was negligible.[21]

In 2010, Ramakrishnan and Qasba published the crystal structure of β4GalT7 from *Drosophila melanogaster*, revealing a strong protein sequence similarity with human β4GalT7.[22] It was shown that binding of manganese and UDP induced a conformational change from an open to a closed form of the enzyme. Even though a crystal structure could not be obtained with bound xylose, amino acids Asp^{211} and Asp^{212} were suggested to be involved in the binding of the xylose moiety by forming hydrogen bonds to O2, O3, and O4. The side chain of Tyr^{177} causes steric hindrance and thus singles out xylose as the acceptor substrate.

In 2013, an N-terminally truncated human β4GalT7 fused to human galectin-1 was expressed in *E. coli*. Crystal structures of two different conformations of human β4GalT7 were presented, one open and one closed form, as well as the crystal structure of β4GalT7 from *Drosophila* with both acceptor and donor substrate present.[23] The crystal structures of human β4GalT7 confirmed that conformational changes occur upon binding of UDP or UDP-Gal and Mn^{2+}.[22] The acceptor binding pocket was shown to be hydrophobic. However, the region surrounding the active site is highly positively charged. The crystal structure of β4GalT7 from *Drosophila* is the first example of a galactosyltransferase in a Michaelis complex, here with UDP-Gal, xylobiose, and manganese, and an S_N2-type catalytic mechanism was proposed.

Fournel-Gigleux and co-workers used molecular docking simulations and a β4GalT7 enzyme assay to further investigate the active site.[24] Computational analysis with 4-methylumbelliferyl β-D-xylopyranoside **1** (Figure 4) positioned in the active site revealed a potentially important hydrophobic cluster of three Tyr residues. The authors suggested that Tyr^{194} might stabilize both the donor and the acceptor by making a hydrogen bond to a β-phosphate oxygen of UDP and a π-stacking interaction with the aglycon. Furthermore, Tyr^{196} is believed to make a hydrogen bond to the side chain of Asp^{229} that then can form a bond to O2 of xylose. Tyr^{199} was suggested to form a hydrogen bond to O2 of the galactose moiety. Point mutagenesis and assays using **1** as acceptor substrate, showed that all three tyrosine

* Enzyme Commission number (EC number) indicates the reaction that the particular enzyme catalyzes. 2 stands for transferases, 2.4 stands for transferases that act on glycosides, 2.4.1 stands for glycosyltransferases that catalyze the transfer of a hexose, and 2.4.1.133 stands for glycosyltransferase that catalyze the reaction between UDP-galactose and an *O*-β-D-xyloprotein.

residues were important for activity. The results were corroborated with cellular studies. In addition, investigations of the structural role of His[195] predicted that the nitrogen atom of the peptide backbone forms a hydrogen bond to the carbonyl group of the aglycon in **1**.

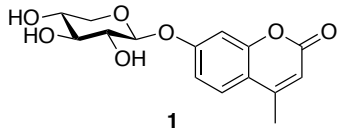

1

Figure 4. Investigated acceptor substrate for β4GalT7.

1.3.2 Assays

In addition to cell studies, galactosyltransferase I activity has been evaluated in early investigations using assays employing partially purified enzyme from different cell extracts.[25-30] However, since the first expression and characterization of β4GalT7,[10-11] several enzyme assays have been developed. Almeida et al. evaluated a full-length construct expressed in insect cells, and an estimated K_M value of 0.89 mM was reported for **1** as well as a K_M of 56 mM for UDP-Gal.[11] The catalytic activity resembled previous results where partially purified enzyme extracts have been used.

Wild-type and mutant human β4GalT7 has also been expressed in yeast *Pichia pastoris*,[31] HeLa cells,[21, 32] CHOpgsB-618 cells,[20, 32] and *E. coli*,[19-21, 24, 32-34] which is often preferred for large scale production. To avoid aggregation of the recombinant enzyme, often formed when using *E. coli*, fusion tags i.e. the maltose-binding protein (MBP),[20-21] galectin-1,[33] glutathione *S*-transferase (GST),[19, 24, 32] or a His tag[34], have been utilized. The β4GalT7 activity have been evaluated by use of absorbance or fluorescence detection of the products,[21, 24, 31, 34] measuring the radioactive incorporation of the product by the use of radiolabeled UDP[^{14}C]Gal,[11, 32] or through an NADH coupled assay.[34]

1.4 Xylosides and GAG synthesis

In 1969, Helting and Rodén showed that D-xylose **2** as well as methyl β-D-xylopyranoside **3** and *O*-β-D-xylopyranosyl-L-serine **4** could be galactosylated using an embryotic chicken cartilage enzyme system (Figure 5).[25] A few years later, it was established that xylosides with β linkage to the aglycon, such as *p*-nitrophenyl and 4-methylumbelliferyl β-D-xylopyranoside **5** and **1**, could act as exogenous substrates, presumably for galactosyltransferase I, and initiate CS GAG synthesis independently

of the core protein.[27, 35-38] It was observed that the nature of the aglycon affected the extent of GAG synthesis, where hydrophobic aglycons proved to generate the most efficient substrates. Esko and co-workers later reported that β-D-xylopyranosides bearing hydrophobic, aromatic aglycons, such as 2-naphthyl and 3-estradiol β-D-xylopyranoside **6** and **7**, also primed HS GAG chains in addition to CS/DS chains.[39-40]

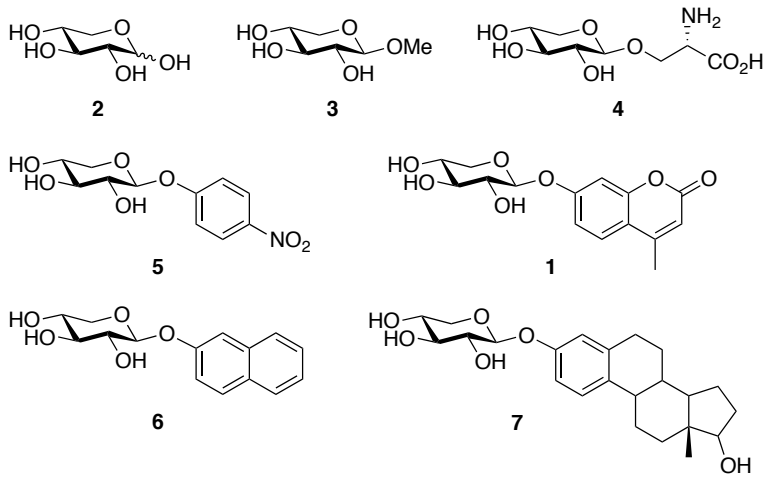

Figure 5. D-Xylose and β-D-xylopyranosides as primers of GAG synthesis.

1.4.1 Xyloside analogs with modifications of the xylose moiety

In 1996, Lugemwa et al. studied benzyl β-D-xylopyranoside analogs, where the hydroxyl groups were epimerized, deoxygenated, or alkylated.[41] In addition, 3-fluoro and 3-amino derivatives, as well as a 4-keto analog and a derivative with an axial methyl group in position 4 were examined. Their GAG priming ability was investigated and only compounds **8-12** were active (Figure 6). The authors suggested that 2-OH and 3-OH can function as hydrogen atom acceptors while 4-OH functions as a hydrogen bond donor, and that the enzyme tolerates axial substituents at C4.

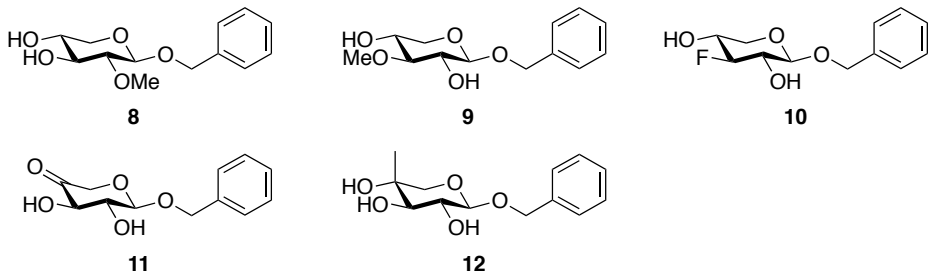

Figure 6. Xyloside analogs that function as primers of GAG synthesis.

In order to determine the function of the C2 phosphorylation of the xylose moiety found in both CS/DS and HS GAG chains, Gulberti et al. examined C2 phosphorylated xyloside **13** and its unphosphorylated analog **14** as substrate for β4GalT7 (Figure 7).[31] It was shown that **13** is not a substrate for β4GalT7, in contrast to **14**, suggesting that phosphorylation prevents recognition and/or transfer of Gal onto the xylose moiety and that it might be involved in the regulatory mechanism of PG biosynthesis. This is in agreement with previous investigations,[42] where phosphorylation is observed once Xyl has been galactosylated. Further studies have identified the kinase responsible for the phosphorylation of the xylose moiety, namely Fam20B.[43] It was shown that this enzyme required a minimal Gal-Xyl disaccharide motif for activity and loss of phosphorylation resulted in premature termination of the linker tetrasaccharide synthesis. In addition, β3GalT6, was much more active when phosphorylated Gal-Xyl-Bn was used as substrate, compared to when the corresponding unphosphorylated analog was used.

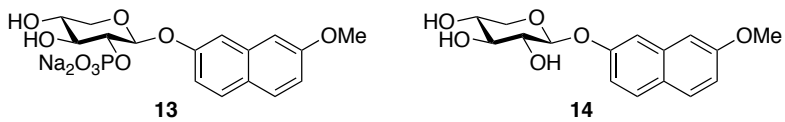

Figure 7. Phosphorylated xyloside **13** and its unphosphorylated analog **14**.

In 2008, Kuberan and co-workers synthesized 4-deoxy-4-fluoroxylosides with various aglycons attached via a triazole linkage and investigated their ability to affect the biosynthesis of GAG chains.[44] Due to the lack of a hydroxyl group in position 4, these xylosides, especially **15** and **16** (Figure 8), could act as inhibitors of PG biosynthesis. The hydrophobicity of the aglycon was determined to be crucial for strong inhibition. In 2010, an additional 6 compounds showed inhibition of PG biosynthesis, where the 4-nitrophenol derivatives **17** and **18** were the most potent ones.[45] **17** and **18** were also showed to inhibit tumor-associated angiogenesis, which is likely to be correlated to the strong inhibition of HS PG biosynthesis.[46]

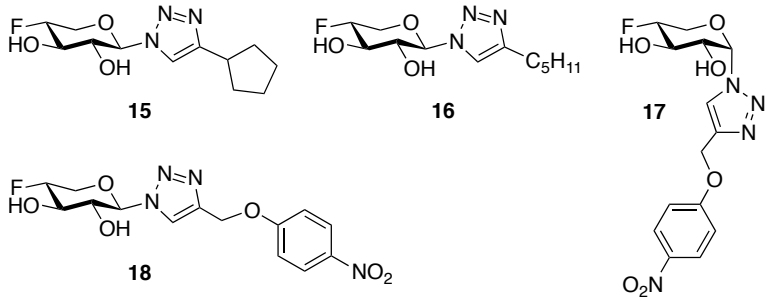

Figure 8. 4-Deoxy-4-fluoroxylosides that act as inhibitors of GAG biosynthesis.

Siegbahn et al. synthesized 2-naphthyl β-D-xylopyranoside analogs where the hydroxyl groups of the xylose residue were epimerized, deoxygenated, methylated, or replaced by a fluorine atom.[47] In this study, the authors concluded that all modifications rendered inactive compounds regarding GAG priming and the 4-deoxy and 4-deoxy-4-fluoro analogs **19** and **20** showed weak inhibition of endogenous GAG synthesis (Figure 9).

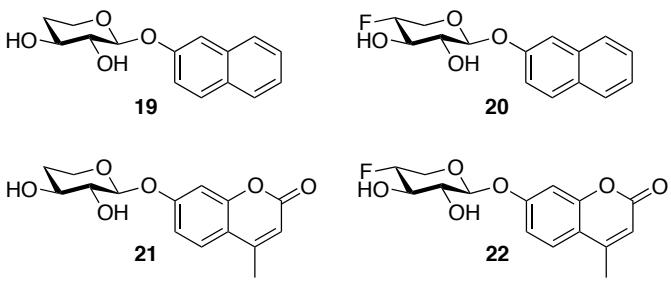

Figure 9. Xyloside analogs modified at position 4 that possess inhibitory activity of GAG synthesis.

Four years later, Fournel-Gigleux and co-workers evaluated xyloside analogs **19**, **21**, and **22** (Figure 9) as inhibitors of β4GalT7 using an enzyme assay and cell studies.[24] These investigations showed that **22** was the most potent derivative with 60% inhibition in the β4GalT7 assay with an IC_{50} value of 0.06 mM. The authors suggested that the possible interaction of His^{195} with the carbonyl group in the umbelliferyl aglycon might offer an explanation to the stronger inhibitory activity of **21** and especially **22**, compared to naphthyl analog **19**. Kuberan and co-workers showed that 4-fluoro compounds containing a *p*-nitrophenol group (**17** and **18**) were potent inhibitors.[45] The authors speculate that a hydrogen bond between the His^{195} backbone and the nitro group might be responsible for this effect.[24] Later, **17** proved to possess anti-fibrotic properties due to its inhibitory activity of β4GalT7.[48]

Synthesis of both CS/DS and HS PGs were inhibited in primary lung fibroblasts and **17** showed antiproliferative activity towards fibroblasts.

1.4.2 Xyloside analogs with modifications of the endocyclic oxygen atom

5-Thioglycosides, i.e. carbohydrate analogs where the endocyclic oxygen atom has been replaced by a sulfur atom, were first synthesized in the 1960's, where 5-thio-D-xylopyranose and methyl 5-thio-α-D-xylopyranoside were two of the first compounds reported.[49-53] More recently, 5-thioxylosides have been synthesized and investigated in terms of antithrombotic activity. The glycosaminoglycan heparin is a well known antithrombotic and anticoagulant. It is known that GAG chains possess antithrombotic activity,[54] and that β-D-xylopyranosides are good antithrombotic agents where the β-D-xylopyranose moiety is the pharmacophore responsible for this activity, being necessary for priming of these GAG chains.[55-56]

In order to design metabolically robust substances, especially concerning glycosidic bond cleavage, 5-thioxylopyranosides were investigated of which **23-26** (Figure 10), known as Naroparcil, Beciparcil, Iliparcil, and Odiparcil, proved to be efficient antithrombotics.[56-59] In addition, it was shown that these compounds are substrates for β4GalT7, and a trend in galactosylation was observed: β-D-xylosides < 1-thio-β-D-xylosides < 5-thio-β-D-xylosides < 1,5-dithio-β-D-xylosides.[56] The results were corroborated with a cell study where GAG synthesis was initiated by the xyloside analogs, and the GAG chains possessed antithrombotic activity.

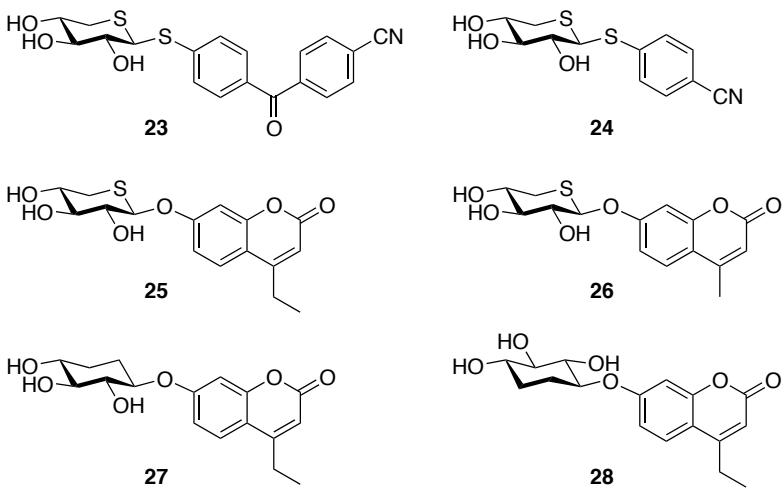

Figure 10. 5-Thioxylosides **23-26** and 5a-carba-xylosides **27** and **28** that possess antithrombotic activity.

Carbasugars, where a methylene group has replaced the endocyclic oxygen atom, are interesting compounds due to their similarity to true carbohydrates. It is possible for carbasugars to be recognized by enzymes and carbasugars are potentially more metabolically stable.[60] 5a-Carba-xylosides,[†] which are derivatives of dihydroconduritol B or F, can be found as part of larger structures. Simple carbaxylosides have, on the other hand, not been studied to any great extent. 5a-Carba-xyosides have, as for the thioxylosides, been investigated as antithrombotic agents in order to gain increased bioavailability compared to xylosides, however, not as extensively. The carbaxyloside analog of Iliparcil has been synthesized, as well as its L-xylo-enantiomer (**27** and **28**, Figure 10).[61-62] Interestingly, the authors reported that **28** showed much higher antithrombotic activity than **27** and only **28** was reported as a substrate for β4GalT7. In general, L-xylosides are not active towards β4GalT7.[62-64]

1.4.3 Xylosides with modifications at the anomeric position

Xylosides with α-linkage to the aglycon, i.e. methyl, phenyl, benzyl, and *p*-nitrophenyl α-D-xylosides, were investigated as primers of GAG synthesis in early studies, and concluded not to be active.[27, 36-38, 65] In 1990, Kolset et al. showed that phenyl α-D-xylopyranoside had a small stimulative effect on GAG synthesis.[66] Remarkably, in 1993, Freeze et al. reported an inhibitory effect on glycolipid synthesis in human melanoma cells of both α and β *p*-nitrophenyl D-xylopyranoside.[67] The authors suggested that both anomers became galactosylated.

Kuberan and co-workers have shown that a triazole linkage between the xylose moiety and the aglycon allows both α and β anomers (Figure 8) to function as primers and inhibitors of GAG synthesis.[45, 68] However, for priming, the β anomers are more efficient compared to the corresponding α anomers.

The oxygen atom in the glycosidic linkage has been exchanged for sulfur, carbon, and nitrogen to investigate the effect on the synthesis of GAG chains. In 1975, Robinson et al. investigated phenyl β-D-thioxylopyranoside **30** (Figure 11), amongst others, and showed that it had similar activity as a GAG primer as the corresponding xyloside **29**, suggesting that β4GalT7 does not distinguish between oxygen and sulfur in the anomeric position.[27] The GAG priming property of thioxylosides has later been corroborated in several studies.[38, 40, 66, 69-70] Kolset et al. showed that hexyl thioxyloside **33** initiated CS GAG synthesis, and that **33** possessed antiproliferative activity.[66]

[†] 5a indicates that the structure is an aldopyranose.

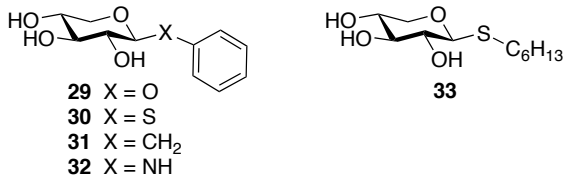

Figure 11. Xyloside derivatives with variation in the exocyclic position.

Sobue et al. examined derivatives of phenyl β-D-xylopyranoside where S, CH_2, and NH replaced the exocyclic oxygen atom (**29**-**32**, Figure 11).[69] This study clearly showed that the *C*-xyloside **31** was less effective as a GAG synthesis initiator compared to **29** and **30**, and *N*-xyloside **32** was even less efficient. The low activity of *C*-xylosides has also been reported by Kolset et al.,[66] Malmberg et al.,[63] and Pineau et al.[71]. Sartorelli and co-workers have synthesized and tested a range of xylosides with an *N*-linked phenyl with various substituents, and a few of these xylosides induced GAG priming and antiproliferative effects.[72] Kuberan and co-workers have shown that triazole-linked xylosides can act as GAG primers,[68, 73-76] and a few derivatives are reported to inhibit invasion of a highly invasive glioma cell line.[77]

1.4.4 Xylosides with variations of the aglycon

The aglycon has an important role in the GAG priming ability of xylosides, which was concluded early on, as mentioned above. Fritz el al. have investigated the amount of HS GAG synthesized by various xylosides with different aglycons.[40] It was concluded that the concentration of the xyloside affected the type of GAG chains synthesized and that making the compounds more hydrophobic by introducing a 4-carbon spacer between the xylose moiety and the aromatic aglycon as in **35** or using it as a tail as in **37** reduced the amount of HS but not the total amount of GAG synthesized (Figure 12). A 2-carbon spacer, as in **34** and **36**, did not have any affect compared to the parent xyloside **6**. It was also concluded that the introduction of a heteroatom in the aromatic system decreased the amount of HS formed and increased steric bulk of the aglycon, as in biphenyl and phenanthryl xylosides **38** and **39**, had little or no effect compared to **6**. The authors suggested that the hydrophobicity and particular structure of the aglycon affect the amount of GAG chains synthesized, as well as their composition.

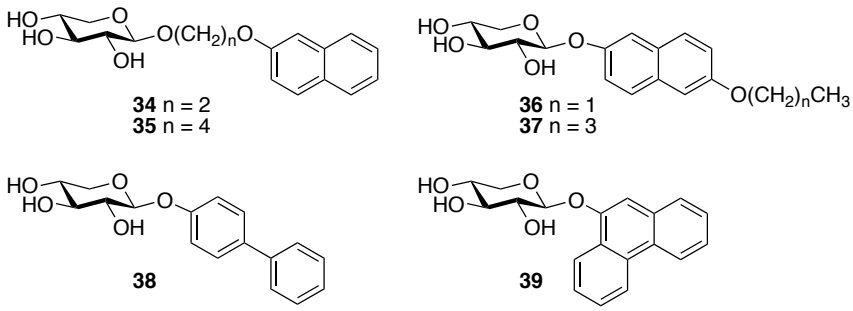

Figure 12. Xylosides that all prime HS GAGs to different extent in addition to CS/DS chains.

In 1998, Mani et al. reported that introducing a hydroxyl group in the naphthyl moiety, i.e. **40** (Figure 13), resulted in inhibition of growth of transformed cells.[64] This was not the case for **6** or its thio-analog, or *p*-nitrophenyl xyloside **5**. The authors postulated that the priming of HS chains may be responsible for the inhibitory effect on cell growth, and that a free hydroxyl group in the aglycon was necessary for the antiproliferative effect to be obtained.[64, 78] In a number of consecutive studies, the selective antiproliferative effect was investigated. Regioisomers where the naphthyl moiety is hydroxylated at other positions, thio-analogs, bis-xylosylated derivatives where both naphthyl hydroxyl groups have been xylosylated, as well as acetylated analogs of the mono- and bis-xylosides have been examined.[70, 79-81] No correlation between hydrophobicity and GAG priming or antiproliferative effect could be observed, and the effect of the xylosides was diverse in different cell lines. In 2010, Nilsson et al. showed that GAG chains primed on **40** in cancer cells were toxic, whereas GAG chains primed in normal cells were inactive as well as the GAG chains primed on **6** in both cell lines.[82] In addition, treatment with **40** selectively lowered levels of histone H3 acetylation in cancer cells. In 2016, Persson et al. carefully examined the GAG chain structure primed on **40** and **6**, and showed that CS/DS GAGs primed on both xylosides in a breast carcinoma cell line were cytotoxic.[83] This effect was inhibited by HS chains primed of **6**. The GAG chains had different disaccharide composition depending on the cell line, which again displays the effect of small variations of the aglycon structure on their activity as well as the effect observed in different cell lines.

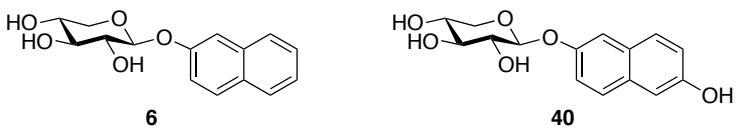

Figure 13. Xyloside **6** and antiproliferative xyloside **40**.

Kuberan and co-workers have synthesized a large library of triazole-linked xylosides with various aglycons.[68, 73] Most of the tested xylosides acted as GAG primers in a concentration-dependent manner. The effect of substituents on a connected phenyl ring showed that the position of the substituent is important, but not its electronic property. Including a spacer between the triazole and aromatic moiety to gain flexibility was investigated in terms of GAG priming as well as the effect of hydrophobicity of different aglycons. Taken all the results together, the authors speculated that the aglycon might aid in the selective transport of xylosides to different Golgi compartments that possess different combinations of enzymes involved in the biosynthesis GAG chains. This can explain the differences in GAG type, disaccharide composition, sulfation pattern, and chain length observed in these studies.

In an effort to form fluorescent xylosides, Tran et al. synthesized xylosides with triazole-linked fluorophores (**41**-**45**, Figure 14).[76] Dansyl derivative **41** and fluorescein derivative **42** did not induce GAG priming, which was suggested to be due to the amine in **41** and carboxylic acid in **42** that might be charged and thus hindering the xylosides from transport across the cell membranes. Xylosides bearing carboxylic acid functionality have been shown to be poor GAG primers.[38, 69, 72, 84] However, Johnsson et al. investigated dansyl xyloside **46** and (9-antracenyl)methyl xyloside **47** and showed that both derivatives entered cells but did not induce GAG synthesis.[85-86] The authors speculated that this might be due to the size of the aglycon and/or the hydrophobicity of the xylosides. On the other hand, pyrene xyloside **43** and umbelliferyl xylosides **44** and **45** proved to initiate GAG synthesis.[76] Unfortunately, **43** could not to be detected by fluorescence measurements. Examining the GAG chains synthesized by **44** and **45** showed that longer chains and a higher degree of HS were obtained compared to well-known 4-methylumbelliferyl xyloside **1**. The effects of these xylosides differed in different cell lines.

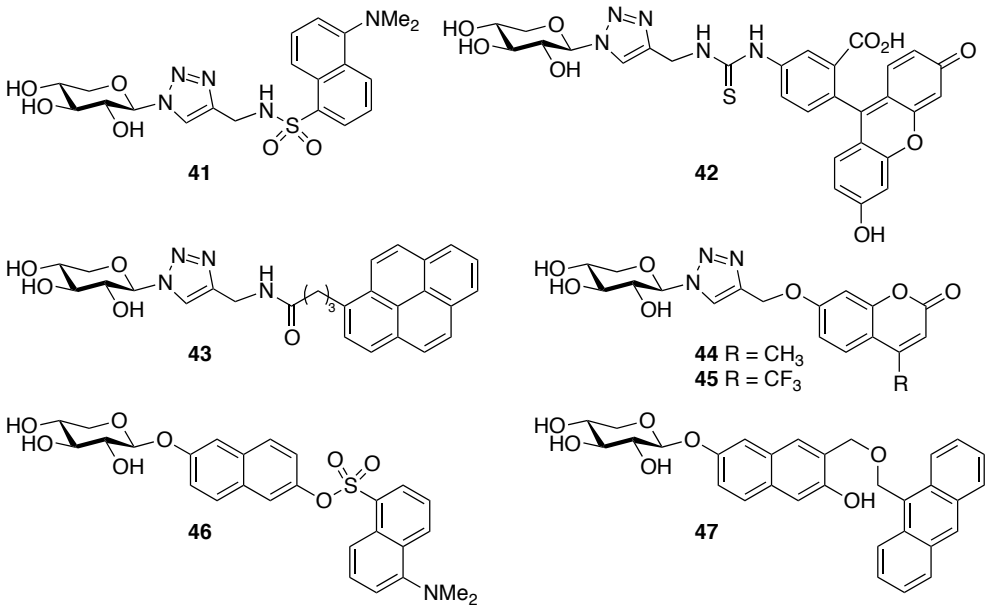

Figure 14. Xyloside analogs linked to fluorophores.

In 2011, Garcia-Garcia et al. used xylosides with a 3-carbon amide linker and showed that the xylopyranosyl-serine **48** was efficiently galactosylated by β4GalT7 (Figure 15).[34] Some of the xylosides, e.g. **48**-**50**, possessed cytotoxic activity towards a lung carcinoma cell line.

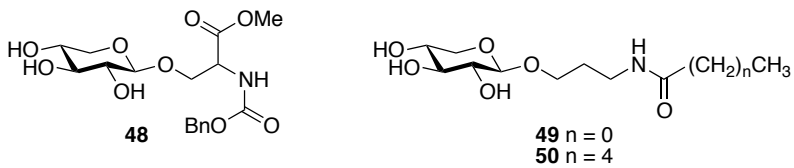

Figure 15. Xylosides with amide aglycon.

Xylobiosides have been examined by Chatron-Colliet et al. and reported to be less active as GAG primers compared to the corresponding xylosides (Figure 16).[87] This was investigated by treating cells with propargyl derivatives that were later clicked with an azide-containing fluorescent probe. The xyloside was taken up to a much higher extent than the xylobioside. In addition, a β4GalT7 enzyme assay indicated that the xylobioside **51** was a less efficient substrate for β4GalT7 than the xyloside **52**.

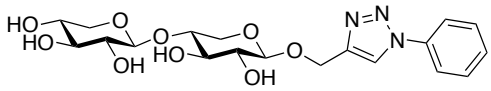

51

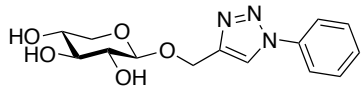

52

Figure 16. Xylobioside **51** and xyloside **52**.

1.5 Enzyme kinetics

Enzymes catalyze a reaction by stabilizing the transition state by specific interactions in the active site, which provides a three-dimensional unique microenvironment. Hence, enzymes have great catalytic power and they work in a highly specific manner, catalyzing a specific reaction with a specific substrate. Enzymes cannot alter the equilibrium of a reaction, just the rate. The fact that a maximum velocity of an enzyme-catalyzed reaction is observed, indicate that a substrate-enzyme complex, ES, is formed at a certain concentration, at which all active sites are saturated. In 1913, Leonor Michealis and Maud Menten proposed a model for enzyme kinetics (Equation 1).

$$E + S \underset{k_{-1}}{\overset{k_1}{\rightleftharpoons}} ES \xrightarrow{k_2} E + P \qquad (1)$$

To simplify the rate equation, a steady-state assumption is applied, meaning that the concentration of ES is constant even though the concentrations of the substrate and product are changing, which occurs when the rates of formation and break down are equal. It is also assumed that the enzyme is present in much lower concentration than the substrate, hence the total concentration of substrate, i.e. free substrate and substrate combined with the enzyme, equals the concentration of free substrate. This gives the equation for the velocity, also known as the Michaelis-Menten equation (Equation 2).

$$V = V_{max} \frac{[S]}{[S] + K_m} \qquad (2)$$

K_m is the Michaelis constant defined as $(k_{-1} + k_2)/k_1$. However, since a series of steps may follow ES formation k_2 is usually exchanged for k_{cat} (Equation 3).

$$K_m = \frac{k_{-1} + k_{cat}}{k_1} \quad (3)$$

When the substrate concentration equals K_m, $V = V_{max}/2$, thus K_m is the concentration where half the active sites are occupied. When the substrate concentration is much less than K_m, the reaction is first order with the rate directly proportional to the substrate concentration. On the other hand, when the substrate concentration is much higher than K_m, the rate of reaction equals the maximum velocity V_{max}. The Michaelis-Menten equation accounts for the kinetics illustrated in Figure 17a.

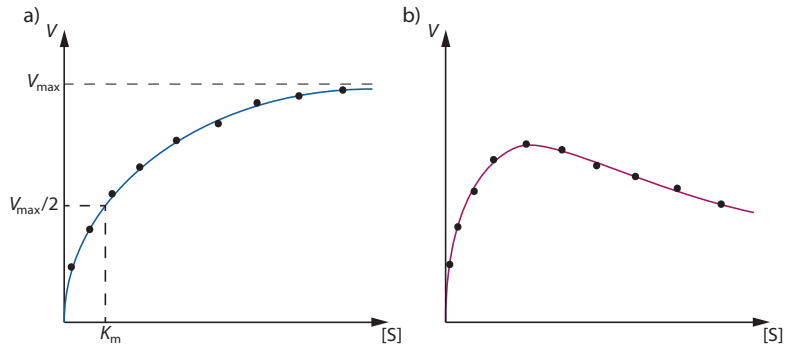

Figure 17. a) A plot of reaction velocity V as a function of substrate concentration [S]. The Michaelis-Menten equation is fitted to the measured data points. b) A plot of reaction velocity V as a function of substrate concentration [S] when substrate inhibition is observed.

K_m for an enzyme depends on the substrate and the conditions, such as pH, temperature, and ionic strength of the solution. K_m indicates the concentration of substrate that is required for significant catalysis to occur, and K_m values are generally between 10^{-1} and 10^{-7} M. V_{max} is the maximum velocity and indicates the turnover number of an enzyme, k_{cat}, i.e. the number of substrates converted into product by an enzyme molecule in a unit time when the enzyme is fully occupied with substrate. The value k_{cat}/K_m is a measure of the catalytic efficiency of an enzyme, since this accounts for both the rate of catalysis with a specific substrate (k_{cat}) as well as the strength of the enzyme-substrate interaction (K_m). Hence, this is a useful value when comparing the preference for different substrates by an enzyme.

Enzymes may be inhibited either irreversibly or reversibly, which in turn can be competitive, uncompetitive, or noncompetitive in its inhibitory action. Inhibition is a naturally regulatory mechanism for many enzymes. Competitive inhibitors often resembles the substrate and binds to the same site as the substrate but it does not form the product, instead it hinders the substrate from forming the enzyme-substrate complex. This slows down the enzyme-catalyzed reaction, i.e. lowers K_m, but V_{max}

may still be obtained, but at higher concentration of substrate than in the absence of inhibitor. Uncompetitive inhibitors bind to the enzyme when the enzyme-substrate complex has been formed, which hinders product formation. This type of inhibition lowers both V_{max} and K_m. Noncompetitive inhibitors binds to a different site than the substrate, and lowers the turnover number, leading to a lowering of V_{max}. Another type of inhibition is substrate inhibition where the velocity of the reaction starts to decrease at a certain substrate concentration (Figure 17b).[88-89] Substrate inhibition has been seen for many enzymes, including β4GalT7,[34] and different mechanisms of this regulatory inhibition have been proposed, and it is likely that the inhibitory mechanism is diverse amongst the enzymes showing this type of kinetics.

1.6 Histone acetyltransferases

Histone acetyltransferases (HATs) play a major role in the regulation of gene expression by catalyzing the transfer of an acetyl group from acetyl-CoA to the ε-amino group of lysine side-chains of histone proteins. This acetylation neutralizes the positively charged amino acid, and thus reduces the interaction between the histone protein core and DNA, generating a more extended structure, which promotes transcription.[90-92] The acetyl group is removed by histone deacetylases (HDACs), leading to transcriptional repression. HATs and HDACs exist and act in multisubunit complexes, which influence their substrate specificity and acetylation preference. In addition, HATs and HDACs also acetylates/deacetylates non-histone proteins such as transcriptional factors, nuclear import-factors, and structural proteins.[93]

Dysfunction of HATs and HDACs, leading to an aberration in the acetylation balance, is often found in cancer cells. Increased HDAC activity, caused by over-expression or malfunction, has been associated with many cancer types.[94-96] HATs have been found to act as suppressors as well as oncogenes in cancer, depending on cancer type and specific genetic alterations.[95, 97]

The antitumor effects of HAT inhibitors have been less studied in comparison to HDAC inhibitors.[94, 98] Bisubstrate analogs, consisting of acetyl-CoA connected to a lysine-containing peptide,[99] have been reported as inhibitors as well as synthetic compounds such as isothiazolones connected to a substituted aromatic system[100] or substituted quinolines.[101-102] Among the natural products with HAT inhibitory activity, anacardic acid **53**,[103] garcinol **54**,[104] and curcumin **55**[105] have proven to be the most important (Figure 18).[95] Curcumin, which is the most studied HAT inhibitor among natural compounds, has been evaluated in clinical trials for the therapy of several cancers, as well as of Alzheimer's disease, inflammatory bowel disease, diabetes, and arthritis among others.[106] Unfortunately, poor bioavailability, due to low absorption and rapid metabolism, limits its therapeutic value. Analogs of

the natural HAT inhibitors have been synthesized, where e.g. the free aromatic hydroxyl groups have been alkylated, largely affecting their HAT inhibitory activity and HAT enzyme selectivity.[98, 107-109]

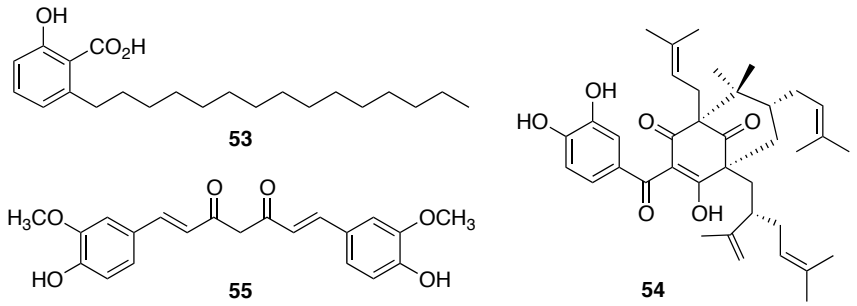

Figure 18. The natural products anacardic acid **53**, garcinol **54**, and curcumin **55**, which all inhibit histone acetyltransferases (HATs).

GAG chains and PGs have also been reported to inhibit HATs, and the inhibition was dependent upon the length of the chain as well as the sulfation pattern.[110] The authors suggested that the HAT inhibition properties of certain GAG chains are dependent on the ability of the GAGs to access the nucleus to interact with HAT, rather on a specific GAG sequence. Furthermore, the role of HS PG in cancer has been studied by examining heparanase, an enzyme that cleaves HS chains of PGs.[111] It was shown that high expression of heparanase, leading to decreased levels of HS PG in the nucleus, generated an increase in HAT activity, which correlates with an aggressive tumor phenotype.

2 Objectives

Although some aspects are known regarding the biosynthesis and xyloside-induced synthesis of GAG chains, many questions still remain regarding, e.g. the formation of specific GAG structures and how these structural features affects specific biological properties. In order to investigate these mechanistic issues, tools such as efficient primers and inhibitors of GAG synthesis would be highly useful. Such tools would also be valuable for method development in e.g. structural investigation of GAG chains. In addition, biological applications of primers and inhibitors could potentially be found useful for treatment of diseases where the synthesis and/or degradation of GAGs are malfunctioning.

In order to design and synthesize efficient substrates and efficient inhibitors of GAG synthesis, we set out to investigate xylosides and xyloside analogs in a β4GalT7 enzyme assay. We aimed towards finding structural features that would generate active compounds, which we envisioned to obtain by performing synthetic modifications of the xylose moiety, the endocyclic and exocyclic positions, and the aglycon (Figure 19). The overall aim of the thesis is to pinpoint the structural requirements of efficient substrates and efficient inhibitors.

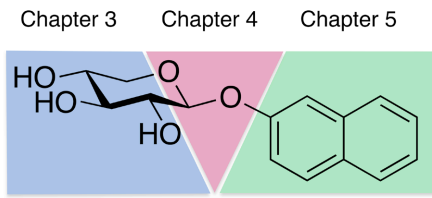

Figure 19. Site of modifications of xylosides, and the chapter in which these results will be presented.

3 Modifications of the xylose moiety

3.1 Monosubstituted xylopyranoside analogs (Paper II)

Intrigued by the prior results of modifications of the xylose moiety (section 1.4.1), we decided to develop an enzyme assay with β4GalT7 to examine the active site in order to define the requirements for efficient galactosylation as well as the terms of inhibition of β4GalT7. We wanted to primarily use an enzyme assay, since this gives direct answers on the enzyme's preference for a certain substrate through kinetic parameters. Cell studies can, of course, also provide useful information. However, in addition to the substrate affinity of the enzyme, parameters such as cell permeability, transport to the correct compartment(s) within the cell, cell type, and cell line affects the results.

Specifically, we aimed towards defining the steric restrictions of the active site of β4GalT7. Hence, we synthesized the methylated analogs **56**-**63** (Figure 20). The previously synthesized xyloside analogs to **6**, where the hydroxyl groups have been epimerized or exchanged for a methoxy group, fluorine atom, or a hydrogen atom,[47] were also included in our investigation of β4GalT7 (Figure 20). The possible effects of these modifications are summarized in Figure 21. We hypothesized that the active site of β4GalT7 contains a precise set of hydrogen bond acceptors and that few modifications are tolerated with retained galactosylation activity. Furthermore, we hypothesized that it is possible to synthesize analogs that act as efficient inhibitors of β4GalT7.

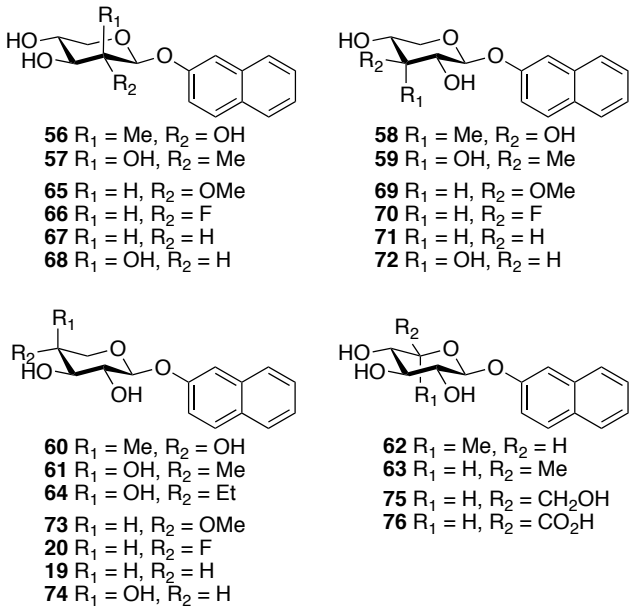

Figure 20. Synthesized methylated analogs **56**-**63** of 2-naphthyl β-D-xylopyranoside **6** as well as the examined monosubstituted analogs.

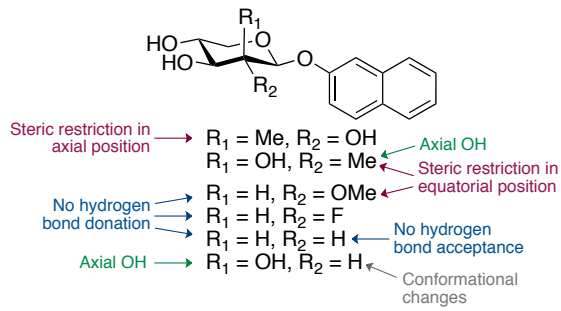

Figure 21. Effect of modifications, exemplified at C2.

3.1.1 Synthesis of methylated analogs

The synthesis of the methylated analogs **56**-**61** started from xyloside **6**, which was benzylated under phase transfer conditions to yield dibenzylated derivatives as previously published.[47] The free hydroxyl group at position 2, 3, and 4, respectively, was then subjected to oxidation using Dess-Martin periodinane (DMP) followed by Grignard addition to install the methyl group (Scheme 2). Hydrogenolysis[112] of the benzyl protective groups furnished the methylated analogs **56**-**61** (Figure 20). It was

of great importance that the oxidation reaction consumed all of the starting material and that the products from the Grignard reaction were carefully purified. Otherwise traces of **6** may contaminate the target methylated analogs, giving rise to a false response in the biological evaluations. This was initially observed with a few of our non-priming derivatives where a low amount of **6** was sufficient to induce GAG priming.

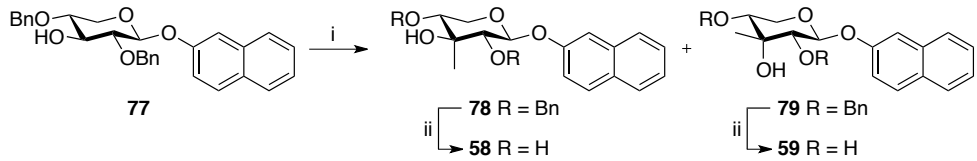

Scheme 2. Synthesis of methylated xyloside analogs, exemplified for position 3. Reagents and conditions: i) 1) DMP, CH_2Cl_2; 2) MeMgBr, Et_2O, **78** (19%), **79** (68%); ii) Pd/C, H_2, HCl, DMF, **58** (76%), **59** (49%).

The methylated derivatives **62** and **63** were synthesized from commercially available peracetylated 6-deoxy-α-L-idopyranose **80** and 2-naphthyl β-D-glucopyranoside **82**, respectively (Scheme 3). **75** and **76** are commercially available.

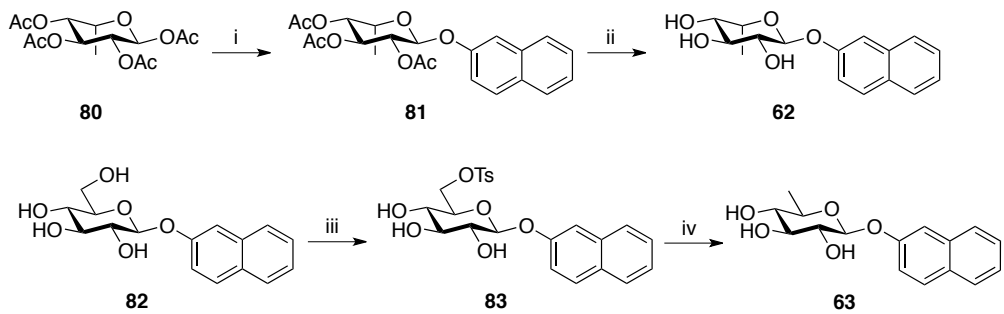

Scheme 3. Synthesis of 5-methylated xyloside analogs. Reagents and conditions: i) $BF_3{\cdot}Et_2O$, Et_3N, 2-naphthol, CH_2Cl_2, 0 °C, 78%; ii) 1 M NaOMe, MeOH, 81%; iii) TsCl, $ZnBr_2$, Py, -25 °C, 86%; iv) $LiAlH_4$, THF, 30 °C, 61%.

As a control, we wanted to include 4-deoxy-4-methyl xyloside **86**, i.e. a methylated analog lacking the hydroxyl group at position 4, in our investigation. Hence, **6** was protected at positions 2 and 3 by an isopropylidene acetal (Scheme 4). **84** was then subjected to a Swern oxidation-Wittig reaction sequence followed by hydrogenation, which produced **86** in trace amounts. Instead, the diastereomer **87**, with the methyl group in an axial position, was formed as the major product. Similar attempts at position 2 also generated the methyl group in an axial orientation,[113] and no further efforts were made to synthesize **86**. The isopropylidene protected **84** was instead

found useful in the synthesis of the ethyl analog **64** (Figure 20), where EtMgBr was used in a Grignard reaction after the above-mentioned Swern oxidation.

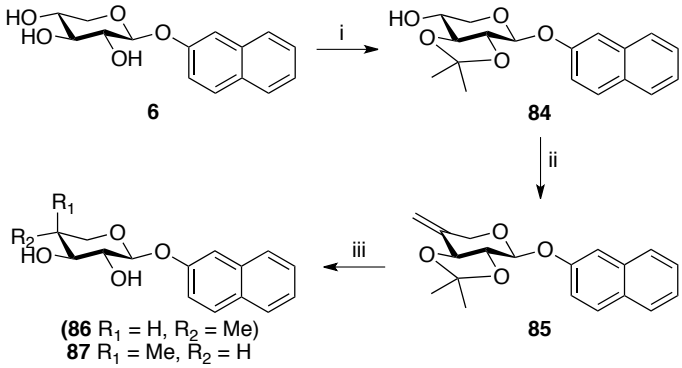

Scheme 4. Reagents and conditions: i) 2-methoxypropene, CSA, DMF, (51%); ii) 1) $(COCl)_2$, DMSO, CH_2Cl_2, -78 °C; 2) Ph_3PCH_2Br, *n*-BuLi, THF, -78 °C → rt, (74%); iii) Pd/C, H_2, HCl, DMF, **87** (47%).

3.1.2 β4GalT7 assay

The β4GalT7 assay was set up in such a manner that the kinetics would follow Michaelis-Menten kinetics (Section 1.5), i.e. initial velocities were measured. Hence, the reaction was quenched after 30 minutes, since approximately less than 10% of the substrate was converted into product at this time. Also, the reaction should show first-order dependence of enzyme concentration. A fixed amount of DMSO was added due to solubility problems of the substrates. The concentration of DMSO had to be the same in all experiments, since the activity of β4GalT7 decreased with increasing amounts of DMSO. The backward reaction must be negligible for the applicability of Michaelis-Menten kinetics. Galactosylated **6** was added to β4GalT7, which showed no reaction. No significant difference in fluorescence between monosaccharide and produced disaccharide could be observed. Hence, the production of galactosylated substrate was determined using reverse-phase HPLC with fluorescence detection, and the formed products were identified by LC-HRMS.

The methylated analogs **56-63** (Figure 20) were investigated in our β4GalT7 assay together with previously published monosubstituted xyloside analogs by Siegbahn et al[47]. Both galactosylation by, and inhibition of, β4GalT7 were examined. Xyloside **6** was chosen as a reference compound when analyzing the data obtained from examinations of the modified analogs, since it is a well-known primer of GAG chains in several different cell types.[40, 64, 78]

3.1.2.1 Galactosylation

In regard to galactosylation, the modified analogs were either not active or significantly less active than **6** (blue bars, Figure 22). The enzyme activity was too low for Michaelis-Menten kinetic parameters to be calculated, hence, the activity is given as percentage of galactosylation observed for **6** at a certain concentration (1.5 mM). These results were corroborated with a cell study where none of the methylated analogs **56**-**63** induced GAG priming to any significant extent. The analogs **19**, **20**, and **65**-**74** have previously been shown not to act as primers of GAG synthesis.[47]

In terms of the size of the binding pocket, our investigation indicate that it is quite narrow since all methylated analogs, except **56** and **62**, as well as the methoxy derivatives were inactive. The analogs with modified hydrogen bonding properties, i.e. the methoxy and fluoro analogs, suggests that hydrogen bond donation is crucial for galactosylation activity since all compounds except for the 2-fluoro analog **66** were inactive. The deoxygenated and epimerized analogs, with exception for **67**, did not generate galactosylated products, which emphasizes the importance of hydrogen bond donors in all three equatorial positions of the xylose moiety. Interestingly, 2-deoxy analog **67** generated two galactosylated products (two blue bars in Figure 22), which was interpreted as galactosylation at either 3-OH or 4-OH. As seen for the C5 analogs, generally no modifications were tolerated. However, since compound **67** lacks substituents in C2 and C5, it is pseudo-symmetric and may fit in the active site in two orientations so that either 3-OH or 4-OH get in position for galactosylation.

These results, together with conformational analysis by NMR studies and molecular docking simulations (with *Drosophila* β4GalT7 mutant D211N), led us to propose a binding pattern of **6** in the active site of β4GalT7 (Figure 23), where 2-OH is hydrogen bonding to Asp^{212} and 3-OH and 4-OH are hydrogen bonding to Asp^{211}. All hydroxyl groups are hydrogen bond donors, and C5 is suggested to have a hydrophobic interaction with Tyr^{177}. The hydrogen bond donation from 4-OH makes this hydroxyl group nucleophilic and it is in close proximity to C1 of UDP-Gal, which makes an S_N2 mechanism plausible. Hence, removing 4-OH renders inactive compounds in terms of galactosylation.

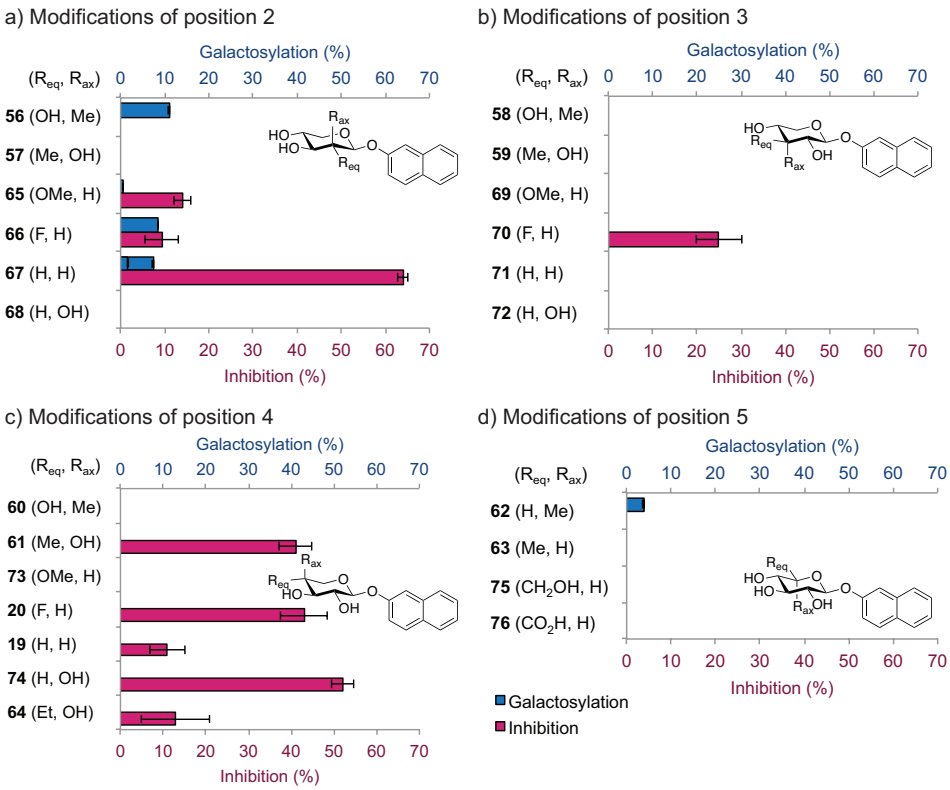

Figure 22. Galactosylation and inhibition of β4GalT7. Blue bars represents galactosylation, and is given as percentage of the effect shown by **6** (at 1.5 mM). Purple bars represents inhibition of galactosylation of **6** by β4GalT7, and is given as percentage of control without the addition of xyloside analog (0.5 mM of **6** and 2.0 mM of xyloside analog).

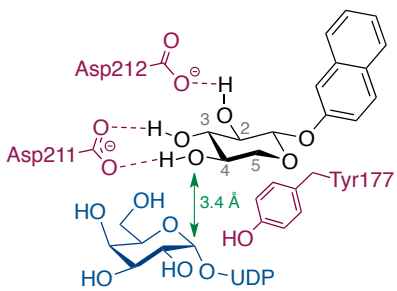

Figure 23. Proposed binding pattern of xyloside **6** and UDP-Gal in the active site of β4GalT7 (*Drosophila* β4GalT7 mutant D211N).

3.1.2.2 Inhibition

Next, we examined the inhibitory activity of the monosubstituted analogs, by treating β4GalT7 with both xyloside **6** (0.5 mM) and xyloside analog **19**, **20**, **56-76** (2.0 mM), where the formation of galactosylated **6** was analyzed (purple bars, Figure 22). As for galactosylation, almost all modifications at position 3 rendered inactive compounds. For position 2, the deoxygenated analog **67** strongly inhibited β4GalT7 activity. Almost all of the analogs modified at position 4 generated inhibitors, where the equatorially methylated **61**, the 4-deoxy-4-fluoro analog **20**, and the epimerized analog **74** proved to be strong inhibitors. To verify that the inhibition seen in the β4GalT7 assay was transferable to in vitro studies, analogs **61** and **20** were investigated in a cell study, where a decrease in GAG priming of **6** was observed (50% for **61**, and 25% for **20**).

The strong inhibition observed by **67** was somewhat surprising, and it may originate from the suggested possibility of adopting two different orientations in the binding pocket of β4GalT7. On the other hand, it is not unexpected that modifications at position 4 severely affects the β4GalT7 activity since it is at 4-OH that galactosylation takes place in the natural substrate (xylose connected to a core protein). The fact that an equatorial methyl group is tolerated, i.e. giving inhibition, but not an axial one, displays the steric restrictions of the active site. **61** fits in the active site but due to the orientation of 4-OH, no interaction with Asp^{211} is possible. Hence, 4-OH of **61** is not nucleophilic and galactosylation does not occur, and the activity of β4GalT7 is inhibited. A similar reasoning explains the inhibitory activity of the arabino-analog **74**. The fluoro analog **20** also fit in the active site, and a hydrogen bond acceptor seems to be accepted at this position. However, due to the absence of 4-OH no galactosylation can occur.

For inhibition, modifications at position 4 clearly appeared to be the most potent. We propose that equatorial substituents are tolerated and sufficient interactions with the enzyme are obtained when the hydroxyl group is exchanged for a hydrogen bond acceptor.

3.2 Disubstituted xylopyranoside analogs (Paper VI)

To further investigate the active site of β4GalT7, and to find the minimal binding epitope, we wanted to examine doubly deoxygenated xylopyranoside analogs. Based on our previous results (Section 3.1), we hypothesized that 3-OH is crucial for both galactosylation and inhibition of β4GalT7 and that at least one more substituent needs to be present for galactosylation to occur. In addition, we aimed to compare two different synthetic routes to the deoxygenated analogs, i.e. a chiral pool approach and a de novo synthesis.

3.2.1 Synthetic strategy

The synthesis of deoxygenated carbohydrates has drawn considerable interest due to their biological activities, and both chiral pool approaches and de novo syntheses have been employed.[114-116] Monosaccharides possess a high density of functional groups and are structurally diverse. Generally, they are found in their D-configuration, such as D-glucose and D-galactose. De novo synthesis is thus an appealing approach, especially towards unnatural carbohydrates.

The doubly deoxygenated xyloside analogs **(-)-88**-**90**, referred to as oxanes, were synthesized as pure enantiomers using the chiral pool approach starting from **6** (originally obtained from D-xylose) (Figure 24). To obtain the unnatural enantiomers, racemic mixtures of the oxanes were synthesized from the simple starting materials **91**,[117] **92**,[118] and **93**,[119] obtained from achiral sources.

The chiral pool approach rely on deoxygenations using the Barton-McCombie radical deoxygenation reaction,[120] which is frequently used for removal of hydroxyl groups in carbohydrates.[121] The Barton-McCombie reaction is a mild method and generally insensitive towards steric strain, which makes this reaction suitable for carbohydrate chemistry. Most commonly, AIBN is utilized as the radical initiator, in combination with nBu$_3$SnH as the hydrogen atom source. However, the toxic nature of nBu$_3$SnH and organotin residues as well as the difficulty of removing these compounds from reaction mixtures,[122] are disadvantages. Hence, other hydrogen atom sources have been developed, such as silanes,[123] dialkyl phosphites and H_3PO_2,[124] phosphine-boranes,[125] cyclohexadienes,[126] trialkylborane/H_2O,[127] $(Bu_4N)_2S_2O_8$/HCO_2Na,[128] and carbene boranes.[129]

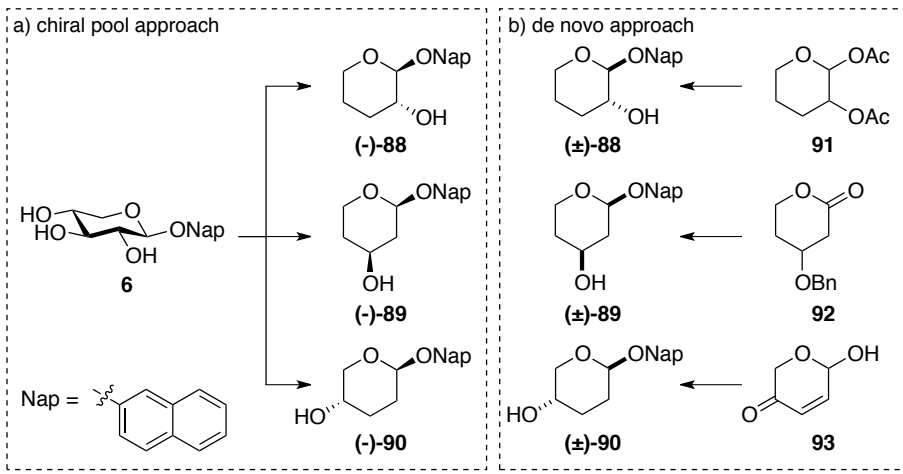

Figure 24. Synthetic strategy of the target oxanes **88**-**90** using either a) a chiral pool approach, or b) a de novo approach.

3.2.2 Synthesis of deoxygenated analogs from xyloside **6**

The synthesis of enantiomerically pure **(-)-88**-**90** was envisioned to start from the known deoxygenated compounds **71** and **19** (Scheme 5), which can be obtained from **6** in three steps each.[47] It would also be possible to form **(-)-89** and **(-)-90** from 2-deoxy analog **67**. Unfortunately, this compound is acid sensitive and therefore not suitable as starting material.

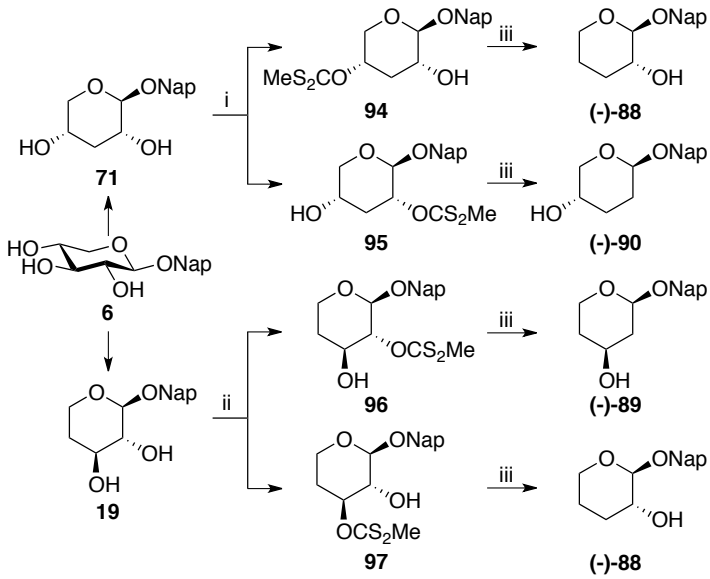

Scheme 5. Synthesis of target oxanes **(-)-88**-**90** using chiral pool approach. Reagents and conditions: i) 1) DBU, CS_2; 2) MeI, DMF, **94** (40%), **95** (47%); ii) 1) NaH; 2) CS_2; 3) MeI, THF, **96** (32%), **97** (16%); iii) 1) H_3PO_2, TEA; 2) AIBN, 1,4-dioxane, reflux, **(-)-88** (82% from **94** or 76% from **97**), **(-)-89** (42%), **(-)-90** (12%). Nap = 2-naphthyl.

Methods for selective monosubstitution with xanthate ester were investigated to avoid the use of protective groups (Table 1 and 2). Generally, methyl xanthate esters are easily formed in high yields by treating an alcohol in THF with NaH, CS_2, and MeI, successively. Using these standard conditions with **71** and a limited amount of either NaH or MeI, produced the disubstituted derivative as the major component (Table 1, entries 1 and 2). Hence, another method was needed. Phase transfer conditions[130] did not prove successful (entry 3), where only disubstitution occurred. Schlessinger and Schultz reported monosubstitution of a compound containing two sterically hindered hydroxyl groups by using 4 equivalents of DBN and CS_2 and MeI in excess in DMF.[131] We thus examined the use of DBU, a functionally similar base (entries 4-8). The addition of 1.5 equivalents of DBU (entry 7) to the reaction mixture generated 87% of the desired products **94** and **95** in approximately 1:1 ratio.

Table 1. Optimization of the formation of methyl xanthate ester **94** and **95** from **71**.

		Yield			
Entry	Conditions	Di[a]	**94**	**95**	**71**
1	1.2 eq NaH, excess CS_2, excess MeI, THF, rt	32%	9%	26%	20%
2	excess NaH, excess CS_2, 1.2 eq MeI, THF, rt	29%	11%	13%	4%
3	1.1 eq MeI, 0.1 eq nBu$_4$NHSO$_4$, NaOH(aq)/CS_2[130]	[b]			
4	4 eq DBU, excess CS_2, excess MeI, DMF, rt	19%	33%	37%	4%
5	2 eq DBU, excess CS_2, excess MeI, DMF, rt	13%	39%	44%	trace
6	1.6 eq DBU, excess CS_2, excess MeI, DMF, rt	6%	36%	46%	trace
7	1.5 eq DBU, excess CS_2, excess MeI, DMF, rt	9%	40%	47%	trace
8	1.2 eq DBU, excess CS_2, excess MeI, DMF, rt	5%	32%	43%	18%

[a] "Di" indicates disubstituted product.

[b] Disubstituted derivative formed as the major component. No further purification occurred.

Transferring the optimized conditions for methyl xanthate ester formation of **71** to **19**, did not give the xanthate esters **96** and **97** to any great extent. Hence, optimization for **19** was also needed (Table 2). DBU was not suitable as base (entries 1-6). Instead, we focused on the use of NaH/CS_2/MeI, limiting the amount of either NaH (entry 7) or MeI (entries 8-10). This generated the target xanthate esters **96** and **97** in approximately 50%. Interestingly, when NaH was used in limited amounts, 3-xanthylated **97** was obtained as the major product, whereas the inversed ratio of products was obtained when MeI was used in limited amounts.

Table 2. Optimization of the formation of methyl xanthate ester **96** and **97** from **19**.

		Yield			
Entry	Conditions	Di[a]	**96**	**97**	**19**
1	1.5 eq DBU, excess CS_2, excess MeI, DMF, rt	-	10%	8%	64%
2	1.5 eq DBU, excess CS_2, excess MeI, DMF, rt (longer reaction time)	[b]			
3	1.5 eq DBU, excess CS_2, excess MeI, DMF, 80 °C	[b]			
4	2 eq DBU, excess CS_2, excess MeI, DMF, rt	[b]			
5	4 eq DBU, excess CS_2, excess MeI, DMF, rt	[b]			
6	8 eq DBU, excess CS_2, excess MeI, DMF, rt	[b]			
7	1.2 eq NaH, excess CS_2, excess MeI, THF, rt	22%	18%	35%	18%
8	excess NaH, excess CS_2, 1.3 eq MeI, THF, rt	35%	30%	17%	11%
9	excess NaH, excess CS_2, 1.1 eq MeI, THF, rt	19%	32%	16%	16%
10	excess NaH, excess CS_2, 1.0 eq MeI, THF, rt	18%	31%	17%	18%

[a] "Di" indicates disubstituted product.

[b] Starting material **19** was observed as the major component of the reaction mixture. No further separation or purification was performed.

With the xanthate esters **94-97** in hand, deoxygenation reactions were performed with H_3PO_2 as the hydrogen atom source and AIBN as the radical initiator (Scheme 5). Deoxygenation of position 3 and 4, i.e. **94** and **97**, successfully resulted in **(-)-88** in high yields. As expected, deoxygenation at C2 of **95** to give **(-)-90** and of **96** to give **(-)-89** proved problematic. Withers and co-workers have investigated the rate of hydrolysis of monosubstituted deoxy β-D-glycopyranosides and showed a clear trend in reactivity: 2-deoxy > 4-deoxy > 3-deoxy ≈ 6-deoxy.[132] In addition, Jensen and Bols have shown that the orientation of polar substituents has a great impact on their electron-withdrawing effects. Equatorial hydroxyl groups are more electron-withdrawing compared to axial ones, which in turn affects the rate of glycoside hydrolysis.[133] Even though the pH was carefully monitored to avoid neutral or acidic pH, moderate to low yields were obtained for **(-)-89** and **(-)-90**, due to hydrolysis. For the low-yielding deoxygenation of **95**, the use of AIBN/$n$$Bu_4SnH$ as well as $(Bu_4N)_2S_2O_8/HCO_2Na$, a method generally suitable for acid-labile compounds, were investigated without success.

3.2.3 Chiral pool vs de novo synthesis

The de novo approach starting from **91-93** (Figure 24) provided access to the unnatural enantiomers **(+)-88-90**, though as racemates. Resolution using chiral HPLC proved successful on an analytical scale. However, on a preparative scale, separation was obtained for **89** and **90**, but not for **88**. This is a drawback for the, in other aspects successful, de novo synthesis that generally required fewer steps and gave higher yields, especially for **88**. The synthesized enantiomerically pure oxanes **(-)-88-90** were utilized for the determination of the stereochemistry of the resolved enantiomer from the de novo synthesis by comparison of the specific rotation. In addition, **(-)-88-90** were also used in the elucidation of the relative stereochemistry of **(+)-88-90**, which was difficult to assign by NMR spectroscopic techniques due to conformational uncertainties.

3.2.4 β4GalT7 assay

The synthesized oxanes **(-)-88**, **(±)-88**, **(-)-89**, **(+)-89**, **(-)-90**, and **(+)-90** were investigated in our β4GalT7 assay. None of the oxanes induced galactosylation by β4GalT7, nor did they inhibit its activity. This clearly indicates that only one hydroxyl group on an oxane ring is insufficient to form any significant interactions with β4GalT7. Hence, we conclude that 3-OH is necessary to gain galactosylation activity as well as inhibition, although at least one additional substituent at position 2 and/or 4 is needed.

3.3 Methyl xanthate ester as protective group (Paper VII)

In our search for efficient synthetic routes to xyloside analogs, we wanted to explore the possibility of using the methyl xanthate ester as a protective group. In a context of synthesis of modified carbohydrates, this may shorten synthetic pathways where deoxygenations using xanthate esters are included.

Methyl xanthate esters are easily formed by different methods, of which NaH/CS_2/MeI is the most common. Other strong bases, such as Na,[134] *n*-BuLi,[135] *t*-BuOK,[136] and NaHMDS[137] have been employed, as well as other conditions, e.g. NaOH and TBAHS under phase transfer conditions,[130] cesium base/TBAI in DMF,[138-139] KF-Al_2O_3,[140] Triton-B[141] or basic resin[142] in DMSO, and KO_2/Et_4NBr in DMF.[143] In addition, the methyl xanthate ester has low polarity, no chiral centers, and a simple NMR spectroscopic signature (i.e. a singlet at around 2.56 ppm in ^{1}H-NMR spectrum and signals at around 216 and 19 ppm in ^{13}C-NMR spectrum).

In 1960, Willard and Pacsu reported that xanthate esters could be cleaved from carbohydrates by the action of $Hg(OAc)_2$.[144] Reductive removal using $LiAlH_4$ has also been presented[131, 145] as well as H_2O_2/LiOH[146] and hydrolysis,[147] including the use of AIBN/$n$$Bu_3SnH$.[148]

3.3.1 Cleavage of methyl xanthate esters

We wanted to develop a method for methyl xanthate ester cleavage that is facile and orthogonal to other common alcohol protective groups. We discovered that methyl xanthate esters were efficiently cleaved simply by heating the substrate in diethylenetriamine (neat) at 160 °C (microwave) for 30 minutes. No precautions against atmospheric air or moisture were needed and aqueous work-up gave the pure alcohols. Diethylenetriamine has recently been employed in the removal of

unactivated carbamates and ureas, including a few thio derivatives, in the presence of amides.[149]

With this new protocol in hand, we examined the substrate scope (Table 3) including primary (entry 1), secondary (entries 2 and 3), phenolic (entries 4 and 5), and carbohydrate (entries 6-8) methyl xanthate esters. All were cleaved in excellent yields, and the same conditions were applied for the vicinal diol (entry 8).

Table 3. Scope of cleavage of methyl xanthate ester.[a]

Entry	Substrate	Product	Yield
1	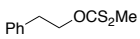	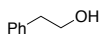	92%
2	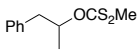	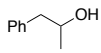	97%
3	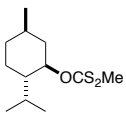	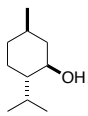	94%
4	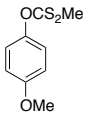	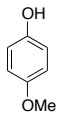	94%
5	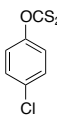	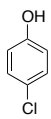	88%
6	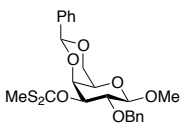	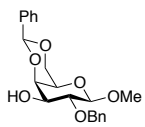	99%
7	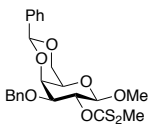	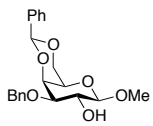	99%
8	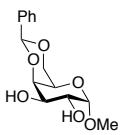	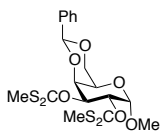	96%

[a] Diethylenetriamine, 160 °C, 30 min, MW.

Attempts to synthesize a tertiary methyl xanthate ester failed due to the difficulty of introducing a methyl xanthate ester at such a sterically hindered position (Scheme 6). As an alternative, neopentyl alcohol **100** was substituted as a methyl xanthate ester. However, isolation of the assumed regenerated alcohol after reaction with

diethylenetriamine failed. Syntheses of an allylic methyl xanthate ester were also attempted, with cinnamyl alcohol **102** and farnesol **104**. Due to the propensity of rearrangement,[150-152] it proved problematic to purify the xanthate esters and they were thus excluded from the study.

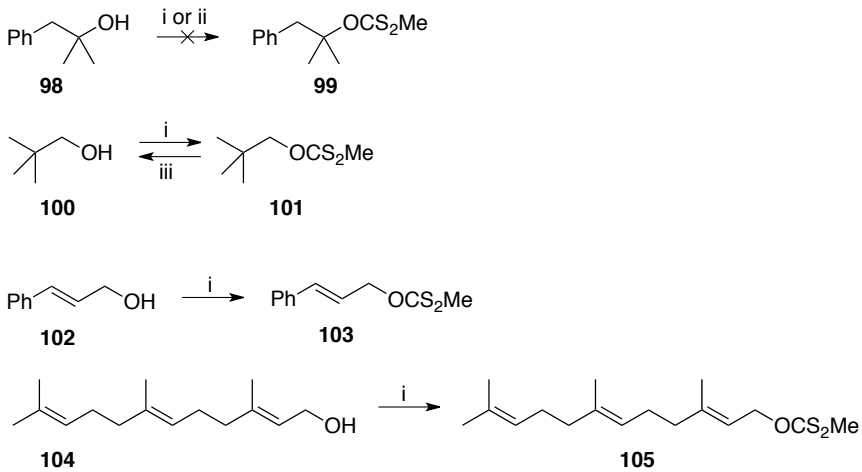

Scheme 6. Reagents and conditions: i) 1) NaH; 2) CS_2, reflux for **98**, 60 °C for **100**, rt or 60 °C for **102** and **104**; 3) MeI, rt, (52% for **101**); ii) CS_2, Cs_2CO_3, TBAI, MeI, DMF, 0 °C → rt; iii) Diethylenetriamine, 160 °C, 30 min, MW.

To investigate the use of methyl xanthate ester as a protective group, we first monosubstituted 1,6-hexanediol as xanthate ester and then introduced and subsequently and chemoselectively removed a range of common alcohol protective groups (Table 4). We also chemoselectively cleaved the methyl xanthate ester in the presence of the other protective groups (Table 5), which proceeded smoothly in excellent yields, except for the acetate (entry 1) that did not tolerate the deprotection conditions.

Table 4. Introduction and chemoselective cleavage of alcohol protective groups in the presence of methyl xanthate ester.

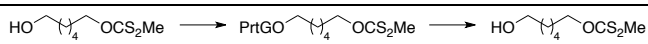

		Introduction		Cleavage	
Entry	PrtG	Reagents	Yield	Reagents(s)	Yield
1	Ac	Ac_2O, Py	98%	1 M LiOH	87%
2	THP	DHP, *p*TSA	94%	*p*TSA	93%
3	MOM	$CH_2(OMe)_2$ LiBr, *p*TSA	89%	1 M HCl	96%
4	Bn		[153]	$BF_3{\cdot}Et_2O$, TBAI	96%
5	TBDPS	TBDPSCl, DMAP, Py	90%	TBAF, AcOH	96%
6	TIPS	TIPSOTf, 2,6-lutidine	96%	TBAF, AcOH	84%

Table 5. Chemoselective cleavage of the methyl xanthate ester in the presence of other alcohol protective groups.[a]

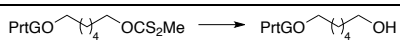

Entry	PrtG	Yield
1	Ac	14%[b]
2	THP	92%
3	MOM	96%
4	Bn	quant
5	TBDPS	99%
6	TIPS	quant

[a] Diethylenetriamine, 160 °C, 30 min, MW.

[b] 78% of 1,6-hexanediol was isolated after column chromatography.

During our efforts in finding a facile way of cleaving the methyl xanthate ester we investigated its reactivity towards a variety of reagents (Table 6). Generally, methyl xanthate esters are not particularly sensitive towards acids, bases, and Lewis acids, whereas it is moderately sensitive towards reducing agents and nucleophiles, especially alkoxides. Methyl xanthate esters do not tolerate oxidizing agents.

Table 6. Reactivity chart of methyl xanthate esters.

Reagents	Unreactive	Reactive
Acids	*p*TSA, HCl, AcOH	$MeSO_3H$
Bases	Py, aq LiOH	RO^-
Lewis acids	$BF_3{\cdot}Et_2O$, TMSI	
Nucleophiles	TBAF	NaOMe, RO^-, diethylenetriamine
Reducing agents	$NaBH_4$, $NaBH_3CN$	$LiAlH_4$, L-Selectride, $LiBH_4$, $BH_3{\cdot}SMe_2$
Oxidative agents		*m*CPBA, $NaIO_4$, H_2O_2/LiOH
Miscellaneous	Ac_2O, Pd/C H_2	AIBN/nBu$_3$SnH

To summarize, the methyl xanthate ester is easily introduced and cleaved and it is orthogonal to common alcohol protective groups. Methyl xanthate ester can thus be used as a protective group.

3.4 Conclusions

We set out to examine the active sit of β4GalT7, especially to investigate the steric restrictions, with the aim to pinpoint the requirements for efficient substrates and inhibitors. We found that none of the modifications generated more efficient substrates for β4GalT7 compared to **6**. We thus conclude that for galactosylation, xylose is the optimal substrate. On the other hand, in terms of inhibition, several compounds were found active. Generally, analogs with modifications at position 4 showed inhibitory activity. Although small substituents at the equatorial position at C4 seemed to be tolerated by the enzyme, the steric restrictions of the other positions appeared to be more pronounced, especially at C3. Hence, we conclude that the acceptor binding pocket is narrow with a precise set of hydrogen bond acceptors. In addition, at least two substituents of the xylose moiety seems vital for sufficient interactions to β4GalT7 to occur, leading to galactosylation or inhibition.

4 Modifications of the endocyclic and exocyclic positions

As part of our investigation of the active site of β4GalT7, we wanted to explore the function of the endocyclic and exocyclic oxygen atom of xylosides. A few 5-thio-β-D-xylosides and 1,5-dithio-β-D-xylosides, as well as one carba analog, have been shown to possess GAG priming abilities and to function as substrates for β4GalT7 (Section 1.4.2). However, only partially purified enzyme extracts from chicken cartilage has been used.[56] Hence, we synthesized and examined naphthyl 5-thio- and naphthyl 1,5-dithio-β-D-xylopyranoside **106** and **107** as well as naphthyl 5a-carba-β-xylopyranoside in both D- and L-configuration, **108** and **109** (Figure 25). We also investigated xyloside derivatives with sulfur, sulfoxide, sulfone, and methylene linkages to the naphthyl aglycon **110**-**114**.

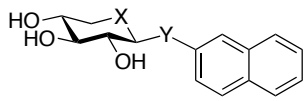

6 X = O, Y = O
106 X = S, Y = O
107 X = S, Y = S
108 X = CH_2, Y = O
110 X = O, Y = S
111 X = O, Y = SO $(S)_S$
112 X = O, Y = SO $(R)_S$
113 X = O, Y = SO_2
114 X = O, Y = CH_2

Figure 25. Naphthyl xyloside analogs with modifications of the endocyclic and/or exocyclic positions.

The exocyclicly modified xylosides **110**[40] and **114**[63] have been synthesized previously. Thio-analog **110** was shown to be a good primer of GAG chains,[40] whereas carba-analog **114** was shown to be a poor primer.[63] This trend has also been found amongst other 1-*S* and 1-*C* xyloside derivatives (Section 1.4.3). **110** and **114** were included in our studies since they have not been directly tested as substrates for β4GalT7, and for comparison reasons.

4.1 Endocyclic analogs (Paper VIII)

4.1.1 Synthesis

The thio analogs **106** and **107** were synthesized from the known bromide donor **115**[154] (Scheme 7). Formation of **106** proved quite problematic since the major products from the glycosylation reaction were *C*-xylosides. It is well-known that *C*-xylosylation occurs with thio-donors and that anomerization and thermodynamically favored O→C rearrangements occur for *O*-xylosides.[155-157] However, we obtained enough quantity of **106**, using ZnO-$ZnCl_2$ as promoter,[158] to be able to examine its activity in the β4GalT7 assay. Synthesis of **107** proceeded smoothly.

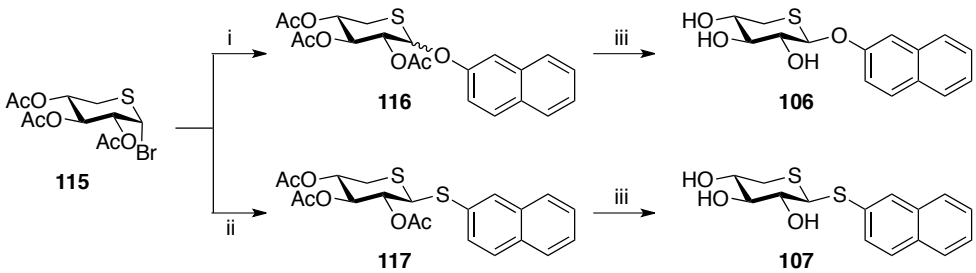

Scheme 7. Reagents and conditions: i) 2-naphthol, ZnO-$ZnCl_2$, toluene:MeCN (1:1), 13X molecular sieves, 60 °C, α/β 0.9:1; ii) 2-naphthalenethiol, ZnO-$ZnCl_2$, toluene:MeCN (1:1), 13X molecular sieves, 45 °C, (54%); iii) 1 M NaOMe, MeOH, **106** (2% over two steps), **107** (97%).

The D- and L- analogs of 5a-carba-β-xylopyranoside were synthesized from α/β-mixtures of the known D- and L-4,5,6-tris(benzyloxy)cyclohex-2-enol **118** and **119** (Scheme 8). Enol **118**, with D-xylo configuration, was obtained from commercially available methyl α-D-glucopyranoside following procedures developed by Madsen and co-workers.[159-160] Methyl α-L-glucopyranoside is not commercially available, and L-glucose is rather expensive compared to monosaccharides in the more abundant D-configuration. Instead, L-enol **119** was synthesized from D-xylose, using similar synthetic methods according to procedures developed by Kornienko and d'Alarcao.[161-162] The naphthyl moiety was installed by a Mitsunobu reaction (Scheme 8). The benzyl groups were then removed by hydrogenolysis,[112] which simultaneously saturated the alkene functionality, generating **108** and **109**.

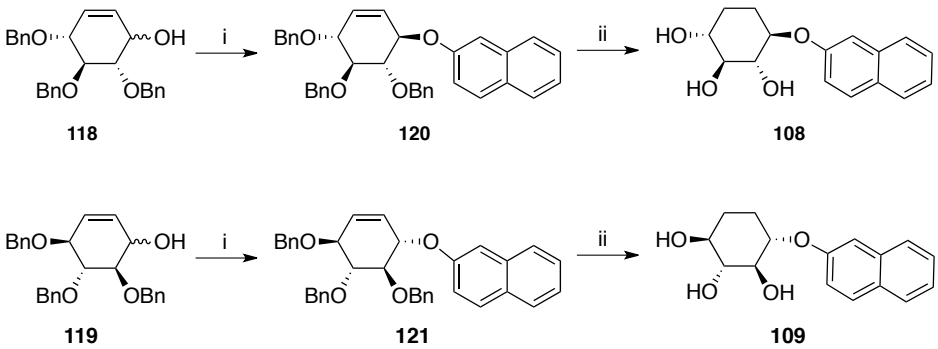

Scheme 8. Reagents and conditions: i) 2-naphthol, PPh_3, DIAD, THF, **120** (51%), **121** (24%); ii) Pd/C, H_2, HCl, DMF, **108** (31%), **109** (50%).

4.1.2 β4GalT7 assay

The xyloside analogs **106-109** were examined together with xyloside **6** and thio derivative **110**. All compounds except L-carbaxyloside **109** acted as substrates for β4GalT7 (Table 7).

Table 7. Kinetic paramteres for galactosylation by β4GalT7.

Entry	Compound	K_m (μM)	V_{max} (pmol s^{-1})	k_{cat} (s^{-1})	K_m/k_{cat} (mM^{-1} s^{-1})
1	**6**	780	2.6	3.1	4.0
2	**110**	360	2.2	2.7	7.5
3	**106**	34	1.7	2.0	59
4	**107**	25	1.3	1.6	64
5	**108**	390	2.3	2.7	6.9
6	**109**	-	-	-	-

A clear trend in galactosylation amongst the thio analogs was observed: β-D-xyloside < 1-thio-β-D-xyloside < 5-thio-β-D-xyloside < 1,5-dithio-β-D-xyloside, which is similar to what has been reported previously.[56] **106** and **107** were galactosylated by β4GalT7 approximately 15 times more efficiently compared to the parent xyloside **6**.

For the carba-analogs, the results were somewhat surprising. The D-analog **108** acted as a substrate for β4GalT7 and was galactosylated slightly more efficiently than **6**. The corresponding L-analog was not galactosylated by β4GalT7. This is opposite to previously reported, and structurally similar, carbaxylosides (**27** and **28**, Figure 10).[62] In this study, the authors reported that the compound with L-xylo configuration (**28**) acted as a substrate, and the compound with D-xylo configuration (**27**) did not.

However, other L-xylosides and L-xyloside analogs have been reported not to act as primers of GAG chains,[62-64] which we also show is true for the L-analog of **6** (Section 5.1.2).

Taking a closer look at this discrepancy regarding the absolute stereochemistry of the active carbaxylosides, the sign of the specific rotation of **108** is the same as the active compound **28**, i.e. (-). Both **27** and **28** were synthesized as racemates from achiral starting materials and resolved by formation and separation of sulfoximide diastereomers. We have experienced difficulties in correctly assigning stereochemistry of diastereomers (Section 3.2.3, Paper IV). Since carbaxylosides **108** and **109** were synthesized from the chiral pool following published procedures, we are certain concerning their stereochemistry. An explanation for the inconsistency regarding the absolute stereochemistry of the active carbaxylosides might therefore be that the stereochemistry of **27** and **28** is incorrectly assigned in the literature.

4.1.3 Conformational analysis and molecular docking simulations

We crystallized **107**, as well as xyloside **6**, in order to investigate what structural features that result in substrates that are efficiently galactosylated by β4GalT7 (Figure 26). The crystal structures revealed that the bond length between the carbon atoms (C1 and C5) and sulfur atoms were approximately 0.4 Å longer in **107** compared to the corresponding bonds in **6** (Table 8, entries 1-3), which is reasonable due to the larger size of sulfur compared to oxygen. In addition, we observed that the bond angles at the endocyclic and exocyclic positions (entries 4 and 6) were smaller in **107** compared to **6**.

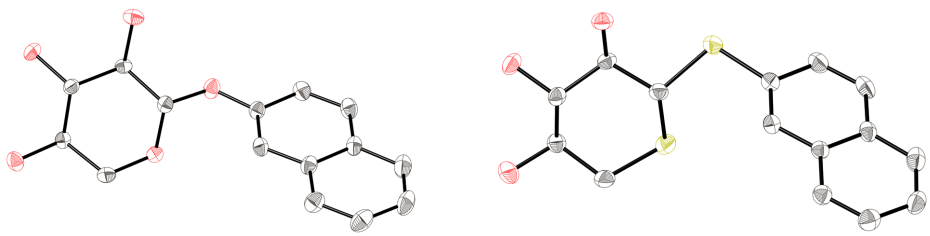

Figure 26. Thermal ellipsoid representations (atoms depicted at 30% probability level and hydrogen atoms excluded for clarity) of the crystal structures of **6** and **107**.

Table 8. Selected bond lengths and bond angles of **6** and **107**, measured from the crystal structures.

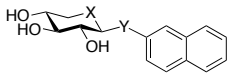

Entry	Bond lengths/angles	Compound **6**	Compound **107**
1	C5-X	1.44 Å	1.80 Å
2	X-C1	1.42 Å	1.81 Å
3	C1-Y	1.41 Å	1.81 Å
4	C5-X-C1	114°	97.2°
5	X-C1-Y	107°	108°
6	C1-Y-C(2Nap)	118°	104°

NMR experiments of **107** in CD_3OD at 37 °C showed that the conformation in solution is similar to that obtained in the crystal structure, i.e. $^4C_1$.

Molecular docking simulations (with *Drosophila* β4GalT7 mutant D211N) confirmed that **107** fits in the active site of β4GalT7. Comparing the modeling of **107** to **6**, a more pronounced π-stacking with parallel displacement geometry was observed between the naphthyl moiety of **107** and the side chain of a tyrosine residue (Tyr[179], Figure 27). Parallel displacement is a favorable π-stacking geometry.[163] This geometry was also observed for 1-thio-xyloside **110**.

In addition, a slightly different orientation of 4-OH was observed for **107** compared to **6**, which presumably affects the distance between O4 of the xyloside and the endocyclic oxygen atom of UDP-Gal. During the catalytic reaction, O4 of xylose is assumed to be deprotonated, which would cause electronic repulsion between the alkoxide and the endocyclic oxygen atom of galactose. It has been suggested for β-1,4-galactosyltransferase 1, a similar enzyme that also catalyzes an S_N2 reaction, that the electronic repulsion that occurs when O4 of the acceptor gets deprotonated promotes a conformational change of the donor, which facilitates the reaction.[164] It has been proposed that β4GalT7 may follow a similar mechanism.[23] Hence, the observed difference in orientation of 4-OH of the xylosides may influence the catalytic efficiency of β4GalT7.

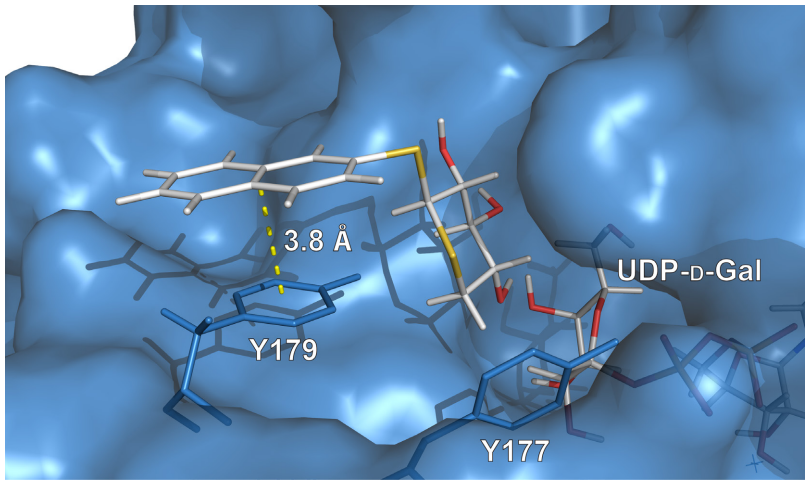

Figure 27. Molecular docking of **107** in *Drosophila* β4GalT7 mutant D211N.

4.2 Exocyclic analogs (Paper III and IX)

We envisioned the syntheses of sulfoxides and sulfone **111-113** to start from the known acetylated thioxyloside **123**[40], easily accessible from peracetylated β-D-xylopyranose **122**. It is known that equatorial thioglycosides show poor stereoselectivity in oxidation reactions towards sulfoxides, compared to the corresponding axial derivatives, which is also true for xylosides.[165-167] These observations are explained by the exo-anomeric effect, i.e. the orientation of the aglycon so that a free electron pair of the sulfur atom overlaps with the unoccupied σ*-orbital of the bond between the endocyclic oxygen atom and C1. Generally, only the (*R*)$_S$ sulfoxide is formed for axial thioglycosides, since the pro-*S* electron pair is sterically hindered by the pyranose ring while the pro-*R* electron pair is available for attack (Figure 28). In equatorial glycosides, the difference in steric hindrance is smaller between the pro-*S* and pro-*R* electron pairs, hence both diastereomers are often formed and the major product usually have the (*S*)$_S$-configuration. The absolute configuration of the sulfoxide sulfur atom may be assigned using NMR spectroscopy[166, 168-169] and/or CD spectroscopy.[168, 170] However, the absolute stereochemistry of most glycosyl sulfoxides has been determined by X-ray crystallography.[165, 167, 171-172]

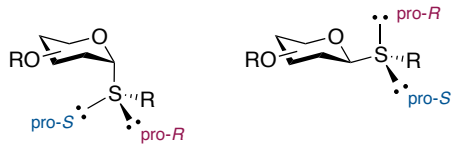

Figure 28. Preferred conformations of axial and equatorial thioglycosides dictated by the exo-anomeric effect.

4.2.1 Synthesis

The sulfoxides **111** and **112** were synthesized from 5-thio-xyloside **123** by careful oxidation with *m*CPBA at -78 °C followed by deacetylation (Scheme 9). As expected, the oxidation step generated a diastereomeric mixture, and the sulfoxides **124** and **125** were obtained in excellent yield as an inseparable mixture in approximately 3:1 ratio[‡]. Using Zemplén conditions for deacetylation of the mixture of **124** and **125** resulted in partial cleavage of the glycosidic bond forming methyl β-D-xylopyranoside, which was difficult to separate from **111** and **112**. Instead, deacetylation was accomplished by using a solution of guanidine/guanidinium nitrate[173]. Sulfoxides **111** and **112** could then be separated by column chromatography and obtained in 64% and 21% yield, respectively.

The sulfone derivative **113** was synthesized from 5-thio-xyloside **123** by oxidation with *m*CPBA in excess at 0 °C, yielding **126** in 91% (Scheme 9). Subsequent deacetylation under Zemplén conditions generated sulfone **113**.

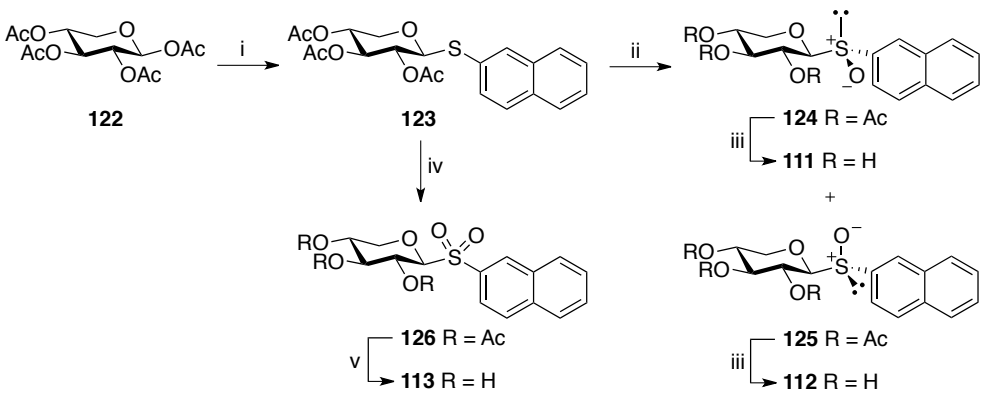

Scheme 9. Reagents and conditions: i) $BF_3{\cdot}Et_2O$, 2-naphthalenethiol, MeCN, (79%); ii) *m*CPBA (1.06 eq), CH_2Cl_2, -78 °C, (95%); iii) guanidine/guanidinium nitrate, CH_2Cl_2/MeOH, **111** (64%), **112** (21%); iv) *m*CPBA (4 eq), CH_2Cl_2, 0 °C, (91%); v) 1 M NaOMe, MeOH, (69%).

[‡] Based on ratio observed in ^{1}H-NMR spectrum

The absolute configuration of the sulfoxides **111** and **112** was elucidated by the use of ^{1}H, ^{13}C, and NOE NMR spectroscopy, and **111** was assigned $(S)_S$ configuration and **112** was assigned $(R)_S$ configuration.

4.2.2 β4GalT7 assay

All xylosides with variations at the exocyclic position (**110-114**) were galactosylated by β4GalT7 (Table 9). Excess-substrate inhibition (Section 1.5) was observed for **110-113** (entries 2-5), hence the kinetic parameters were calculated using the concentrations up to the highest observed reaction rate. β4GalT7 galactosylated all thio-derivatives more efficiently compared to parent xyloside **6** (entries 2-5). The galactosylation efficiency was approximately 13 times higher for sulfone **113** than for **6**. β4GalT7 also showed higher catalytic efficiency for the sulfoxides **111** and **112** compared to **6**. The $(R)_S$ sulfoxide **112** was slightly more efficiently galactosylated than the corresponding $(S)_S$ sulfoxide **111**. However, in catalytic efficiency, both **111** and **112** resembled thioxyloside **110** to a much larger extent than sulfone **113**. *C*-xyloside **114** (entry 7) proved to be a less suitable substrate for β4GalT7 compared to **6**.

Table 9. Kinetic parameters for galactosylation by β4GalT7.

Entry	Compound	K_m (mM)	V_{max} (pmol s^{-1})	k_{cat} (s^{-1})	K_m/k_{cat} (mM^{-1} s^{-1})
1	**6**	0.70	1.6	1.2	1.6
2	**110**[a]	0.30	1.7	1.8	5.8
3	**111**[a]	0.37	2.5	2.5	6.9
4	**112**[a]	0.14	1.1	1.1	7.8
5	**113**[a]	0.10	2.1	2.2	21
6	**6**[b]	0.58	1.1	1.5	2.6
7	**114**[b]	2.4	1.8	2.5	1.0

[a] Excess-substrate inhibition were observed, hence the kinetic parameters were calculated using the concentrations up to the highest observed reaction rate.

[b] *C*-xyloside **114** (entry 7) was assayed at another occation than analogs **110-113** with a different batch of β4GalT7, hence slightly different kinetic parameters for **6** (entries 1 and 6) are obtained. The kinetic parameters of **114** can therefore only be compared to **6** (entry 6).

To investigate if the great increase in galactosylation of sulfone **113** by β4GalT7 was transferrable to cell studies, GAG priming of **6**, **110**, and **113** were examined. 5-Thioxyloside **110** was shown to induce GAG priming to a similar extent as **6**, whereas sulfone **113** primed GAG chains approximately 3.4 times as much as **6**.

4.3 Conclusions

We set out to investigate the endocyclic and exocyclic positions of xyloside **6** to identify the effects on β4GalT7 activity as part in the overarching aim to pinpoint requirements for efficient substrates and inhibitors. We found that thio analogs were more efficient substrates for β4GalT7 compared to **6**, where the 1,5-dithioxyloside and exocyclic sulfone were the most potent. Although molecular docking simulations are still ongoing with these compounds and β4GalT7, we suggest that small differences in the binding orientation greatly affect the activity towards β4GalT7. Furthermore, we propose that an exchange of the exocyclic oxygen atom to a sulfur atom enables a favorable π-stacking with parallel geometry between the naphthyl moiety and a tyrosine residue.

5 Variations of the aglycon

5.1 Size, electronic properties, and distance to aromatic aglycon (Paper I and III)

It has previously been shown that the aglycon has a large effect on the GAG priming ability of xylosides (Section 1.4.4). We wanted to conduct a comprehensive study of the interactions between β4GalT7 and xylosides with variations in the aglycon, including different sizes and electronic properties, as well as different distances between the xyloside and the aromatic part of the aglycon. Hence, we investigated xylosides **3**, **29**, **34**, **38**, **40**, and **127**-**136** as substrates for β4GalT7, with 2-naphthyl xyloside **6** as reference compound (Figure 29). We hypothesized that it is possible to form efficient substrates for β4GalT7 by optimizing the aglycon structure.

Xyloside **3** is commercially available and xylosides **29**,[40] **38**,[40] **40**,[64] **127**,[40] **134**,[78] and **135**[84] have been reported previously.

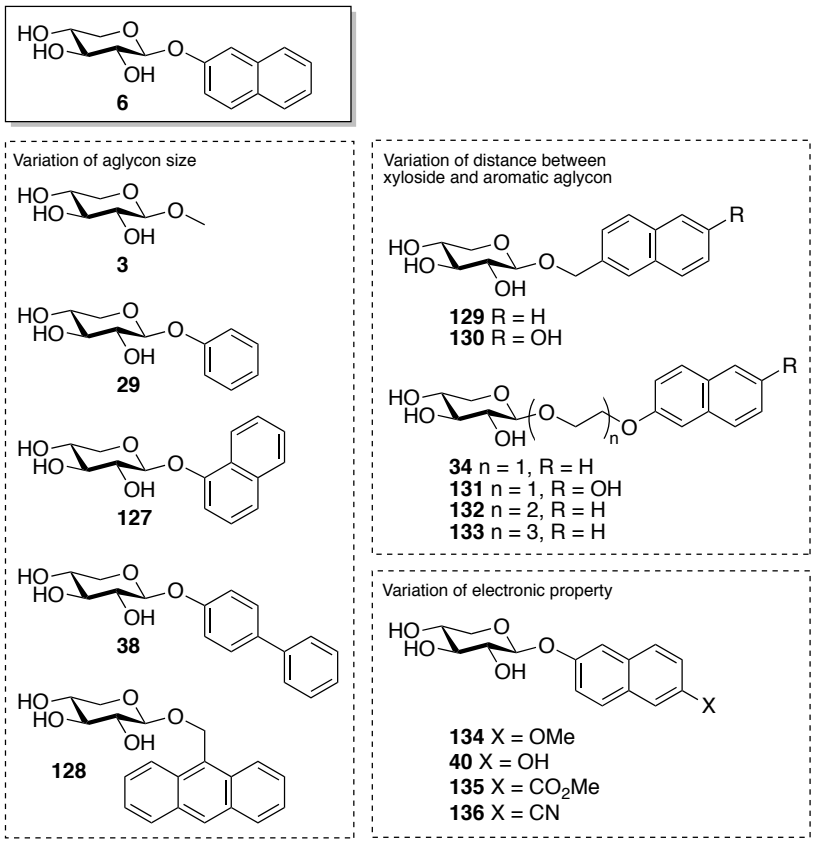

Figure 29. Xylosides with different variations in the aglycon structure.

5.1.1 Synthesis of xylosides with a spacer between xylose and the aromatic part of the aglycon

To investigate the effect of xylosides with different distances between the xylose part and the aromatic aglycon, we synthesized naphthyl xylosides where the naphthyl moiety is separated by a methylene bridge or oligoethylene glycol (OEG) spacers of three different lengths. OEG spacers were chosen since they are inexpensive, polar, and commercially available in a variety of different lengths. Due to the antiproliferative effect of **40**, we also synthesized hydroxylated analogs **130** and **131** to investigate the effect of the distance on the antiproliferative activity.

Xylosides **34** and **129-133** were synthesized from peracetylated xylose **122** (Scheme 10). The methylene-bridged derivatives were formed through glycosylation with 2-naphthalenemethanol and 6-acethoxy-2-naphthalenemethanol, respectively, followed

by deacetylation. The synthesis of **137** gave a range of byproducts that were not easily separated from **137**, hence deacetylation was performed with the crude mixture. Synthesis of the corresponding hydroxylated derivative **130** was on the other hand straightforward.

The synthesis of the OEG-bridged xylosides **34, 131-133** were initiated by xylosylation of the OEG spacers. For the shortest spacer, 2-bromoethanol was used. However, the bromide analogs of diethylene glycol and triethylene glycol were not commercially available, hence, the chloride equivalents were used. In contrast to the synthesis of **142** from bromide **139**, coupling of 2-naphthol to chlorides **140** and **141** proved difficult and gave low yields of **144** and only traces of **145** under the same reaction conditions, i.e. K_2CO_3 in DMF. This might be due to the weaker leaving group-property of chloride compared to bromide. In addition, we speculate that the longest spacer may form a crown ether-like interaction with potassium ions, thereby obstructing the substitution reaction. When adding 18-crown-6, which complexes to potassium ions, to the reaction mixtures the yields were increased for both **144** and **145** and the reaction times were decreased from 48 hours to 6 hours.

Coupling of 6-acethoxy-2-naphthol to bromide **139** resulted in partial cleavage of the aromatic acetate. This compound was not possible to separate from **143**, hence deacetylation was performed with this mixture. Deacetylation of **142**, **144**, and **145** proceeded smoothly, generating the target xylosides **34**, **132**, and **133** in good yields.

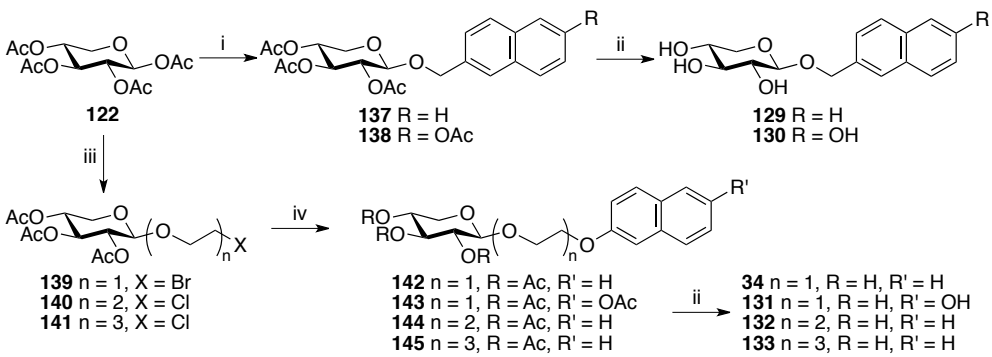

Scheme 10. Reagents and conditions: i) 2-naphthalenemethanol, $BF_3{\cdot}Et_2O$, CH_2Cl_2, 0 °C; 6-acethoxy-2-naphthalenemethanol, $BF_3{\cdot}Et_2O$, CH_2Cl_2, 0 °C, **138** (79%); ii) 1 M NaOMe, MeOH, **129** (11% over two steps), **130** (68%), **34** (90%), **131** (39% over two steps), **132** (73%), **133** (66%); iii) 2-bromoethanol, $BF_3{\cdot}Et_2O$, CH_2Cl_2, 0 °C, **139** (69%); 2-(2-chloroethoxy)-ethanol, $BF_3{\cdot}Et_2O$, CH_2Cl_2, 0 °C, **140** (43%); 2-[2-(2-chloroethoxy)ethoxy]-ethanol, $BF_3{\cdot}Et_2O$, CH_2Cl_2, 0 °C, **141** (61%); iv) 2-naphthol, K_2CO_3, DMF, 80 °C, **142** (63%); 6-acethoxy-2-naphthol, K_2CO_3, DMF, 80 °C; 2-naphthol, K_2CO_3, 18-crown-6, DMF, 80 °C, **144** (22%), **145** (29%).

Further attempts to increase the yields of **144** and **145** were made by exchanging the chloride of the diethylene and triethylene glycol spacers for an iodide by simply performing a Finkelstein reaction with NaI in acetone. However, glycosylation of this triethylene glycol derivative proved to be problematic, not forming **147** to any significant extent, and the diethylene glycol derivative gave modest yields of **146** (Scheme 11). However, substitution reaction of **146** with 2-naphthol generated **144** in approximately 50% yield, with modest purity. We also investigated the possibility to perform the reactions in a reversed order by coupling the OEG iodide spacers to 2-naphthol before xylosylation. Again, synthesis to form the derivative with the longest spacer failed, whereas **149** was formed in high yield. The subsequent glycosylation reaction failed, thus we abandoned this approach without further examination. Finally, we examined the substitution reaction between ethylene glycol derivative **139** and diethylene glycol derivative **149** in an attempt to form **145**. Unfortunately, no product was obtained. In addition, Cs_2CO_3 was briefly examined as base instead of K_2CO_3 in the reaction between **141** and 2-naphthol, without increased yields.

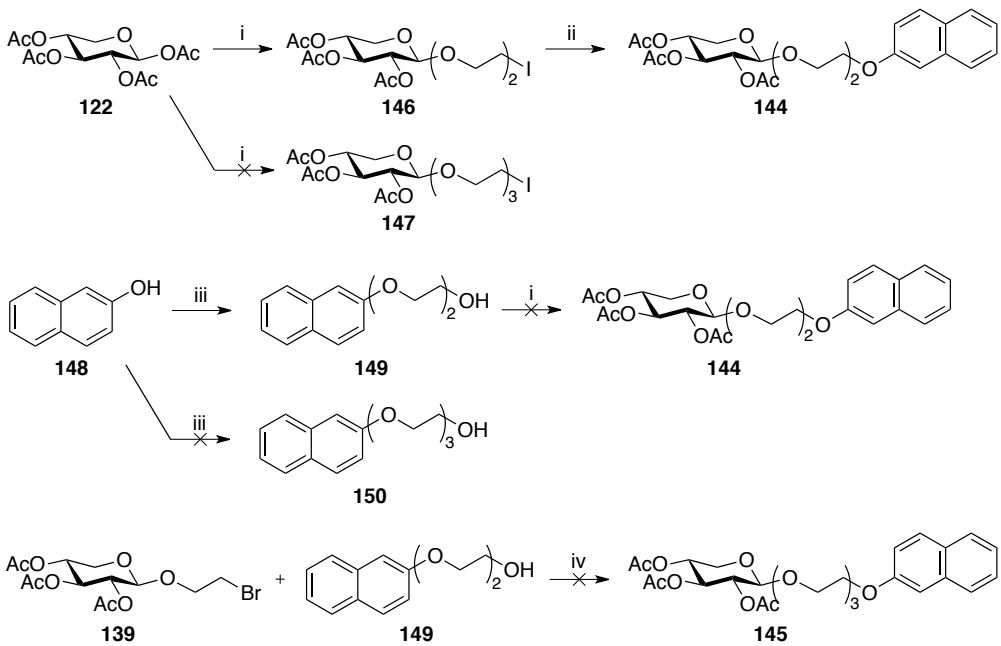

Scheme 11. Reagents and conditions: i) 2-(2-iodoethoxy)-ethanol, $BF_3{\cdot}Et_2O$, CH_2Cl_2, 0 °C, **146** (41%); 2-[2-(2-iodoethoxy)ethoxy]-ethanol, $BF_3{\cdot}Et_2O$, CH_2Cl_2, 0 °C; **122**, $BF_3{\cdot}Et_2O$, CH_2Cl_2, 0 °C; ii) 2-naphthol, K_2CO_3, DMF, 50 °C; iii) 2-(2-iodoethoxy)-ethanol, K_2CO_3, DMF, 80 °C, **149** (82%); 2-[2-(2-iodoethoxy)ethoxy]-ethanol, DBU, DMF, 80 °C; iv) K_2CO_3 or DBU, DMF, 80 °C.

The hydrophobicity of xylosides has been argued to affect which class of GAG chains that is synthesized and to what extent (Section 1). Gradient retention times can be

used to substitute log *P* values,[174-175] where *P* is the partition coefficient of a compound in two immiscible solvents, usually octanol-water. To elucidate the effect of the spacers on the hydrophobicity of these xylosides, we measured the HPLC retention times using a C18 column with a MeCN gradient in water (0.1% TFA). We observed a clear trend between the retention times of **6**, **34**, **40**, and **129**-**133**, which is correlated to hydrophobicity, and the distance between the xylose part and the aromatic aglycon (Table 10). The hydrophobicity of these xylosides seemed to increase with increasing spacer length, despite the use of OEG spacers.

Table 10. Retention times and xylose-naphthyl distance.

Entry	Xyloside	Rentention time (min)[a]	Xylose-naphthyl distance (nm)[b]
1	**6**	32.25 ± 0.012	0.24
2	**129**	33.39 ± 0.010	0.37
3	**34**	35.61 ± 0.005	0.60
4	**132**	36.90 ± 0.004	0.95
5	**133**	37.70 ± 0.003	1.31
6	**40**	22.26 ± 0.034	0.24
7	**130**	25.97 ± 0.014	0.37
8	**131**	27.22 ± 0.008	0.60

[a] The retention times are the mean values of three separate measurements. The gradient of MeCN was increased from 1 minute by 1.2% per minute.

[b] The xylose-naphthy distances were calculated from the anomeric carbon of xylose to the carbon in position 2 of the naphthyl moiety. The calculations were performed using density functional theory at the B3LYP/6-31G** level and default settings in Spartan'10 for Macintosh.

5.1.2 β4GalT7 assay

In an effort to explore the surroundings of the acceptor pocket of the active site, we investigated xylosides with different aglycons, varying in size, electronic property, and distance to the aromatic moiety, as substrates for β4GalT7. Naphthyl xyloside **6** was used as reference compound to which the activities of the xylosides with the above-mention variations were compared.

In addition to these xylosides, we synthesized and examined the α-analog and L-analog to **6** (**151** and **152**, Figure 30). Both α-xylosides (Section 1.4.3) and L-xylosides (Section 1.4.2) have been reported not to function as GAG primers. As anticipated, **151** and **152** did not induce galactosylation by β4GalT7.

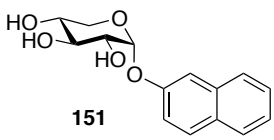

151

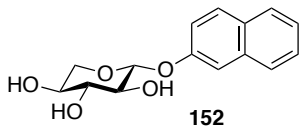

152

Figure 30. 2-Naphthyl α-D-xylopyranoside **151** and 2-naphthyl β-L-xylopyranoside **152**.

5.1.2.1 Variation of aglycon size

Our β4GalT7 assay is based on fluorescence detection (Section 3.1.2), and since methyl xyloside **3** and phenyl xyloside **29** are not fluorescent, it was not possible to detect galactosylation by these compounds with this method. Instead, galactosylation was measured indirectly by adding **6** as well as **3** and **29**, respectively, and measure the decrease in galactosylation of **6**. Even though the concentrations of **3** and **29** were four times that of **6**, a minor decrease of 21% ± 13 for **3** and 44% ± 3 for **29** were observed. This showed that **3** and **29**, compared to **6**, were less efficient substrates for β4GalT7.

The remaining xylosides with different aglycon sizes, namely **38**, **127**, and **128**, were all showed to act as substrates for β4GalT7 (Table 11). The difference in binding orientation of the naphthyl moiety has only a minor effect on the galactosylation (entry 2). The larger xylosides **38** and **128** were galactosylated approximately twice as efficiently as **6** (entries 3 and 4).

Table 11. Kinetic parameters for galactosylation by β4GalT7.

Entry	Compound	Aglycon	K_m (mM)	V_{max} (pmol s^{-1})	k_{cat} (s^{-1})	K_m/k_{cat} (mM^{-1} s^{-1})
1	**6**	2-Naphthyl	0.58	1.1	1.5	2.6
2	**127**	1-Naphthyl	0.57	1.3	1.8	3.2
3	**38**[a]	Biphenyl	0.17	0.72	1.0	6.0
4	**128**[a]	(9-Antracene)-methyl	0.12	0.43	0.60	5.1

[a] Excess-substrate inhibition were observed, hence the kinetic parameters were calculated using the concentrations up to the highest observed reaction rate.

These results are in agreement with earlier cell studies where **3** has been shown to be a less good GAG primer than xylosides with aromatic aglycons,[39] and **29**, **38**, and **127** have been shown to induce GAG priming to a similar extent as **6**.[40] Molecular docking simulations with **6** in the active site of β4GalT7 showed that the aglycon extends from the active site and interacts with the exterior of the enzyme, which mainly consist of aromatic amino acids. The molecular modeling also revealed a π-π interaction between the naphthyl moiety of **6** and the side chain of a tyrosine residue (Tyr^{179} in *Drosophila* β4GalT7 mutant D211N). This interaction is not possible for

3, hence the lower activity. Since only a slight increase in galactosylation efficiency by β4GalT7 of the xylosides containing a larger aglycon than **6** were observed, we suggest that the presumably favorable π-π interaction is not increased to a significant extent by increasing the size of the aromatic aglycon.

5.1.2.2 Variation of the spacer length between xylose and naphthyl moiety

The xylosides **129**, **34**, **132**, and **133**, with increasing distances between xylose and naphthyl, were investigated in our β4GalT7 assay. All xylosides were more efficiently galactosylated by β4GalT7 than **6** (Table 12), where the two derivatives with the longest spacers proved most efficient, with k_{cat}/K_m values approximately 6 times higher than that for **6** (entries 4 and 5). However, no clear correlations between the kinetic parameters and the spacer length and/or hydrophobicity of the xylosides (Section 5.1.1) were observed (Figure 31). Molecular docking simulations indicated that **129**, **34**, **132**, and **133** have a slightly different orientation in the active site compared to **6**, with a more pronounced CH-π interaction from H5 to a tyrosine residue (Tyr^{177} in *Drosophila* β4GalT7 D211N mutant).

Table 12. Kinetic parameters for galactosylation by β4GalT7.

Entry	Compound	Xyl-Nap distance (nm)	K_m (mM)	V_{max} (pmol s^{-1})	k_{cat} (s^{-1})	K_m/k_{cat} (mM^{-1} s^{-1})
1	**6**	0.24	0.77	1.2	1.7	2.2
2	**129**	0.37	0.48	1.9	2.6	5.5
3	**34**	0.60	0.60	2.0	2.7	4.6
4	**132**	0.95	0.091	0.93	1.3	14
5	**133**	1.31	0.24	2.4	3.3	13

Cell studies were also performed with **129**, **34**, **132**, and **133**, using two different cell lines. The investigated xylosides induced GAG priming to a higher extent than **6**, and plotting biological activity versus the xylose-naphthyl distance, a plateau in priming was observed (Figure 31). In addition, the hydroxylated analogs **130** and **131** were also examined and generally showed to prime GAG chains to a larger extent than **40**, and also compared to their non-hydroxylated analogs **129** and **34**. Due to the selective antiproliferative activity of **40**, we investigated the toxicity of **34** and **129-133**. However, none of the xylosides, except **131** showed any distinct selective antiproliferative effect towards the tested cancer cell line (human breast carcinoma cells (HCC70)) compared to the normal cell line (human breast fibroblast cells (CCD-1095Sk)).

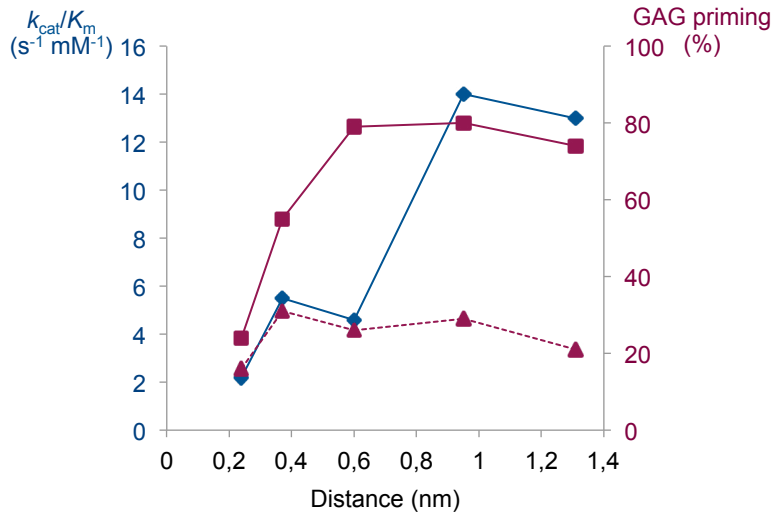

Figure 31. Galactosylation by β4GalT7 and GAG priming plotted versus the distance between the anomeric carbon of xylose to the carbon in position 2 of the naphthyl moiety. The proportion of GAG priming is given as the integrated value of fractions from cells treated with xyloside, divided by the integrated value of fractions from untreated cells. Blue diamonds indicate k_{cat}/K_m values (s^{-1} mM^{-1}), purple solid line with squares indicate GAG priming in human breast fibroblast cells (CCD-1095Sk), and purple dashed line with triangles indicate GAG priming in human breast carcinoma cells (HCC70 cells).

5.1.2.3 Variation of the electronic property of naphthyl substituents

To investigate the effect on galactosylation of naphthyl substituents having different electronic properties ranging from electron-withdrawing to electron-donating, we examined xylosides **40** and **134-136**. They were all galactosylated by β4GalT7 slightly more efficiently then **6** (Table 13). However, no trend in galactosylation could be deduced, which is in agreement with conclusions for a triazole-linked system.[68]

Table 13. Kinetic parameters for galactosylation by β4GalT7.

Entry	Compound	Substituent	K_m (mM)	V_{max} (pmol s^{-1})	k_{cat} (s^{-1})	K_m/k_{cat} (mM^{-1} s^{-1})
1	**6**	H	0.58	1.1	1.5	2.6
2	**134**[a]	OMe	0.58	1.6	2.2	3.8
3	**40**	OH	0.31	1.2	1.6	5.2
4	**135**[a]	CO_2Me	0.31	1.1	1.5	4.8
5	**136**	CN	0.60	2.0	2.8	4.7

[a] Excess-substrate inhibition were observed, hence the kinetic parameters were calculated using the concentrations up to the highest observed reaction rate.

5.2 Arabinosides with different aglycons (Paper III)

Intrigued by our results and others of modifications of the xylose moiety (Section 3.1), the anomeric position (Section 4.2), as well as variations of the aglycon (Section 5.1), we wanted to examine if these findings could be combined to generate an efficient inhibitor. We hypothesized that a xyloside that is an efficient substrate for β4GalT7 will be a good starting point for the design of inhibitors by modifying the xylose part by, e.g. epimerization at C4, thus eliminating the possibility of the compound to act as a substrate.

We decided to synthesize glycosides based on arabinose, since 2-naphthyl α-L-arabinoside **74** is one of the most potent inhibitors we have tested, as it fits in the active site of β4GalT7, but cannot be galactosylated due to the orientation of 4-OH (Section 3.1.2.2). In addition, L-arabinose is commercially available, making arabinosides easily accessible. Furthermore, arabinosides are stable, in contrast to for example the 2-deoxy xyloside **67**. We thus synthesized methyl and phenyl arabinoside as well as naphthyl arabinosides with oxygen, sulfur, or sulfone in the anomeric position, and analogs with either a methylene bridge or a diethylene glycol spacer between arabinose and the naphthyl moiety (**153-158**, Figure 32). These compounds were then tested as inhibitors of β4GalT7.

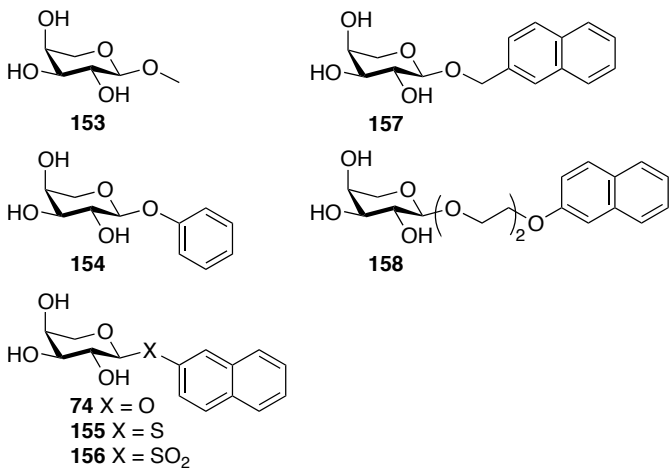

Figure 32. Arabinosides investigated as inhibitors of β4GalT7.

5.2.1 Synthesis of arabinosides

Arabinoside **153** is commercially available and **154**[176] and **74**[47] are known compounds.

Arabinosides **155-157** were synthesized from peracetylated β-L-arabinopyranosyl bromide **159**[177] obtained from L-arabinose in two steps (Scheme 12). For **160**, phase transfer conditions were used to install the thionaphthyl moiety, which is a mild method that usually give excellent anomeric stereoselectivity. This reaction proceeded in modest yield. We also investigated the use of Koenigs-Knorr reaction conditions and the use of acetate donor with $BF_3{\cdot}Et_2O$ for the synthesis of **160**, which did not prove successful. Deacetylation yielded **155** in 95%. Oxidation of the 1-thio derivative **160** with *m*CPBA as described above (Section 4.2.1), generated the sulfone **161** in excellent yield, which was deacetylated to form **156**.

The methylene bridged naphthyl arabinoside **157** was synthesized from the bromide donor **159** using Koenigs-Knorr reaction conditions, i.e. glycosylation in the presence of a silver salt, followed by deacetylation. This procedure could also be used for the glycosylation to form **164**. However, using the acetate donor and $BF_3{\cdot}Et_2O$ increased the yield of **164** from 13% to 30%, calculated from L-arabinose. Hence, this route was used, where acetylation of L-arabinose generated an α/β-mixture (approximately 5.4:1), which was used directly in the glycosylation reaction. Coupling of **164** to 2-naphthol was performed according to the procedure developed for the xyloside analog as previously described (Section 5.1.1), and deacetylation generated arabinoside **158**.

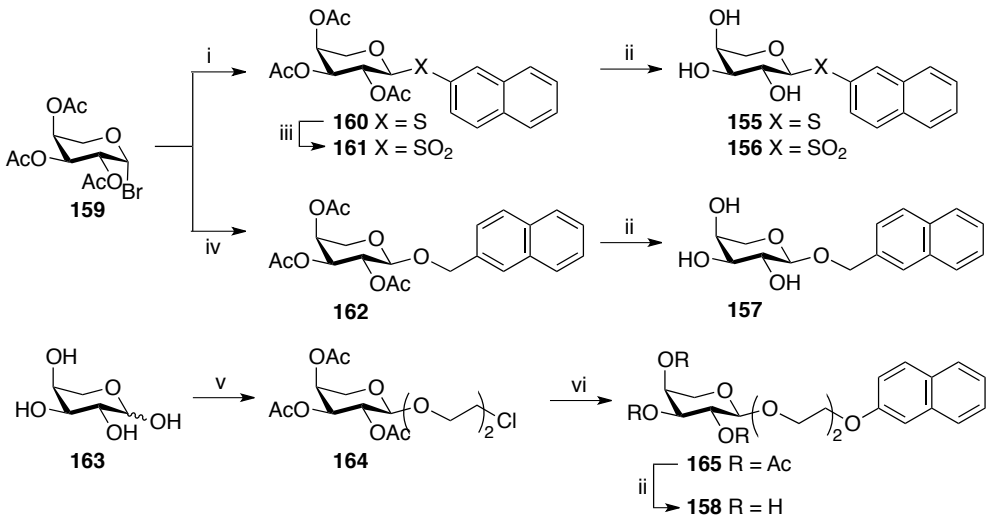

Scheme 12. Reagents and conditions: i) 2-naphthalenethiol, TBAHS, 1 M Na_2SO_4, EtOAc, (39% over three steps from L-arabinose); ii) 1 M NaOMe, MeOH, **155** (95%), **156** (45%), **157** (90%), **158** (90%); iii) *m*CPBA, CH_2Cl_2, 0 °C, (96%); iv) 2-naphthalenemethanol, Ag_2O, 4Å molecular sieves, CH_2Cl_2, (20% over three steps from L-arabinose); v) 1) KOAc, Ac_2O; 2) $BF_3{\cdot}Et_2O$, 2-(2-chlororethoxy)-ethanol, CH_2Cl_2, (30% over two steps from L-arabinose); vi) 2-naphthol, K_2CO_3, 18-crown-6, DMF, 80 °C, (40%).

5.2.2 β4GalT7 assay

To study the inhibitory effect of **153-158** on galactosylation by β4GalT7, we added both xyloside **6** and arabinoside to β4GalT7 and studied the decrease in galactosylation of **6** by β4GalT7 (Section 3.1.2.2). None of the tested arabinosides inhibited galactosylation to the same extent as the previously reported naphthyl arabinoside **74** (Table 14). This clearly shows that the corresponding arabinoside of an efficiently galactosylated xyloside is not necessarily an efficient inhibitor. We therefore conclude that an efficient substrate cannot generally be considered a suitable starting point for the design of efficient inhibitors of β4GalT7.

Table 14. Inhibition of galactosylation of **6** by β4GalT7. The decrease in galactosylated **6** is expressed in % of the amount Gal-**6** formed without added arabinoside.

Entry	Arabinoside	Inhibition (% of control)
1	**153**	11 ± 3
2	**154**	28 ± 8
3	**74**	63 ± 5
4	**155**	22 ± 3
5	**156**	38 ± 3
6	**157**	0
7	**158**	10 ± 0.3

5.3 Disubstituted naphthyl xylosides (Paper V)

In an effort to further study the selective antiproliferative effect of **40**,[82] we wanted to investigate the accompanying decrease in acetylation of histone H3. GAGs and PGs have been shown to inhibit histone acetyltransferases (HATs) (Section 1.6). We hypothesized that it is possible to design xylosides, which act either directly, or more likely, that prime GAG chains that functions as HAT inhibitors. Hence, we synthesized analogs to **40** with substitution patterns in the naphthyl moiety that resembles the aromatic moiety of known natural HAT inhibitors (Figure 18, Section 1.6), i.e. hydroxyl groups and/or methoxy groups in ortho positions with respect to each other (Figure 33). Xylosides **14**, **40**, **134**, and **166-170** were investigated in our β4GalT7 assay and **167-170** were examined in terms of GAG priming ability, HAT and HDAC inhibition, effect on histone H3 acetylation, and antiproliferative activity towards cancer cells and normal cells.

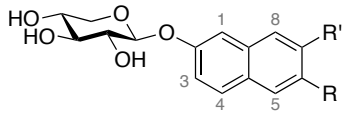

40 R = OH, R' = H
166 R = H, R' = OH
134 R = OMe, R' = H
14 R = H, R' = OMe

167 R = OH, R' = OH
168 R = OH, R' = OMe
169 R = OMe, R = OH
170 R = OMe, R'= OMe

Figure 33. 2-Naphthyl xylosides with different substituents in the naphthyl moiety.

5.3.1 Synthesis of disubstituted naphthyl xylosides

The synthesis towards **167-170** inevitably involves functionalization of the aromatic system, since 2,3,6-nahthalenetriol that would be the aglycon of choice for the synthesis of these compounds is not commercially available. We initially examined the use of Friedel-Crafts acylation, which we envisioned as the first step towards the addition of a hydroxyl functionality in the naphthalene moiety, followed by Baeyer-Villiger oxidation and subsequent hydrolysis of the formed ester. However, the reaction conditions using strong Lewis acids proved too harsh for fully acetylated **40**, and cleavage of the glycosidic bond was observed.

Instead, we turned our focus towards directed ortho metalation (D*o*M), which regioselectively introduces an electrophile ortho to a substituent that functions as a directed metalation group (DMG). This method is relatively mild, and since an ortho relation between the hydroxyl/methoxy groups in **167-170** is desired, we considered this approach appealing, envisioning **40** and **166** as starting points for theses syntheses.

A few oxygen-based DMGs have been reported, including *O*-carbamates that are considered to be one of the most powerful. *O*-Carbamates have been found useful in synthetic strategies of aromatic systems involving D*o*M reactions.[178-181] Hence, we chose to utilize *O*-aryl *N*,*N*-diethyl carbamate as DMG for the synthesis of **167-170**. Several different electrophiles can be introduced to generate the target hydroxyl group, such as boronic esters (oxidized with H_2O_2),[179, 182] dimethylsilane (Fleming-Tamao oxidation),[183] and direct treatment of the lithiated species with lithium *tert*-butyl peroxide.[184-185] We investigated these procedures using 2-naphthyl-*N*,*N*-diethyl *O*-carbamate **171** (Figure 34). Unfortunately, direct treatment by *tert*-butyl hydroperoxide of the lithiated species did not generate the wanted alcohol. Hence, we chose to utilize boronic esters as intermediates in the synthesis of **167-170** since this protocol gave the highest yield of **172** and **173**. In addition to **172** and **173**,

anionic ortho-Fries rearrangement occurred during the reaction, generating **174**, which was also formed in the reaction with chlorodimethylsilane. It is known that **171** is lithiated at both position 1 and 3, with preference for position 3, and that anionic rearrangement of the carbamate occurs,[179, 186] which we also observed.

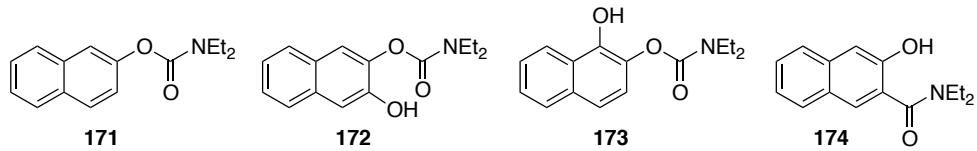

Figure 34. Aromatic hydroxylation of **171** by DoM generated **172**-**174**.

Initially, we examined the possibility to use *N*,*N*-diethyl carbamate as protective group as well, which would shorten the synthetic route compared to the use of other protective groups that have to be introduced and removed orthogonally to the carbamate. However, substituting **40** with *N*,*N*-diethyl carbamate at all hydroxyl positions was not possible. Hence a one-pot procedure was developed where the aromatic hydroxyl group was converted to the *O*-carbamate, followed by benzylation of the aliphatic hydroxyl groups to form **175** (Scheme 13). ortho-Lithiation of **175**, subsequent treatment with $B(OMe)_3$, and oxidation of the formed boronic species with $NaOH/H_2O_2$ generated the desired 7-hydroxylated compound **176** as well as the 5-hydroxylated derivative **177** in 27% and 14% yield, respectively. Fortunately, we observed no anionic ortho-Fries rearrangement during this reaction.

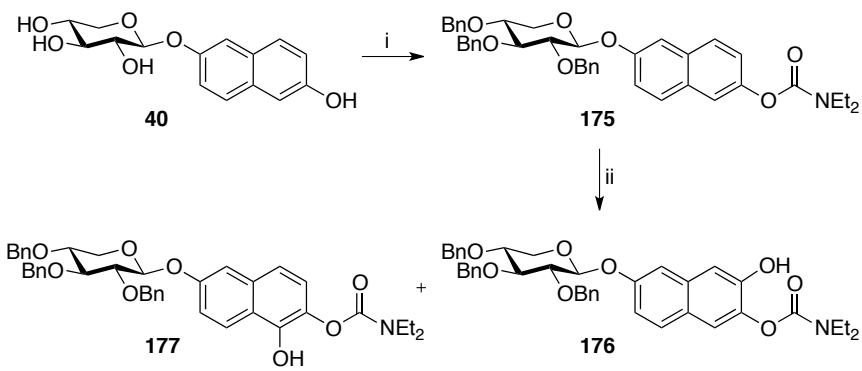

Scheme 13. Reagents and conditions: i) 1) K_2CO_3, Et_2NCOCl, DMF, 80 °C; 2) Bu_4NI, NaH, BnBr, DMF, 0 °C → rt, (55%); ii) 1) TMEDA, *s*-BuLi, $B(OMe)_3$, THF, -78 °C → rt; 2) AcOH, H_2O_2, **176** (53%), **177** (23%).

However, **176** was obtained as an inseparable mixture together with its regioisomer **178** (Figure 35). The carbamate appeared to migrate during the oxidation step from

its original position at O6 to the newly formed, and deprotonated, O7. Carbamoyl migration has been reported to occur when performing a D*o*M reaction with $B(OMe)_3$ and subsequent oxidation of the boronic derivative with NaOH and H_2O_2.[187] In addition, various O → C carbamoyl migrations have been utilized in e.g. the formation of benzofuranones and 4-hydroxycoumarins.[188-189] To circumvent the carbamoyl migration, we instead used H_2O_2 with acetic acid,[190] which generated **176** without formation of the regioisomer **178**. In addition, this oxidizing protocol increased the yield, forming **176** and **177** in 53% and 23% yield, respectively (Scheme 13).

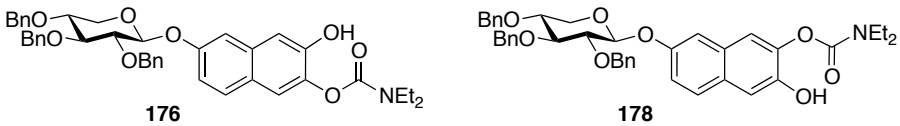

Figure 35. Desired product **176** and its regioisomer formed by carbamate migration.

With the hydroxylated derivative **176** in hand, we performed methylation with MeI and NaH, which formed the desired compound **179** together with its regioisomer **180** (Scheme 14). Using a weaker base such as K_2CO_3 did not prevent carbamoyl migration, and **179** and **180** were isolated in approximately a 3:1 mixture in 91% yield. At this point, deprotection of the aromatic hydroxyl group was achieved by reflux with NaOH in ethanol, generating **181** and **182** as an inseparable mixture in 88% yield. Subsequent hydrogenolysis[112] yielded the desired monomethylated naphthyl xylosides **168** and **169**, which could be separated by HPLC. Performing the deprotection steps in reverse order was not possible, since the debenzylated compounds did not tolerate the harsh hydrolysis conditions. Acidic hydrolysis, reduction with $LiAlH_4$, or the use of Schwartz reagent ($Cp_2Zr(H)Cl$)[191] did not prove successful either. However, with this protocol in hand, generating both **168** and **169**, no further efforts to avoid carbamoyl migration were attempted.

Removing the *O*-carbamate in **176** by basic hydrolysis, as described above, generated only trace amounts of the wanted product **183**. Instead, $LiAlH_4$ reduction of **176** yielded dihydroxy compound **183** in good yield. **183** was then debenzylated to form **167**, or fully methylated before hydrogenolysis to form **170**.

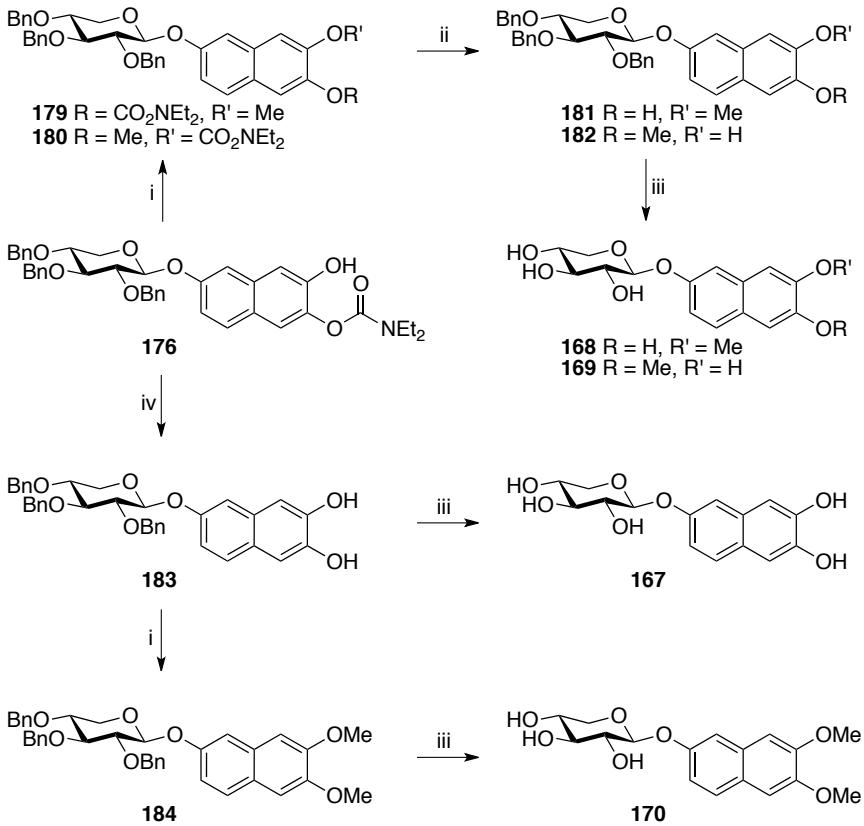

Scheme 14. Reagents and conditions: i) K_2CO_3, MeI, DMF, **179** + **180** (91%), **184** (82%); ii) NaOH, EtOH, refluxe, **181** + **182** (88%); iii) Pd/C, H_2, HCl, DMF, **167** (54%), **168** (41% from **176**), **169** (12% from **176**), **170** (66%); iv) $LiAlH_4$, THF, (81%).

5.3.2 β4GalT7 assay

The disubstituted naphthyl xylosides **167-170** were investigated in our β4GalT7 assay together with **6** and monosubstituted naphthyl xylosides **14**, **40**, **134**, and **166**. Compounds **40** and **134** have been investigated previously (Section 5.1.2.3), but were included as comparison. All investigated xylosides induced galactosylation by β4GalT7, and to approximately the same extent (Table 15). For all of the disubstituted naphthyl xylosides **167-170**, we observed excess-substrate inhibition, hence the kinetic parameters were calculated using the concentrations up to the highest observed reaction rate. **40**,[64] **134**,[78] and **166**[79] have all been shown to induce GAG priming, and **14**[31] was shown by Gulberti et al. to act as a substrate for β4GalT7.

Table 15. Kinetic parameters for galactosylation by β4GalT7.

Entry	Compound	K_m (mM)	V_{max} (pmol s^{-1})	k_{cat} (s^{-1})	K_m/k_{cat} (mM^{-1} s^{-1})
1	**6**	0.76	1.2	1.7	2.2
2	**40**	0.22	0.87	0.98	4.5
3	**166**	0.43	1.1	1.3	3.0
4	**134**	0.72	1.6	1.9	2.6
5	**14**	0.34	0.95	1.1	3.2
6	**167**[a]	0.23	0.81	0.92	3.9
7	**168**[a]	0.12	0.40	0.45	3.8
8	**169**[a]	0.26	1.0	1.1	4.5
9	**170**[a]	0.42	1.2	1.4	3.2

[a] Excess-substrate inhibition were observed, hence the kinetic parameters were calculated using the concentrations up to the highest observed reaction rate.

5.3.3 Cell studies and effect on HAT acetylation

The disubstituted naphthyl xylosides **167-170** were showed to induce GAG priming, as expected from the results of the β4GalT7 assay (Section 5.3.2), and **167** was observed to prime GAG chains to a lesser extent than **168-170**. The GAG priming ability did not correspond to the trend seen in the k_{cat}/K_m values (Table 15), which may be explained by differences in cellular uptake of the xylosides.

To investigate the inhibitory effect on HAT activity by xylosides **167-170**, a commercially available HAT assay with nuclear extracts was used with anacardic acid (**53**) as positive control. We observed approximately 50% reduction of HAT activity for **167-169**, whereas **170** was not affecting the HAT activity to any significant extent (Figure 36). However, none of the xylosides were as efficient as anacardic acid. Interestingly, dimethylation of the phenolic groups in a garcinol (**54**) analog rendered an inactive compound.[108] Furthermore, a study with curcumin (**55**) showed that exchanging the methoxy substituent for a hydroxyl group generated an active compound whereas curcumin itself was inactive in this report.[107] Our results are in line with these observations.

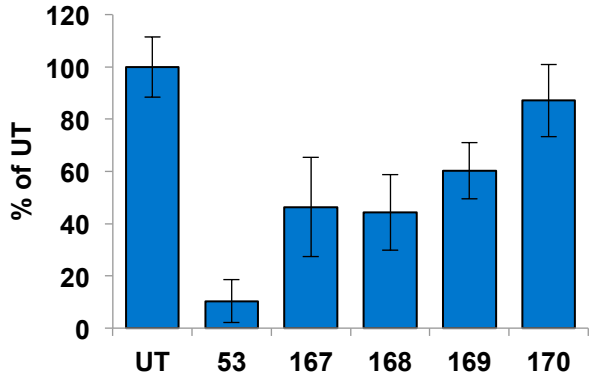

Figure 36. HAT activity upon treatment with xylosides **167**-**170** and anacardic acid (**53**). (Mean values of five separate assays.)

GAG chains primed on **167** and **170** were isolated and examined in the HAT assay. We observed no reduction in HAT activity by these GAG chains. In addition, using a commercially available HDAC assay, we showed that none of the disubstituted naphthyl xylosides **167**-**170** or xyloside-primed GAG chains were inhibitors of HDAC, indicating that **167**-**169** acts specifically on HAT enzymes regarding the inhibition of histone acetylation.

To examine if the result from the HAT assay was transferrable to cell studies, the effect on histone H3 acetylation of **167**-**170** were investigated. Unfortunately, even though we observed inhibition of HAT activity of xylosides **167**-**169** in the nuclear extracts, no reduction of the acetylation of histone H3 in the cells were observed to any great extent. This may be due to the recruitment of the xylosides to the GAG priming machinery, and we showed that the GAG chains are not active regarding reduction of histone acetylation. Finally, investigation of the antiproliferative effect of **167**-**170** showed that none of the xylosides was particularly selectively toxic towards cancer cells. In summary, xylosides **167**-**170** are not functioning as HAT inhibitors.

5.4 Conclusions

In the final part of our investigation of the active site of β4GalT7, we set out to investigate the effect of the aglycon in order to identify efficient substrates with the aim of transferring these structural features to possible inhibitors. In this study, we found that aromatic aglycons, separated from xylose with short OEG spacers generated the most efficient xylosides in terms of galactosylation by β4GalT7. Our

results indicate that the effect of the aglycon originates from a favorable π-π interaction between the aromatic aglycon and a tyrosine residue of β4GalT7.

To elucidate if efficient substrates are a good starting point for the design of inhibitors, we synthesized and tested arabinosides with different aglycons and modifications of the exocyclic position. Unfortunately, we found no efficient inhibitor. We thus conclude that another approach of designing inhibitors is needed. The results are in line with our suggestion that small differences in the binding orientation in the active site of β4GalT7 affects the activity to a great extent.

In addition, disubstituted naphthyl xylosides were investigated as possible HAT inhibitors in an effort to explore the antiproliferative effect observed for **40**. However, none of the investigated compounds, or xyloside-primed GAG chains, functioned as HAT inhibitors in cells.

6 Concluding remarks and future perspectives

We set out to pinpoint the structural requirements for efficient substrates and efficient inhibitors of β4GalT7, by performing synthetic modifications of the xylose moiety, the endocyclic and exocyclic positions, and the aglycon.

The results from our studies clearly demonstrate the importance of all three hydroxyl groups of the xylose moiety for galactosylation by β4GalT7to occur efficiently. The acceptor binding pocket of β4GalT7 is shallow and decorated with a precise set of hydrogen bond acceptors. Generally, no modifications at position 3 are accepted by β4GalT7, whereas deoxygenation at position 2 and various modifications at position 4 generate inhibitors. Small substituents in the equatorial position at C4, such as methyl and ethyl, fits in the active site of β4GalT7, whereas the donor UDP-Gal limits the available space in the axial position. Specifically, the arabinose analogs, i.e. epimerization at position 4 of the parent xyloside, and the 4-deoxy-4-fluoro analog were active in terms of inhibition of β4GalT7.

Further on, we demonstrate that exchanging the endocyclic and/or exocyclic oxygen atom for sulfur generates xyloside analogs with more potent galactosylation activity towards β4GalT7 compared to the parent xyloside. We found that the 1,5-dithio analog and the exocyclic sulfone were the most efficiently galactosylated substrates.

We also show that aromatic aglycons, especially when separated from the xylose moiety by a short OEG spacer, generate xylosides that are efficient substrates for β4GalT7.

With the results of our β4GalT7 assay in combination with conformational analysis by NMR spectroscopy and molecular docking simulations, we propose that the above-mentioned modifications of the endocyclic and exocyclic positions as well as the variations of the aglycon affect the binding orientation of these compounds in the acceptor binding pocket of β4GalT7. Even though some of these interactions only differ to a small extent, significant variations in the activity can be observed. In addition to the interactions seen between the xylose moiety and amino acids in the active site, we suggest that a favorable π-π interaction between the aromatic aglycon and a tyrosine residue of β4GalT7 may have a pronounced effect on the activity of the xylosides.

All these results were used in an attempt to design efficient inhibitors. The structural features generating efficient substrates, i.e. sulfur and sulfone in the exocyclic position and separation of the aromatic aglycon and xylose by a spacer, were combined with a modification of the xylose moiety shown to give an inhibitor, i.e. epimerization at C4. We hypothesized that these compounds would be potent inhibitors of β4GalT7. However, we found only modest to weak inhibition by these arabinosides. Hence, we conclude that another approach is needed for the design of inhibitors.

To summarize, we have performed a series of studies involving modifications of different positions of naphthyl xyloside and concluded that modifying the endocyclic and exocyclic positions as well as varying the aglycon can generate efficient substrates (Figure 37). Molecular docking simulations with β4GalT7 and analogs with modifications at the endocyclic and exocyclic positions are still ongoing to determine the exact origin of this efficiency.

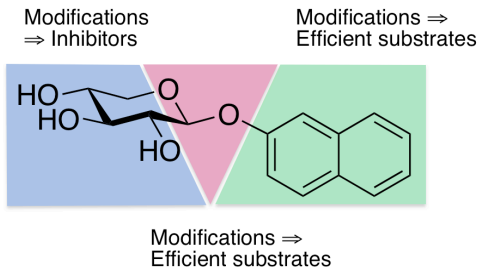

Figure 37. Effects of modifications of the xylose moiety, the endocyclic and exocyclic positions, and the aglycon on the β4GalT7 activity.

Strong inhibitors would be valuable tools in GAG research. However, it still remains unclear what makes a good inhibitor of β4GalT7. Our investigations set the stage for further studies. To our knowledge, transition state analogs have not been synthesized and tested as inhibitors of β4GalT7. UDP is required for the conformational change of β4GalT7 from an open structure to a closed structure forming the acceptor binding pocket. It would be highly interesting to investigate e.g. xylosides connected to a UDP moiety via O4 and a short spacer. Such analogs may possess interesting biological features with different kinetic parameters to what we have observed for our compounds so far. Furthermore, naphthyl arabinosides with aromatic substituents designed to interact with nearby amino acids of β4GalT7 might prove to be efficient inhibitors.

7 Acknowledgements

Detta arbete hade inte varit möjligt att genomföra utan följande personer, därmed vill jag rikta ett stort tack till…

Ulf Ellervik, min handledare, för att du tog in mig i din grupp och för allt du har lärt mig. Du är en av de absolut mest positiva människor jag någonsin träffat. Din entusiasm och oändliga optimism är inspirerande.

Sophie Manner, min biträdande handledare, för att du är allt en biträdande handledare bör vara. Det är få förunnat att få dela labb med en sådan källa av kunskap – både när det gäller kemi och allt annat som är viktigt och mindre viktigt här i livet.

Grupp UE, från då och nu, för att ni har gjort arbetet och livet i labbet till en fröjd, särskilt:

Anna Siegbahn, för att du är en great mind! Inte visste jag när jag började i gruppen att jag skulle hitta en sådan klippa som är gjord av det rätta virket. Du ska även ha stort tack för att du korrekturläst detta alster.

Markus Ohlin, för att du alltid är så himla glad och positiv och gärna delar med dig av tips och trix.

Andrea Persson, för allt arbete du gör på BMC, och för att du är noggrann och nitisk.

Emil Tykesson, för att du är allt man kan önska av en kollega, ingenting är svårt eller besvärligt när man frågar dig om hjälp.

Daniel Willén, för att du faktiskt har stått ut med en ganska stressad kollega ända sedan du kom till vårt labb och för att du första julen överlevde all julmusik.

Göran Widmalm och medlemmar av *grupp GW* som har varit involverade i alla projekt genom årens gång, för ett trevligt och mycket givande samarbete.

Maria Levin, *Bodil Eliasson* och *Katarina Fredriksson*, för all hjälp och allt stöd som ni bidragit med, ni är avdelningens ryggrad.

Sofia Essén och *Einar Nilsson*, för alla HRMS som ni kört genom åren.

Magnus Johnson, för att du snabbt och smidigt har kört röntgenkristallografi.

Karl-Erik Bergquist och *Anders Sundin*, för support vid problem med NMR och IT.

Alla seniorer på CAS som delar med sig av sin enorma kunskap.

Alla kollegor på CAS, från då och nu, för att ni har gjort detta till en trevlig arbetsplats, särskilt fikamaffian: *Dan Killander*, *Ritha Gidlöf*, *Eira Ruud Furuseth*, *Rikard Larsson*, *Torbjörn Wixe*, *Björn Borgström*, *Alexander Holmkvist*, *Kristoffer Peterson*, *Victor Abrahamsson*, och fler därtill. Det är framför allt ni som förgyllt arbetsdagen med massa skratt och mycket udda samtalsämnen och sett till (så länge fikamaffian fortfarande fanns) att jag tog fikapauser.

Min familj, för att ni är så positiva fast att ni inte har en aning om vad det är jag gör om dagarna, särskilt:

Mor och *Far* för att ni alltid är så stöttande och tror att jag klarar allt jag tar mig för. Er support genom alla år har varit ovärderlig. Jag är enormt tacksam för det och för allt ni gjort för mig.

Marcus, min älskade man, för att vi skrattar så mycket tillsammans och för att du tror på mig och får mig att kämpa vidare. Utan dig hade detta inte varit möjligt. Äntligen börjar ett nytt kapitel i vårt liv.

Alva, vår fina lilla tjej, som förgyller vår tillvaro genom sin blotta närvaro och med sitt underbara skratt. Du är det bästa som hänt mig!

References

1. McNaught, A. D. *Carbohydr. Res.* **1997**, *297*, 1-92.
2. Thorsheim, K.; Siegbahn, A.; Johnsson Richard, E.; Manner, S.; Stalbrand, H.; Widmalm, G.; Ellervik, U. *Carbohydr Res* **2015**, *418*, 65-88.
3. Gulati, K.; Poluri, K. M. *Glycoconjugate J.* **2016**, *33*, 1-17.
4. Kamhi, E.; Joo Eun, J.; Dordick Jonathan, S.; Linhardt Robert, J. *Biol. Rev.* **2013**, *88*, 928-943.
5. Afratis, N.; Gialeli, C.; Nikitovic, D.; Tsegenidis, T.; Karousou, E.; Theocharis, A. D.; Pavao, M. S.; Tzanakakis, G. N.; Karamanos, N. K. *Febs J.* **2012**, *279*, 1177-1197.
6. Yamada, S.; Sugahara, K. *Curr. Drug Discovery Technol.* **2008**, *5*, 289-301.
7. Yip, G. W.; Smollich, M.; Götte, M. *Mol. Cancer Ther.* **2006**, *5*, 2139-2148.
8. Gotting, C.; Kuhn, J.; Zahn, R.; Brinkmann, T.; Kleesiek, K. *J. Mol. Biol.* **2000**, *304*, 517-528.
9. Gotting, C.; Kuhn, J.; Kleesiek, K. *Cell. Mol. Life Sci.* **2007**, *64*, 1498-1517.
10. Okajima, T.; Yoshida, K.; Kondo, T.; Furukawa, K. *J. Biol. Chem.* **1999**, *274*, 22915-22918.
11. Almeida, R.; Levery, S. B.; Mandel, U.; Kresse, H.; Schwientek, T.; Bennett, E. P.; Clausen, H. *J. Biol. Chem.* **1999**, *274*, 26165-26171.
12. Bai, X.; Zhou, D.; Brown, J. R.; Crawford, B. E.; Hennet, T.; Esko, J. D. *J. Biol. Chem.* **2001**, *276*, 48189-48195.
13. Kitagawa, H.; Tone, Y.; Tamura, J.-i.; Neumann, K. W.; Ogawa, T.; Oka, S.; Kawasaki, T.; Sugahara, K. *J. Biol. Chem.* **1998**, *273*, 6615-6618.
14. Mikami, T.; Kitagawa, H. *Biochim. Biophys. Acta, Gen. Subj.* **2013**, *1830*, 4719-4733.
15. Sugahara, K.; Kitagawa, H. *IUBMB Life* **2002**, *54*, 163-175.
16. Mizumoto, S.; Ikegawa, S.; Sugahara, K. *J. Biol. Chem.* **2013**, *288*, 10953-10961.
17. Götte, M.; Kresse, H. *Biochem. Genet.* **2005**, *43*, 65-77.
18. Seidler, D. G.; Faiyaz-Ul-Haque, M.; Hansen, U.; Yip, G. W.; Zaidi, S. H. E.; Teebi, A. S.; Kiesel, L.; Götte, M. *J. Mol. Med.* **2006**, *84*, 583-594.
19. Bui, C.; Talhaoui, I.; Chabel, M.; Mulliert, G.; Coughtrie, M. W. H.; Ouzzine, M.; Fournel-Gigleux, S. *FEBS Lett.* **2010**, *584*, 3962-3968.
20. Rahuel-Clermont, S.; Daligault, F.; Piet, M.-H.; Gulberti, S.; Netter, P.; Branlant, G.; Magdalou, J.; Lattard, V. *Biochem. J.* **2010**, *432*, 303-311.
21. Daligault, F.; Rahuel-clermont, S.; Gulberti, S.; Cung, M.-T.; Branlant, G.; Netter, P.; Magdalou, J.; Lattard, V. *Biochem. J.* **2009**, *418*, 605-614.
22. Ramakrishnan, B.; Qasba, P. K. *J. Biol. Chem.* **2010**, *285*, 15619-15626.
23. Tsutsui, Y.; Ramakrishnan, B.; Qasba, P. K. *J. Biol. Chem.* **2013**, *288*, 31963-31970.

24. Saliba, M.; Ramalanjaona, N.; Gulberti, S.; Bertin-Jung, I.; Thomas, A.; Dahbi, S.; Lopin-Bon, C.; Jacquinet, J.-C.; Breton, C.; Ouzzine, M.; Fournel-Gigleux, S. *J. Biol. Chem.* **2015**, *290*, 7658-7670.
25. Helting, T.; Roden, L. *J. Biol. Chem.* **1969**, *244*, 2790-2798.
26. Schwartz, N. B.; Roden, L. *J. Biol. Chem.* **1975**, *250*, 5200-5207.
27. Robinson, H. C.; Brett, M. J.; Tralaggan, P. J.; Lowther, D. A.; Okayama, M. *Biochem. J.* **1975**, *148*, 25-34.
28. Esko, J. D.; Weinke, J. L.; Taylor, W. H.; Ekborg, G.; Roden, L.; Anantharamaiah, G.; Gawish, A. *J. Biol. Chem.* **1987**, *262*, 12189-12195.
29. Higuchi, T.; Tamura, S.; Takagaki, K.; Nakamura, T.; Morikawa, A.; Tanaka, K.; Tanaka, A.; Saito, Y.; Endo, M. *J. Biochem. Biophys. Methods* **1994**, *29*, 135-142.
30. Parker, G. J.; Handley, C. J.; Robinson, H. C. *Anal. Biochem.* **1995**, *226*, 154-160.
31. Gulberti, S.; Lattard, V.; Fondeur, M.; Jacquinet, J.-C.; Mulliert, G.; Netter, P.; Magdalou, J.; Ouzzine, M.; Fournel-Gigleux, S. *J. Biol. Chem.* **2005**, *280*, 1417-1425.
32. Talhaoui, I.; Bui, C.; Oriol, R.; Mulliert, G.; Gulberti, S.; Netter, P.; Coughtrie, M. W. H.; Ouzzine, M.; Fournel-Gigleux, S. *J. Biol. Chem.* **2010**, *285*, 37342-37358.
33. Pasek, M.; Boeggeman, E.; Ramakrishnan, B.; Qasba, P. K. *Biochem. Biophys. Res. Commun.* **2010**, *394*, 679-684.
34. Garcia-Garcia, J. F.; Corrales, G.; Casas, J.; Fernandez-Mayoralas, A.; Garcia-Junceda, E. *Mol. BioSyst.* **2011**, *7*, 1312-1321.
35. Okayama, M.; Kimata, K.; Suzuki, S. *J. Biochem.* **1973**, *74*, 1069-1073.
36. Schwartz, N. B.; Galligani, L.; Ho, P.-L.; Dorfman, A. *Proc. Natl. Acad. Sci. U. S. A.* **1974**, *71*, 4047-4051.
37. Galligani, L.; Hopwood, J.; Schwartz, N. B.; Dorfman, A. *J. Biol. Chem.* **1975**, *250*, 5400-5406.
38. Robinson, J. A.; Robinson, H. C. *Biochem. J.* **1981**, *194*, 839-846.
39. Lugemwa, F. N.; Esko, J. D. *J. Biol. Chem.* **1991**, *266*, 6674-6677.
40. Fritz, T. A.; Lugemwa, F. N.; Sarkar, A. K.; Esko, J. D. *J. Biol. Chem.* **1994**, *269*, 300-307.
41. Lugemwa, F. N.; Sarkar, A. K.; Esko, J. D. *J. Biol. Chem.* **1996**, *271*, 19159-19165.
42. Ueno, M.; Yamada, S.; Zako, M.; Bernfield, M.; Sugahara, K. *J. Biol. Chem.* **2001**, *276*, 29134-29140.
43. Wen, J.; Xiao, J.; Rahdar, M.; Choudhury, B. P.; Cui, J.; Taylor, G. S.; Esko, J. D.; Dixon, J. E. *Proc. Natl. Acad. Sci. U. S. A.* **2014**, *111*, 15723-15728.
44. Garud, D. R.; Tran, V. M.; Victor, X. V.; Koketsu, M.; Kuberan, B. *J. Biol. Chem.* **2008**, *283*, 28881-28887.
45. Tsuzuki, Y.; Nguyen, T. K. N.; Garud, D. R.; Kuberan, B.; Koketsu, M. *Bioorg. Med. Chem. Lett.* **2010**, *20*, 7269-7273.
46. Raman, K.; Ninomiya, M.; Nguyen, T. K. N.; Tsuzuki, Y.; Koketsu, M.; Kuberan, B. *Biochem. Biophys. Res. Commun.* **2011**, *404*, 86-89.
47. Siegbahn, A.; Aili, U.; Ochocinska, A.; Olofsson, M.; Roennols, J.; Mani, K.; Widmalm, G.; Ellervik, U. *Bioorg. Med. Chem.* **2011**, *19*, 4114-4126.
48. Shaukat, I.; Barre, L.; Venkatesan, N.; Li, D.; Jaquinet, J.-C.; Fournel-Gigleux, S.; Ouzzine, M. *PLoS One* **2016**, *11*, 1-22.

49. Schwarz, J. C. P.; Yule, K. C. *Proc. Chem. Soc., London* **1961**, 417.
50. Adley, T. J.; Owen, L. N. *Proc. Chem. Soc., London* **1961**, 418.
51. Whistler, R. L.; Feather, M. S.; Ingles, D. L. *J. Am. Chem. Soc.* **1962**, *84*, 122.
52. Ingles, D. L.; Whistler, R. L. *J. Org. Chem.* **1962**, *27*, 3896-3898.
53. Adley, T. J.; Owen, L. N. *J. Chem. Soc. C* **1966**, 1287-1290.
54. Teien, A. N.; Abildgaard, U.; Hook, M. *Thromb. Res.* **1976**, *8*, 859-867.
55. Bellamy, F.; Horton, D.; Millet, J.; Picart, F.; Samreth, S.; Chazan, J. B. *J. Med. Chem.* **1993**, *36*, 898-903.
56. Bellamy, F.; Barberousse, V.; Martin, N.; Masson, P.; Millet, J.; Samreth, S.; Sepulchre, C.; Theveniaux, J.; Horton, D. *Eur. J. Med. Chem.* **1995**, *30*, 101s-115s.
57. Masson, P. J.; Coup, D.; Millet, J.; Brown, N. L. *J. Biol. Chem.* **1995**, *270*, 2662-2668.
58. Toomey, J. R.; Abboud, M. A.; Valocik, R. E.; Koster, P. F.; Burns-Kurtis, C. L.; Pillarisetti, K.; Danoff, T. M.; Erhardt, J. A. *J. Thromb. Haemost.* **2006**, *4*, 1989-1996.
59. Myers, A. L.; Upreti, V. V.; Khurana, M.; Eddington, N. D. *J. Clin. Pharmacol.* **2008**, *48*, 1158-1170.
60. Arjona, O.; Gomez, A. M.; Lopez, J. C.; Plumet, J. *Chem. Rev.* **2007**, *107*, 1919-2036.
61. Jeanneret, V.; Vogel, P.; Renaut, P.; Millet, J.; Theveniaux, J.; Barberousse, V. *Bioorg. Med. Chem. Lett.* **1998**, *8*, 1687-1688.
62. Renaut, P.; Millet, J.; Sepulchre, C.; Theveniaux, J.; Barberousse, V.; Jeanneret, V.; Vogel, P. *Helv. Chim. Acta* **1998**, *81*, 2043-2052.
63. Malmberg, J.; Mani, K.; Saewen, E.; Wiren, A.; Ellervik, U. *Bioorg. Med. Chem.* **2006**, *14*, 6659-6665.
64. Mani, K.; Havsmark, B.; Persson, S.; Kaneda, Y.; Yamamoto, H.; Sakurai, K.; Ashikari, S.; Habuchi, H.; Suzuki, S.; Kimata, K.; Malmstrom, A.; Westergren-Thorsson, G.; Fransson, L.-A. *Cancer Res.* **1998**, *58*, 1099-1104.
65. Fukunaga, Y.; Sobue, M.; Suzuki, N.; Kushida, H.; Suzuki, S. *Biochim Biophys Acta* **1975**, *381*, 443-447.
66. Kolset, S. O.; Sakurai, K.; Ivhed, I.; Oevervatn, A.; Suzuki, S. *Biochem. J.* **1990**, *265*, 637-645.
67. Freeze, H. H.; Sampath, D.; Varki, A. *J. Biol. Chem.* **1993**, *268*, 1618-1627.
68. Kuberan, B.; Ethirajan, M.; Victor, X. V.; Tran, V.; Nguyen, K.; Do, A. *ChemBioChem* **2008**, *9*, 198-200.
69. Sobue, M.; Habuchi, H.; Ito, K.; Yonekura, H.; Oguri, K.; Sakurai, K.; Kamohara, S.; Ueno, Y.; Noyori, R.; Suzuki, S. *Biochem. J.* **1987**, *241*, 591-601.
70. Jacobsson, M.; Mani, K.; Ellervik, U. *Bioorg. Med. Chem.* **2007**, *15*, 5283-5299.
71. Pineau, N.; Carrino, D. A.; Caplan, A. I.; Breton, L. *Eur. J. Dermatol.* **2011**, *21*, 359-370.
72. Wang, L.; Maniglia, C. A.; Mella, S. L.; Sartorelli, A. C. *J. Med. Chem.* **1983**, *26*, 629-632.
73. Victor, X. V.; Nguyen, T. K. N.; Ethirajan, M.; Tran, V. M.; Nguyen, K. V.; Kuberan, B. *J. Biol. Chem.* **2009**, *284*, 25842-25853.

74. Tran, V. M.; Victor, X. V.; Yockman, J. W.; Kuberan, B. *Glycoconjugate J.* **2010**, *27*, 625-633.
75. Nguyen, T. K. N.; Tran, V. M.; Sorna, V.; Eriksson, I.; Kojima, A.; Koketsu, M.; Loganathan, D.; Kjellen, L.; Dorsky, R. I.; Chien, C.-B.; Kuberan, B. *ACS Chem. Biol.* **2013**, *8*, 939-948.
76. Tran, V. M.; Kuberan, B. *Bioconjugate Chem.* **2014**, *25*, 262-268.
77. Raman, K.; Kuberan, B. *Mol. BioSyst.* **2010**, *6*, 1800-1802.
78. Mani, K.; Belting, M.; Ellervik, U.; Falk, N.; Svensson, G.; Sandgren, S.; Cheng, F.; Fransson, L.-A. *Glycobiology* **2004**, *14*, 387-397.
79. Jacobsson, M.; Ellervik, U.; Belting, M.; Mani, K. *J. Med. Chem.* **2006**, *49*, 1932-1938.
80. Johnsson, R.; Mani, K.; Ellervik, U. *Bioorg. Med. Chem.* **2007**, *15*, 2868-2877.
81. Nilsson, U.; Jacobsson, M.; Johnsson, R.; Mani, K.; Ellervik, U. *Bioorg. Med. Chem. Lett.* **2009**, *19*, 1763-1766.
82. Nilsson, U.; Johnsson, R.; Fransson, L.-A.; Ellervik, U.; Mani, K. *Cancer Res.* **2010**, *70*, 3771-3779.
83. Persson, A.; Tykesson, E.; Westergren-Thorsson, G.; Malmstroem, A.; Ellervik, U.; Mani, K. *J. Biol. Chem.* **2016**, *291*, 14871-14882.
84. Abrahamsson, C.-O.; Ellervik, U.; Eriksson-Bajtner, J.; Jacobsson, M.; Mani, K. *Carbohydr. Res.* **2008**, *343*, 1473-1477.
85. Johnsson, R.; Mani, K.; Cheng, F.; Ellervik, U. *J. Org. Chem.* **2006**, *71*, 3444-3451.
86. Johnsson, R.; Mani, K.; Ellervik, U. *Bioorg. Med. Chem. Lett.* **2007**, *17*, 2338-2341.
87. Chatron-Colliet, A.; Brusa, C.; Bertin-Jung, I.; Gulberti, S.; Ramalanjaona, N.; Fournel-Gigleux, S.; Brezillon, S.; Muzard, M.; Plantier-Royon, R.; Remond, C.; Wegrowski, Y. *Chem. Biol. Drug Des.* **2017**, *89*, 319-326.
88. Reed, M. C.; Lieb, A.; Nijhout, H. F. *BioEssays* **2010**, *32*, 422-429.
89. Kaiser, P. M. *J. Mol. Catal.* **1980**, *8*, 431-442.
90. Shahbazian, M. D.; Grunstein, M. *Annu. Rev. Biochem.* **2007**, *76*, 75-100.
91. Roth, S. Y.; Denu, J. M.; Allis, C. D. *Annu. Rev. Biochem.* **2001**, *70*, 81-120.
92. Grunstein, M. *Nature* **1997**, *389*, 349-352.
93. Glozak, M. A.; Sengupta, N.; Zhang, X. H.; Seto, E. *Gene* **2005**, *363*, 15-23.
94. Jones, P. *Med. Chem. Commun.* **2012**, *3*, 135-161.
95. Biancotto, C.; Frige, G.; Minucci, S. *Adv. Genet.* **2010**, *70*, 341-386.
96. Minucci, S.; Pelicci, P. G. *Nat. Rev. Cancer* **2006**, *6*, 38-51.
97. Watt, S. A.; South, A. P. *Drug Delivery Lett.* **2013**, *3*, 149-158.
98. Dal Piaz, F.; Vassallo, A.; Rubio, O. C.; Castellano, S.; Sbardella, G.; De Tommasi, N. *Mol. Divers.* **2011**, *15*, 401-416.
99. Lau, O. D.; Kundu, T. K.; Soccio, R. E.; Ait-Si-Ali, S.; Khalil, E. M.; Vassilev, A.; Wolffe, A. P.; Nakatani, Y.; Roeder, R. G.; Cole, P. A. *Mol. Cell* **2000**, *5*, 589-595.
100. Stimson, L.; Rowlands, M. G.; Newbatt, Y. M.; Smith, N. F.; Raynaud, F. I.; Rogers, P.; Bavetsias, V.; Gorsuch, S.; Jarman, M.; Bannister, A.; Kouzarides, T.; McDonald, E.; Workman, P.; Aherne, G. W. *Mol. Cancer Ther.* **2005**, *4*, 1521-1532.
101. Mai, A.; Rotili, D.; Tarantino, D.; Ornaghi, P.; Tosi, F.; Vicidomini, C.; Sbardella, G.; Nebbioso, A.; Miceli, M.; Altucci, L.; Filetici, P. *J. Med. Chem.* **2006**, *49*, 6897-6907.

102. Mai, A.; Rotili, D.; Tarantino, D.; Nebbioso, A.; Castellano, S.; Sbardella, G.; Tini, M.; Altucci, L. *Bioorg. Med. Chem. Lett.* **2009**, *19*, 1132-1135.
103. Balasubramanyam, K.; Swaminathan, V.; Ranganathan, A.; Kundu, T. K. *J. Biol. Chem.* **2003**, *278*, 19134-19140.
104. Balasubramanyam, K.; Altaf, M.; Varier, R. A.; Swaminathan, V.; Ravindran, A.; Sadhale, P. P.; Kundu, T. K. *J. Biol. Chem.* **2004**, *279*, 33716-33726.
105. Balasubramanyam, K.; Varier, R. A.; Altaf, M.; Swaminathan, V.; Siddappa, N. B.; Ranga, U.; Kundu, T. K. *J. Biol. Chem.* **2004**, *279*, 51163-51171.
106. Gupta, S. C.; Patchva, S.; Aggarwal, B. B. *The AAPS Journal* **2013**, *15*, 195-218.
107. Costi, R.; Di Santo, R.; Artico, M.; Miele, G.; Valentini, P.; Novellino, E.; Cereseto, A. *J. Med. Chem.* **2007**, *50*, 1973-1977.
108. Mantelingu, K.; Reddy, B. A.; Swaminathan, V.; Kishore, A. H.; Siddappa, N. B.; Kumar, G. V.; Nagashankar, G.; Natesh, N.; Roy, S.; Sadhale, P. P.; Ranga, U.; Narayana, C.; Kundu, T. K. *Chem. Biol.* **2007**, *14*, 645-657.
109. Eliseeva, E. D.; Valkov, V.; Jung, M.; Jung, M. O. *Mol. Cancer Ther.* **2007**, *6*, 2391-2398.
110. Buczek-Thomas, J. A.; Hsia, E.; Rich, C. B.; Foster, J. A.; Nugent, M. A. *J. Cell. Biochem.* **2008**, *105*, 108-120.
111. Ramani, V. C.; Purushothaman, A.; Stewart, M. D.; Thompson, C. A.; Vlodavsky, I.; Au, J. L. S.; Sanderson, R. D. *Febs J.* **2013**, *280*, 2294-2306.
112. Ochocinska, A.; Siegbahn, A.; Ellervik, U. *Tetrahedron Lett.* **2010**, *51*, 5200-5202.
113. Siegbahn, A. Naphthoxylosides - Probing the β4GalT7 active site. Lund University, 2014.
114. de Lederkremer, R. M.; Marino, C. *Adv. Carbohydr. Chem. Biochem.* **2007**, *61*, 143-216.
115. Aljahdali, A. Z.; Shi, P.; Zhong, Y.; O'Doherty, G. A. *Adv. Carbohydr. Chem. Biochem.* **2013**, *69*, 55-123.
116. Kirschning, A.; Jesberger, M.; Schoning, K.-U. *Synthesis* **2001**, 507-540.
117. Kozikowski, A. P.; Ghosh, A. K. *J. Org. Chem.* **1985**, *50*, 3017-3019.
118. Romero, J. A. C.; Tabacco, S. A.; Woerpel, K. A. *J. Am. Chem. Soc.* **2000**, *122*, 168-169.
119. Ji, Y.; Benkovics, T.; Beutner, G. L.; Sfouggatakis, C.; Eastgate, M. D.; Blackmond, D. G. *J. Org. Chem.* **2015**, *80*, 1696-1702.
120. Barton, D. H. R.; McCombie, S. W. *J. Chem. Soc., Perkin Trans. 1* **1975**, 1574-1585.
121. Crich, D.; Quintero, L. *Chem. Rev.* **1989**, *89*, 1413-1432.
122. Baguley, P. A.; Walton, J. C. *Angew. Chem., Int. Ed.* **1998**, *37*, 3072-3082.
123. Chatgilialoglu, C. *Acc. Chem. Res.* **1992**, *25*, 188-194.
124. Barton, D. H. R.; Jang, D. O.; Jaszberenyi, J. C. *J. Org. Chem.* **1993**, *58*, 6838-6842.
125. Barton, D. H. R.; Jacob, M. *Tetrahedron Lett.* **1998**, *39*, 1331-1334.
126. Studer, A.; Amrein, S.; Schleth, F.; Schulte, T.; Walton, J. C. *J. Am. Chem. Soc.* **2003**, *125*, 5726-5733.
127. Spiegel, D. A.; Wiberg, K. B.; Schacherer, L. N.; Medeiros, M. R.; Wood, J. L. *J. Am. Chem. Soc.* **2005**, *127*, 12513-12515.
128. Park, H. S.; Lee, H. Y.; Kim, Y. H. *Org. Lett.* **2005**, *7*, 3187-3190.

129. Ueng, S.-H.; Fensterbank, L.; Lacote, E.; Malacria, M.; Curran, D. P. *Org. Lett.* **2010**, *12*, 3002-3005.
130. Lee, A. W. M.; Chan, W. H.; Wong, H. C.; Wong, M. S. *Synth. Commun.* **1989**, *19*, 547-552.
131. Schlessinger, R. H.; Schultz, J. A. *J. Org. Chem.* **1983**, *48*, 407-408.
132. Namchuk, M. N.; McCarter, J. D.; Becalski, A.; Andrews, T.; Withers, S. G. *J. Am. Chem. Soc.* **2000**, *122*, 1270-1277.
133. Jensen, H. H.; Bols, M. *Acc. Chem. Res.* **2006**, *39*, 259-265.
134. Majetich, G.; Irvin, T. C.; Thompson, S. B. *Tetrahedron Lett.* **2015**, *56*, 3326-3329.
135. Jin, J.; Newcomb, M. *J. Org. Chem.* **2007**, *72*, 5098-5103.
136. Hagiwara, H.; Kobayashi, K.; Miya, S.; Hoshi, T.; Suzuki, T.; Ando, M. *Org. Lett.* **2001**, *3*, 251-254.
137. Tanaka, R.; Ohishi, K.; Takanashi, N.; Nagano, T.; Suizu, H.; Suzuki, T.; Kobayashi, S. *Org. Lett.* **2012**, *14*, 4886-4889.
138. Salvatore, R. N.; Sahab, S.; Jung, K. W. *Tetrahedron Lett.* **2001**, *42*, 2055-2058.
139. Nagle, A. S.; Salvatore, R. N.; Cross, R. M.; Kapxhiu, E. A.; Sahab, S.; Yoon, C. H.; Jung, K. W. *Tetrahedron Lett.* **2003**, *44*, 5695-5698.
140. Villemin, D.; Hachemi, M. *Synth. Commun.* **1996**, *26*, 2449-2459.
141. Chaturvedi, D.; Ray, S. *Monatsh. Chem.* **2006**, *137*, 1219-1223.
142. Chaturvedi, D.; Ray, S. *J. Sulfur Chem.* **2006**, *27*, 265-270.
143. Singh, S. K.; Singh, K. N. *Phosphorus, Sulfur Silicon Relat. Elem.* **2011**, *186*, 94-97.
144. Willard, J. J.; Pacsu, E. *J. Am. Chem. Soc.* **1960**, *82*, 4347-4350.
145. Kapeller, D. C.; Hammerschmidt, F. *J. Org. Chem.* **2009**, *74*, 2380-2388.
146. Hager, A.; Kuttruff, C. A.; Herrero-Gomez, E.; Trauner, D. *Tetrahedron Lett.* **2014**, *55*, 59-62.
147. Humeres, E.; Soldi, V.; Klug, M.; Nunes, M.; Oliveira, C. M. S.; Barrie, P. J. *Can. J. Chem.* **1999**, *77*, 1050-1056.
148. Barboni, L.; Datta, A.; Dutta, D.; Georg, G. I.; Vander Velde, D. G.; Himes, R. H.; Wang, M.; Snyder, J. P. *J. Org. Chem.* **2001**, *66*, 3321-3329.
149. Noshita, M.; Shimizu, Y.; Morimoto, H.; Ohshima, T. *Org. Lett.* **2016**, *18*, 6062-6065.
150. Suryawanshi, S. N.; Rani, A.; Bhakuni, D. S. *Synth. Commun.* **1990**, *20*, 625-632.
151. Harano, K.; Kiyonaga, H.; Yokote, C.; Hisano, T. *Chem. Pharm. Bull.* **1991**, *39*, 1952-1957.
152. Eto, M.; Tajiri, O.; Nakagawa, H.; Harano, K. *Tetrahedron* **1998**, *54*, 8009-8014.
153. Ueng, S.-H.; Solovyev, A.; Yuan, X.; Geib, S. J.; Fensterbank, L.; Lacote, E.; Malacria, M.; Newcomb, M.; Walton, J. C.; Curran, D. P. *J. Am. Chem. Soc.* **2009**, *131*, 11256-11262.
154. Whistler, R. L.; Es, T. V. *J. Org. Chem.* **1963**, *28*, 2303-2304.
155. Baudry, M.; Barberousse, V.; Collette, Y.; Descotes, G.; Pires, J.; Praly, J.-P.; Samreth, S. *Tetrahedron* **1998**, *54*, 13783-13792.
156. Baudry, M.; Barberousse, V.; Descotes, G.; Pires, J.; Praly, J.-P. *Tetrahedron* **1998**, *54*, 7447-7456.
157. Baudry, M.; Barberousse, V.; Descotes, G.; Faure, R.; Pires, J.; Praly, J.-P. *Tetrahedron* **1998**, *54*, 7431-7446.

158. Collette, Y.; Ou, K.; Pires, J.; Baudry, M.; Descotes, G.; Praly, J. P.; Barberousse, V. *Carbohydr. Res.* **1999**, *318*, 162-166.
159. Skaanderup, P. R.; Poulsen, C. S.; Hyldtoft, L.; Jorgensen, M. R.; Madsen, R. *Synthesis* **2002**, 1721-1727.
160. Andresen, T. L.; Skytte, D. M.; Madsen, R. *Org. Biomol. Chem.* **2004**, *2*, 2951-2957.
161. Kornienko, A.; d'Alarcao, M. *Tetrahedron Lett.* **1997**, *38*, 6497-6500.
162. Kornienko, A.; d'Alarcao, M. *Tetrahedron Asymmetry* **1999**, *10*, 827-829.
163. Neel, A. J.; Hilton, M. J.; Sigman, M. S.; Toste, F. D. *Nature* **2017**, *543*, 637-646.
164. Ramakrishnan, B.; Ramasamy, V.; Qasba, P. K. *J. Mol. Biol.* **2006**, *357*, 1619-1633.
165. Crich, D.; Mataka, J.; Sun, S.; Wink, D. J.; Lam, K. C.; Rheingold, A. L. *Chem. Commun.* **1998**, 2763-2764.
166. Khiar, N. *Tetrahedron Lett.* **2000**, *41*, 9059-9063.
167. Crich, D.; Mataka, J.; Zakharov, L. N.; Rheingold, A. L.; Wink, D. J. *J. Am. Chem. Soc.* **2002**, *124*, 6028-6036.
168. Sanhueza, C. A.; Arias, A. C.; Dorta, R. L.; Vazquez, J. T. *Tetrahedron Asymmetry* **2010**, *21*, 1830-1832.
169. Buist, P. H.; Behrouzian, B.; MacIsaac, K. D.; Cassel, S.; Rollin, P.; Imberty, A.; Gautier, C.; Perez, S.; Genix, P. *Tetrahedron Asymmetry* **1999**, *10*, 2881-2889.
170. Cho, H.; Plapp, B. V. *Biochemistry* **1998**, *37*, 4482-4489.
171. Khiar, N.; Alonso, I.; Rodriguez, N.; Fernandez-Mayoralas, A.; Jimenez-Barbero, J.; Nieto, O.; Cano, F.; Foces-Foces, C.; Martin-Lomas, M. *Tetrahedron Lett.* **1997**, *38*, 8267-8270.
172. Liang, H.; MacKay, M.; Grindley, T. B.; Robertson, K. N.; Cameron, T. S. *Can. J. Chem.* **2010**, *88*, 1154-1174.
173. Ellervik, U.; Magnusson, G. *Tetrahedron Lett.* **1997**, *38*, 1627-1628.
174. Valko, K.; Plass, M.; Bevan, C.; Reynolds, D.; Abraham, M. H. *J. Chromatogr., A* **1998**, *797*, 41-55.
175. Valko, K. *J. Chromatogr. A* **2004**, *1037*, 299-310.
176. Tsuda, Y.; Haque, M. E.; Yoshimoto, K. *Chem. Pharm. Bull.* **1983**, *31*, 1612-1624.
177. Timmons, S. C.; Jakeman, D. L. *Carbohydr. Res.* **2008**, *343*, 865-874.
178. Sibi, M. P.; Snieckus, V. *J. Org. Chem.* **1983**, *48*, 1935-1937.
179. Snieckus, V. *Chem. Rev.* **1990**, *90*, 879-933.
180. Hartung, C. G.; Snieckus, V. *Mod. Arene Chem.* **2002**, 330-367.
181. Snieckus, V.; Anctil, E. J. G. *Met.-Catal. Cross-Coupling React. More* **2014**, *3*, 1067-1133.
182. Rozenberg, V.; Zhuravsky, R.; Sergeeva, E. *Chirality* **2006**, *18*, 95-102.
183. Rayment, E. J.; Summerhill, N.; Anderson, E. A. *J. Org. Chem.* **2012**, *77*, 7052-7060.
184. Julia, M.; Saint-Jalmes, V. P.; Verpeaux, J. N. *Synlett* **1993**, 233-234.
185. Julia, M.; Pfeuty-Saint Jalmes, V.; Ple, K.; Verpeaux, J.-N. *Bull. Soc. Chim. Fr.* **1996**, *133*, 15-24.
186. Groom, K.; Hussain, S. M. S.; Morin, J.; Nilewski, C.; Rantanen, T.; Snieckus, V. *Org. Lett.* **2014**, *16*, 2378-2381.
187. Zhuravsky, R. P.; Rozenberg, V. I.; Sergeeva, E. V.; Vorontsov, E. V. *Russ. Chem. Bull.* **2005**, *54*, 2702-2704.

188. Kalinin, A. V.; Miah, M. A. J.; Chattopadhyay, S.; Tsukazaki, M.; Wicki, M.; Nguen, T.; Coelho, A. L.; Kerr, M.; Snieckus, V. *Synlett* **1997**, 839-841.
189. Reed, M. A.; Chang, M. T.; Snieckus, V. *Org. Lett.* **2004**, *6*, 2297-2300.
190. Beak, P.; Brown, R. A. *J. Org. Chem.* **1982**, *47*, 34-46.
191. Morin, J.; Zhao, Y.; Snieckus, V. *Org. Lett.* **2013**, *15*, 4102-4105.